UNIVERSITY OF GRANADA

FACULTY OF SCIENCES

New developments and applications of Radial Basis Functions in Interpolation, Approximation and Data Science

by

Basim Mustafa

A dissertation presented in fulfillment of the requirements for the Doctor's degree from the University of Granada.

Granada, Spain

2024

Editor: Universidad de Granada. Tesis Doctorales
Autor: Basim Mustafa
ISBN: 978-84-1195-396-2
URI: https://hdl.handle.net/10481/93130

Supervised By

1. Prof. Dr. Miguel Pasadas Fernández (University of Granada, Full Professor of Applied Mathematics).
2. Prof. Dr. Pedro González Rodelas (University of Granada, Associate Professor of Applied Mathematics).

Dissertation Committee:

1. President:
2. Secretary:
3. Vocal:
4. First stand in:
5. Second stand in:
6. Third stand in:

Acknowledgments

I extend my sincere gratitude to all those who have contributed to the completion of this research work and supported my academic journey. Special recognition and heartfelt appreciation go to my esteemed supervisors, Prof. Miguel Pasadas Fernández and Prof. Pedro González Rodelas, for their unwavering dedication, invaluable guidance, and continuous support.
I would like to express my thanks to Professors Abdelouahed Kouibia and Domingo Barrera for their unwavering support.
My deep appreciation goes to my dear mother for her unconditional help and encouragement. I acknowledge the endless support of my wife, Nour, whose solid encouragement has been a driving force. Special thanks to my daughters, Zaina and little Yasmina, for their joyous presence.
I am profoundly indebted to An-Najah National University for their encouragement and financial support.
Thank you to everyone who has been part of this journey, contributing to its success.

Basim Mustafa

Contents

List of Figures

List of Tables

Chapter 1

Introduction

We explore Radial Basis Functions (RBF) and their applications. The journey begins with the solution of integral equations and integro-differential problems, followed by an investigation into numerical solutions for data science, with a focus on density estimation. The exploration concludes with a novel approach using Generalized Wendland radial basis functions for the approximation of bivariate functions. In this thesis, we dive into an in-depth understanding of these mathematical methods and their practical applications.

In the pursuit of advancing the field of Radial Basis Functions (RBF), our exploration begins with a novel approximation method proposed for solving second-kind Volterra integral equation systems. Grounded in the minimization of a functional within a discrete space defined by compactly supported radial basis functions of Wendland type, this methodology achieves not only acceptable accuracy but also remarkably low computational costs. The significance of our contributions is underscored by the proof of two convergence results, a feature notably absent in recent literature.

Volterra integral equations, introduced by Vito Volterra in the early 20th century, serve as one of the fundamental applications for our research. The rich variety of applications includes but is not limited to elasticity, plasticity, semi-conductors, scattering theory, and population dynamics. These integral equations arise naturally when transforming initial value problems into integral forms, simplifying solutions and often revealing connections to systems of ordinary differential equations (ODEs). Exploiting this link, our approach aligns with authors who leverage effective ODE codes for numerical solutions.

Expanding our exploration to linear Volterra integro-differential problems, we introduce an approximation method based on the minimization of

a functional within a finite-dimensional space generated by a finite set of Wendland radial basis functions. Proving the existence and uniqueness of solutions, alongside establishing two convergence results, our methodology is validated through numerical examples. This expansion serves as another evidence of the widespread use of Volterra integral equations in a variety of fields, including quantum physics and population dynamics.

In our next work, we deal with two approximation problems in a finite-dimensional Generalized Wendland space of compactly supported radial basis functions. Namely, we present an interpolation method and a smoothing variational method in this space. Next, the theory of the presented method is justified by proving the corresponding convergence result. Likewise, to illustrate such method, some graphical and numerical examples are presented in $\mathbb{R}^2$ and a comparison with another work is analyzed.

Transitioning seamlessly into the realm of data science, we delve into the importance of density estimation, a fundamental statistical tool with wide-ranging applications. Our focus is on kernel density estimation, a method integral to probabilistic modeling and reasoning with uncertainty. A three-step strategy is employed, adapting an algorithm that subdivides data into high and low-density regions, each assigned a bandwidth parameter. Utilizing Gaussian and Birnbaum-Saunders Power-Exponential (BS-PE) kernel estimators, we introduce a residual-based posteriori error estimator τ_i for each region or class S_i for comprehensive evaluation. A series of simulation studies and real data are realized for evaluating the performance of the procedure proposed. Moreover, our computational methodologies incorporate a proven convergence algorithm, enhancing the reliability and theoretical robustness of our approach. The real-world implications of density estimation span finance, healthcare, environmental science, and machine learning, forming a bridge between theoretical foundations and practical challenges.

Through the combination of these diverse paths of research, our thesis aims to contribute to the evolving landscape of mathematical methodologies and their real-world implications.

So, the thesis is organized as follows: Apart from this introduction, in Chapter 2, we recall some notations and preliminaries. Chapter 3 is an introduction to radial basis functions interpolation with their historical and theoretical background. Chapter 4 is devoted to the detailed numerical solution of integral equations by RBF's, in which the results of our two published articles are included. Our third paper is covered in Chapter 5, which is an application of Generalized Wendland RBFs. Chapter 6 discusses Nonparametric Density Estimation. Finally, chapter 7 ends with conclusions and future work, followed by the references cited throughout the thesis.

Chapter 2

Preliminaries

In the chapter, we establish the groundwork by presenting essential definitions, foundational concepts, and relevant theorems. This serves as a necessary framework for the subsequent chapters.

2.1 Vector spaces

This section is devoted to introduce definitions and some examples of the concept of vector spaces, normed spaces, Banach spaces, Hilbert spaces and Sobolev spaces.

2.1.1 Basic notions on vector spaces

Definition 2.1.1. *[19] Let V be a set of objects, to be called vectors; and let $\mathbb{K}$ be a set of scalars, either $\mathbb{R}$ the set of real numbers, or $\mathbb{C}$ the set of complex numbers. Assume there are two operations: $(u, v) \to u + v \in V$ and $(\alpha, v) \to \alpha v \in V$, called addition and scalar multiplication, respectively, defined for any $u, v \in V$ and any $\alpha \in \mathbb{K}$. These operations are to satisfy the following rules.*

1. *$u + v = v + u$ for any $u, v \in V$ (commutative law);*

2. $(u+v)+w = u+(v+w)$ *for any* $u, v, w \in V$ *(associative law);*

3. *there is an element* $0 \in V$ *such that* $0+u = u$ *for any* $u \in V$ *(existence of the zero element);*

4. *for any* $u \in V$ *there is an element* $-u \in V$ *such that* $u + -u = 0$ *(existence of opposite elements);*

5. $1u = u$ *for any* $u \in V$ *;*

6. $\alpha(\beta u) = (\alpha\beta)u$ *for any* $u \in V$ *any* $\alpha, \beta \in \mathbb{K}$ *(associative law for scalar multiplication);*

7. $\alpha(u+v) = \alpha u + \alpha v$ *and* $(\alpha+\beta)u = \alpha u + \beta u$ *for any* $u, v \in V$ *and any* $\alpha, \beta \in \mathbb{K}$ *(distributive laws).*

Then V *is called a* ***linear space****, or a* ***vector space****.*

Here are some examples of vector spaces.

1. The set of the real numbers $\mathbb{R}$ is a real linear space when the addition and scalar multiplication are the usual addition and multiplication. Similarly, the set of complex numbers $\mathbb{C}$ is a complex linear space.

2. Let d be a positive integer. The letter d is used generally in this work for the spatial dimension. The set of all vectors with d real components, with the usual vector addition and scalar multiplication, forms a linear space $\mathbb{R}^d$. A typical element in $\mathbb{R}^d$ can be expressed as $x = (x_1, \cdots, x_d)^{\mathrm{T}}$ where $x_1, ..., x_d \in \mathbb{R}$. Similarly, $\mathbb{C}^d$ is a complex linear space.

3. For any non-negative integer m, we may define the space $\mathbb{C}^m(\Omega)$ as the space of all the functions that together with their derivatives of orders up to m are continuous on Ω.

4. The space of matrices of real numbers with m rows and n columns, for every $m, n \in \mathbb{N}^*$, is a linear space and is denoted by $\mathcal{M}_{m,n}(\mathbb{R})$.

Definition 2.1.2. *[19] We say $v_1, ..., v_n \in V$ are **linearly dependent** if there are scalars $\alpha_i \in \mathbb{K}, 1 \leqslant i \leqslant n$, with at least one α_i non-zero such that*

$$\sum_{i=1}^{n} \alpha_i v_i = 0.$$

*We say $v_1, ..., v_n \in V$ are **linearly independent** if they are not linearly dependent, meaning that the only choice of scalars α_i for which the last equation is valid is $\alpha_i = 0$ for $i = 1, 2, \cdots, n$.*

We observe that $v_1, ..., v_n$ are linearly dependent if and only if at least one of the vectors can be expressed as a linear combination of the rest of the vectors.

Definition 2.1.3. *[18] The **span** of $v_1, \cdots, v_n \in V$ is defined to be the set of all the linear combinations of these vectors:*

$$span\{v_1, \cdots, v_n\} = \left\{ \sum_{i=1}^{n} \alpha_i v_i, \alpha_i \in \mathbb{K}, 1 \leqslant i \leqslant n \right\}.$$

2.1.2 Normed spaces

Definition 2.1.4. *Given a linear space V a **norm** $\|\cdot\|$ is a function from V to $\mathbb{R}$ with the following properties.*

1. $\|v\| \geqslant 0$ *for any $v \in V$, and $\|v\| = 0$ if and only if $v = 0$;*
2. $\|\alpha v\| = |\alpha| \|v\|$ *for any $v \in V$ and $\alpha \in \mathbb{K}$;*
3. $\|u + v\| \leqslant \|u\| + \|v\|$ *for any $u, v \in V$.*

The space V equipped with the norm $\|\cdot\|$ is called a normed linear space or a ***normed space***. We usually say V is a normed space when the definition of the norm is clear from the context. Two of the famous and widely used norms are:

1. For $x = (x_1, ..., x_d)^{\mathrm{T}}$, the formula

$$\|x\|_2 = \left(\sum_{i=1}^{d} x_i^2 \right)^{1/2}$$

defines a norm in the space $\mathbb{R}^d$, called the *Euclidean norm*, which is the usual norm for the space $\mathbb{R}^d$. When $d = 1$, the norm coincides with the absolute value: $\|x\|_2 = |x|$ for $x \in \mathbb{R}$.

2. More generally, for $1 \leq p \leq \infty$ the formulas

$$\|x\|_p = \left(\sum_{i=1}^{d} |x_i|^p \right)^{1/p} \quad \text{for } 1 \leq p < \infty$$

$$\|x\|_\infty = \max_{1 \leq i \leq d} |x_i|$$

define norms in the space $\mathbb{R}^d$. The norm $\|\cdot\|_p$ is called the *p-norm*, and $\|\cdot\|_\infty$ is called the *maximum norm* or *infinity norm*.

With the notion of a norm at our disposal, we can define the concept of convergence as follows.

Definition 2.1.5. *[18]*

*Let V be a normed space with the norm $\|\cdot\|$. We say that a sequence $\{u_n\} \subseteq V$ is **convergent** to $u \in V$ if*

$$\lim_{n \to \infty} \|u_n - u\| = 0.$$

We say that u is the limit of the sequence $\{u_n\}$, and write $u_n \longrightarrow u$ as $n \longrightarrow \infty$ or $\lim_{n \to \infty} u_n = u$.

2.1.3 Banach spaces

Definition 2.1.6. *[18]*

*Let V be a normed space. A sequence $\{u_n\} \subseteq V$ is called a **Cauchy** sequence if*

$$\lim_{m,n\to\infty} \|u_m - u_n\| = 0.$$

Obviously, a convergent sequence is a Cauchy sequence. In the finite-dimensional space $\mathbb{R}^d$, any Cauchy sequence is convergent. However, in a general infinite-dimensional space, a Cauchy sequence may fail to converge.

Definition 2.1.7. *[18] A normed space is said to be* ***complete*** *if every Cauchy sequence from the space converges to an element in the space. A complete normed space is called a* ***Banach space****.*

Examples:

- The space of real-valued vectors with n components equipped with the standard Euclidean norm

$$\|(x_1, \ldots, x_n)\|_2 = \sqrt{(x_1^2 + \ldots + x_n^2)}.$$

- l^p spaces equipped with with l^p-norm

$$\|(x_1, \ldots,)\|_p = \left(\sum_{k=1}^{\infty} \|x_k\|^p \right)^{\frac{1}{p}}.$$

- $C(J, \mathbb{R})$ the space of all continuous functions from J to $\mathbb{R}$, endowed with the sup-norm $\|\cdot\|_\infty$, defined by

$$\|f\|_\infty = \sup_{t\in J} |f(t)|.$$

It is not hard to prove that any finite-dimensional normed vector space is a Banach space. So completeness is really only an issue for infinite dimensional spaces.

2.1.4 Hilbert spaces

In studying linear problems, inner product spaces are usually used. These are the spaces where a norm can be defined through the inner product and the notion of orthogonality of two elements can be introduced. The inner product in a general space is a generalization of the usual scalar product in the plane $\mathbb{R}^2$ or the space $\mathbb{R}^3$.

Definition 2.1.8. *[18] Let V be a linear space over $\mathbb{K} = \mathbb{R}$ or $\mathbb{C}$.*

*An **inner product** $(\cdot, \cdot)$ is a function from $V \times V$ to $\mathbb{K}$ with the following properties.*

1. *Positivity: For any $u \in V, (u, u) \geq 0$ and $(u, u) = 0$ if and only if $u = 0$.*

2. *Conjugate symmetry: For any $u, v \in V, (v, u) = \overline{(u, v)}$.*

3. *Linearity: For any $u, v, w \in V$ any $\alpha, \beta \in \mathbb{K}$, $(\alpha u + \beta v, w) = \alpha (u, w) + \beta (v, w)$.*

The space V together with the inner product $(\cdot, \cdot)$ is called an ***inner product space***. When the definition of the inner product $(\cdot, \cdot)$ is clear from the context, we simply say V is an inner product space. When $\mathbb{K} = \mathbb{R}$, V is called a real inner product space, while if $\mathbb{K} = \mathbb{C}$, V is a complex inner product space.

Commonly seen inner product spaces are usually associated with their canonical inner products. As an example, the canonical inner product for $x = (x_1, ., x_d)^{\mathrm{T}}, y = (y_1, ., y_d)^{\mathrm{T}} \in \mathbb{R}^d$ is

$$(x, y) = \sum_{i=1}^{d} x_i y_i.$$

This inner product induces the *Euclidean norm*

$$\|x\| = \sqrt{\sum_{i=1}^{d} |x_i|^2} = \sqrt{(x, x)}.$$

Among the inner product spaces, of particular importance are the Hilbert spaces.

Definition 2.1.9. *[18] A complete inner product space is called a **Hilbert space**.*

In what follows, H will always denote a Hilbert space.

A basic example is $L^2(\Omega)$ equipped with the scalar product

$$(u, v) = \int_{\Omega} u(x)v(x)d\mu$$

is a Hilbert space. In particular, ℓ^2 is a Hilbert space.

Definition 2.1.10. *[18]*

Suppose $A = (a_{ij})$, $a_{ij} \in \mathbb{R}$, $1 \leq i \leq m$, $1 \leq j \leq n$ *and* $A \in \mathcal{M}_{m,n}$*(the space of real* $m \times n$ *matrices). We will define in this space the following scalar product*

$$\forall A = (a_{ij}),\ B = (b_{ij}) \in \mathcal{M}_{m,n},\ \langle A, B\rangle_{m,n} = \sum_{i=1}^{m}\sum_{j=1}^{n} a_{ij}b_{ij}\,,$$

and the corresponding matrix norm

$$\forall A \in \mathcal{M}_{m,n},\ \langle A\rangle_{m,n} = \langle A, A\rangle_{m,n}^{1/2}\,.$$

is called the Hilbert-Schmidt *norm.*

2.1.5 Sobolev spaces

In preparation for Sobolev spaces, we first introduce the notion of locally integrable functions and the concept of a weak derivative.

Definition 2.1.11. *[7] Let* $1 \leq p < \infty$*. A function* $v : \Omega \subseteq \mathbb{R}^d \to \mathbb{R}$ *is said to be locally p-integrable,* $v \in L^p_{\text{loc}}(\Omega)$*, if for every* $\mathrm{x} \in \Omega$*, there is an open neighborhood* Ω' *of* $\mathbf{x}$ *such that* $\Omega' \subseteq \Omega$ *and* $v \in L^p(\Omega')$*.*

Definition 2.1.12. *[7] Let* Ω *be a non-empty open set in* $\mathbb{R}^d, v, w \in L^1_{\text{loc}}(\Omega)$*. Then* w *is called a weak* α^{th} *derivative of* v *if*

$$\int_{\Omega} v(\mathbf{x})D^{\alpha}\phi(\mathbf{x})dx = (-1)^{|\alpha|}\int_{\Omega} w(\mathbf{x})\phi(\mathbf{x})dx \quad \forall \phi \in C_0^{\infty}(\Omega).$$

Definition 2.1.13. *[7] Let* k *be a non-negative integer,* $p \in [1, \infty]$*. The* ***Sobolev space*** $W^{k,p}(\Omega)$ *is the set of all functions* $v \in L^1_{loc}(\Omega)$ *such that*

for each multi-index α with $|\alpha| \leq k$, the α^{th} weak derivative $D^\alpha v$ exists and $D^\alpha v \in L^p(\Omega)$. The norm in the space $W^{k,p}(\Omega)$ is defined as

$$\|v\|_{W^{k,p}(\Omega)} = \begin{cases} \left(\sum_{|\alpha|\leq k} \|D^\alpha v\|^p_{L^p(\Omega)}\right)^{1/p}, & 1 \leq p < \infty \\ \max_{|\alpha|\leq k} \|D^\alpha v\|_{L^\infty(\Omega)}, & p = \infty \end{cases}$$

When $p = 2$, we write $H^k(\Omega) \equiv W^{k,2}(\Omega)$.

Usually we replace $\|v\|_{W^{k,p}(\Omega)}$ by the simpler notations $\|v\|_{k,p,\Omega}$, or even $\|v\|_{k,p}$ when no confusion results. The standard semi-norm over the space $W^{k,p}(\Omega)$ is

$$|v|_{W^{k,p}(\Omega)} = \begin{cases} \left(\sum_{|\alpha|=k} \|D^\alpha v\|^p_{L^p(\Omega)}\right)^{1/p}, & 1 \leq p < \infty, \\ \max_{|\alpha|=k} \|D^\alpha v\|_{L^\infty(\Omega)}, & p = \infty. \end{cases}$$

It is not difficult to see that $W^{k,p}(\Omega)$ is a normed space. Moreover, we have the following result.

Theorem 2.1.1. *[7] The Sobolev space $W^{k,p}(\Omega)$ is a Banach space.*

A simple consequence of the theorem is the following result.

Corollary 2.1.14. *[7] The Sobolev space $H^k(\Omega)$ is a Hilbert space with the inner product*

$$(u, v)_k = \int_\Omega \sum_{|\alpha|\leq k} D^\alpha u(\mathbf{x}) D^\alpha v(\mathbf{x}) dx, \quad u, v \in H^k(\Omega).$$

2.2 Notations

In this section, we establish the notations that will be consistently used throughout the thesis.

For $n \in \mathbb{N}$ we denote by $\langle \cdot \rangle_n$ and $\langle \cdot, \cdot \rangle_n$ the Euclidean norm and inner product in $\mathbb{R}^n$.
Given $I = (a, b) \subset \mathbb{R}$ an open bounded real interval and $k \in \mathbb{N}$, let $\mathbb{P}_k(I)$ be the real linear space of the restrictions to I of the polynomials of degree $\leq k$. On the other hand, for $m \geq 1$, we designate by $H^m((0,1); \mathbb{R}^n)$ the Sobolev space of order m of (classes of) functions $\boldsymbol{u} \in L^2((0,1); \mathbb{R}^n)$ together with all j-th derivative functions $\boldsymbol{u}^{(j)}$ of order $j \leq m$, in the sense of distributions. This space is equipped with

- the semi–inner products, for any $\boldsymbol{u}, \boldsymbol{v} \in H^m((0,1);\mathbb{R}^n)$,

$$(\boldsymbol{u}, \boldsymbol{v})_j = \int_0^1 \langle \boldsymbol{u}^{(j)}(t), \boldsymbol{v}^{(j)}(t) \rangle_n dt, \quad 0 \leq j \leq m,$$

- the corresponding semi–norms $|\boldsymbol{u}|_j = (\boldsymbol{u}, \boldsymbol{u})_j^{\frac{1}{2}}$, for $0 \leq j \leq m$,

- the inner product $((\boldsymbol{u}, \boldsymbol{v}))_m = \sum_0^m (\boldsymbol{u}, \boldsymbol{v})_j$,

- and the corresponding norm $\|\boldsymbol{u}\|_m = ((\boldsymbol{u}, \boldsymbol{u}))_m^{\frac{1}{2}}$.

Let $D : H^{2n}(I) \to L^2(I)$ be the differential operator given by

$$Du(t) = \sum_{i=0}^{n} (-1)^i d^i (p_i(t) d^i u(t)), \quad t \in I, \quad u \in H^{2n}(I),$$

where $p_i(t) \in H^i(I)$, for $0 \leq i \leq n$. Consider the integral operator Λ given by

$$\Lambda u(t) = \int_a^t k(t,s) u(s) ds, \quad \forall\, t \in I, \quad \forall\, u \in L^2(I).$$

Let $\mathbb{R}^{n,p}$ be the space of real matrices of n rows and p columns, equipped with the inner product

$$\langle A, B \rangle_{n,p} = \sum_{i=1}^{n} \sum_{j=1}^{p} a_{ij} b_{ij}, \quad \forall A = (a_{ij})_{\substack{1 \leq i \leq n \\ 1 \leq j \leq p}},\ B = (b_{ij})_{\substack{1 \leq i \leq n \\ 1 \leq j \leq p}} \in \mathbb{R}^{n,p},$$

and the corresponding norm $\langle A \rangle_{n,p} = \langle A, A \rangle_{n,p}^{\frac{1}{2}}$.

Chapter 3

Radial Basis Functions

In this chapter we give an introduction to radial basis functions interpolation with their historical and theoretical background. Also some basic results of the interpolation problem are given. Furthermore, we explain the need to use radial basis functions in the interpolation and approximation problems. Finally, we introduce the class of compactly supported radial basis functions (CSRBFs) with some examples.

In mathematics, most functions are not exactly evaluated, even though we typically use them as if they were fully known quantities. The procedure of finding and evaluating a function whose graph passes through a set of given points is known as interpolation. These points may come from measurements in a physical issue or they could come from a function that is well-known.

3.1 Scattered data Interpolation

The following issue arises in many scientific fields. Finding a rule that enables us to infer details about the process we are investigating at locations other than the ones where our measurements were taken is what we want to do with a set of data, such as measurements and the locations at which they were collected. Therefore, we are attempting to identify a function that provides a "good" fit for the provided data. There are various ways to define "good." But, for the purposes of this discussion, we will limit the criteria to the desire that the functions precisely match the provided measurements at the given locations. This approach is known as interpolation; if the measurement sites are not on a uniform or regular grid, the procedure is known as scattered

data interpolation.

Given a set of data points $(x_i, y_i) \in X \times Y$, where $i = 0, 1, \ldots, N$, X and Y are subsets of $\mathbb{R}$ (or $\mathbb{C}$), representing the domains where x_i and y_i reside, respectively. The points x_i are referred to as interpolation nodes and are assumed to be distinct. Provided with a specific linear subspace V of functions in $C(X)$. Find an interpolating function f in V satisfying the interpolating condition

$$f(x_i) = y_i, \ i = 0, 1, \ldots, N.$$

Before going further with the univariate case, it's worth mentioning the fact that we might allow x_i to lie in an arbitrary s-dimensional space $\mathbb{R}^s$ means that the formulation of the Problem above allows us to cover many different types of applications. Here are some examples:

1. If $s = 1$ the data could be a series of measurements taken over a certain time period, thus the "data sites" x_i would correspond to certain time instances.

2. For $s = 2$ we can think of the data being obtained over a planar region, and so x_i corresponds to the two coordinates in the plane.

3. For $s = 3$ we might think of a similar situation in space. One possibility is that we could be interested in the temperature distribution inside some solid body.

4. Higher-dimensional examples might not be that intuitive, but a multitude of them exist, e.g., in finance, optimization, economics or statistics, but also in artificial intelligence or learning theory.

An interpolation function is also called interpolant. The primary purpose of interpolation is to replace a set of data points (x_i, y_i) with a function given analytically, another purpose is to approximate functions with simpler ones, usually polynomials or piecewise polynomials.

We start with the simplest case, when only the values $f_i := f(x_i)$, for $i = 0, ..., N$ are given at the pairwise distinct nodes $x_0, ..., x_N$. We now seek a unique polynomial $P \in \mathbf{P}_N = \mathbb{R}_N[x]$ (a set of polynomials with coefficients in $\mathbb{R}$ and of degree $\leqslant N$), which interpolates f at the $(N + 1)$ nodes $x_0, ..., x_N$, i.e., $P(x_i) = f_i$ for $i = 0, ..., N$.

In order to compute the interpolating polynomial, we need to choose a basis of the space of polynomials $\mathbf{P}_N$.

A polynomial can be represented using many different kinds of bases.

1. Monomial basis: the monomial basis of a polynomial is of the form $\left\{1, x, \ldots, x^N\right\}$.

2. Center basis: the center basis of a polynomial is of the form $\left\{1, (x-c), \ldots, (x-c)^N\right\}$ with $c \neq 0$.

3. Lagrange basis: let $(x_i)_{i=0}^N$, be N distinct points, the associated basis is given by

$$L_i(x) = \prod_{j=0, i\neq j}^{N} \frac{x - x_j}{x_i - x_j}$$

4. Newton basis: let $(x_i)_{i=0}^N$, be N distinct points, the associated basis is given by

$$\left\{1, (x-x_0), (x-x_0)(x-x_1), .., \prod_{k=0}^{N-1}(x-x_k)\right\}.$$

If we write P as above, in coefficient representation

$$P_N(x) = \sum_{i=0}^{N} a_i x^i$$

i.e., with respect to the monomial basis $\left\{1, x, \ldots, x^N\right\}$ of $\mathbf{P}_N$, then the interpolation matrix resulting from interpolation conditions $P_N(x_i) = f(x_i)$ is called Vandermonde matrix. The determinant of Vandermonde matrix is different from zero precisely when the nodes $x_0, \ldots, x_N$ are pairwise distinct. However, the solution of the system requires an excessive amount of computational effort. In addition, the Vandermonde matrices are almost singular in higher dimensions N.

3.1.1 Runge's phenomenon

Theorem 3.1.1. *[97] Let f be a function in $C^{N+1}[a,b]$, and let P_N be a polynomial of degree $\leq N$ that interpolates the function f at $(N+1)$ distinct points $x_0, x_1, \ldots, x_N \in [a,b]$. Then to each $x \in [a,b]$ there exists a point $\xi_x \in [a,b]$ such that*

$$f(x) - P_N(x) = \frac{1}{(N+1)!} f^{(N+1)}(\xi_x) \prod_{i=0}^{N} (x - x_i)$$

Runge phenomenon is a problem of oscillation at the edges of an interval that occurs when using polynomial of high degree over a set of equispaced interpolation points. The discovery was important because it shows that going to higher degree doesn't always improve accuracy [41].

Interpolation at equidistant points is a natural and well-known approach to construct approximating polynomials. Runge's phenomenon demonstrates that interpolation can result in divergent approximations.

Let consider the function

$$f(x) = \frac{1}{1+x^2}.$$

Runge found that if this function is interpolated at equidistant points $x_i = -5 : \frac{10}{N} : 5$, the resulting interpolation oscillates towards the end of the interval. It can be proven that the interpolation error increases when the degree of the polynomial is increased [97].

If we consider the class of functions

$$\mathcal{F} = \left\{ f \in C^{N+1}[a,b], \left| \sup_{\tau \in [a,b]} f^{(N+1)}(\tau) \right| \leq M(N+1)! \right\}$$

for a constant $M > 0$, then the approximation error obviously depends crucially on the choice of the nodes $x_0, \ldots, x_N$ via the expression

$$prod(x) = (x - x_0) \ldots (x - x_N)$$

Also the equidistance between points leads to Lebesgue constant that increases quickly when N increases. Table 3.1 shows the error between Runge's function and its interpolation polynomial when N increase, with $x_{N-1/2} = 5 - \frac{5}{N}$. We remark that

$$\lim_{N \to \infty} \left\| P_N\left(x_{N-1/2}\right) - f\left(x_{N-1/2}\right) \right\|_\infty = +\infty$$

The evaluation of $prod(x) = \prod_{i=0}^{N} (x - x_i)$ is illustrated in table 3.2 , with: $x_i = -5 : \frac{10}{N} : 5$.

Runge's phenonmenon can be avoided by (See for example [41]):

1. Change of the interpolation points

N	$f(x)$	$p_N(x)$	Absolute error
2	0.1379	0.7596	0.6217
10	0.0471	1.5787	1.5317
16	0.0435	-10.1739	10.2174
20	0.0424	-39.9524	39.9949

Table 3.1 : The error between Runge's function and its interpolation polynomial when $N \to \infty$.

x	$f(x)$	$p_{20}(x)$	Absolute error	prod(x)
0.25	0.9412	0.9425	0.0013	$2.0468e + 006$
1.75	0.2462	0.2384	0.0077	$-6.5587e + 006$
3.75	0.0664	-0.4471	0.5134	$-7.5594e + 008$
4.75	0.0424	-39.9524	39.9949	$-7.2721e + 010$

Table 3.2 : The behavior of $prod(x)$.

The oscillation can be minimized by using nodes that are distributed more densely towards the edges of the interval. This set of nodes is Chebyshev nodes for which the maximum error in approximating the Runge function is guaranteed to diminish with increasing polynomial order.

2. Use piecewise polynomials

   The problem can be avoided by using spline curves which are piecewise polynomials, when trying to decrease the interpolation error one can increase the number of polynomials pieces which are used to construct the spline instead of increasing the degree of the polynomial.

3.1.2 Interpolation in higher dimensions

In the univariate setting it is well known that one can interpolate arbitrary data at $N + 1$ distinct data sites using a polynomial of degree N [44]. For the multivariate setting, however, there is a negative result in the coming

theorem of (Mairhuber-Curtis). In order to understand this theorem we need the following definition.

Definition 3.1.2. *[44] Let the finite-dimensional linear function space $\mathcal{B} \subseteq C(\Omega)$ have a basis $\{B_1, \cdots, B_N\}$. Then $\mathcal{B}$ is a Haar space on Ω if*

$$det(A) \neq 0 \tag{3.1}$$

for any set of distinct points $x_1, \cdots, x_N$ in Ω. Here A is the matrix with entries $A_{jk} = B_k(x_j)$.

Theorem 3.1.3. *[44]* ***(Haar-Mairhuber-Curtis)***

If $\Omega \subset \mathbb{R}^s, s \geq 2$, contains an interior point, then there exist no Haar spaces of continuous functions.

Proof. To prove Haar-Mairhuber-Curtis theorem , let $s \geq 2$ and suppose $\mathcal{B}$ is a Haar space with basis $\{B_1, \cdots, B_N\}$ with $N \geq 2$. Then, by the definition of a Haar space

$$det(A) \neq 0 \tag{3.2}$$

for any set of distinct $x_1, \cdots, x_N$. Now consider a closed path P in Ω connecting only x_1 and x_2. This is possible since by assumption contains an interior point. We can exchange the positions of x_1 and x_2 by moving them continuously along the path P (without interfering with any of the other x_i). This means, however, that rows 1 and 2 of the determinant (3.2) have been exchanged, and so the determinant has changed sign. Since the determinant is a continuous function of x_1 and x_2 we must have determinant equal to zero at some point along P. This is a contradiction. □

Remarks

- Note that existence of a Haar space guarantees invertibility of the interpolation matrix A, i.e., existence and uniqueness of an interpolant to data specified at $x_1, \cdots, x_N$ from the space $\mathcal{B}$.

- The only exception would be the one-dimensional case $s = 1$. Univariate polynomials of degree *N-1* form an N-dimensional Haar space for data given at $x_1, \cdots, x_N$.
- The Haar-Mairhuber-Curtis theorem implies that in the multivariate setting we can no longer expect this to be the case. For example, it is not possible to perform unique interpolation with (multivariate) polynomials of degree N to data given at arbitrary locations in $\mathbb{R}^2$.

So as a result of this theorem, if we choose our basis functions independently of the data, we are not guaranteed a well-posed problem.

The Haar-Mairhuber-Curtis theorem tells us that if we want to have a well-posed multivariate scattered data interpolation problem, we can't fix in advance the set of basis functions, but the basis should depend on the data location.

3.2 Radial Basis Functions

In this section, we explore the principal tool underpinning our thesis - Radial Basis Functions. Firstly, we navigate through the Meshfree methods and their historical development, highlighting their advantages and diverse applications. The subsequent subsection is dedicated to unraveling the origins of radial basis functions (RBFs) and furnishing a precise definition of a RBF. To conclude this investigation, the final subsection sheds light on the historical evolution of the RBF interpolation problem, accompanied by a foundational theoretical overview. As a culmination, we present a collection of tables and figures showcasing prominent examples of radial basis functions.

3.2.1 Meshfree methods

Historical landmarks

Originally, the motivation for the basic meshfree approximation methods (radial basis functions) came from applications in geodesy, geophysics, mapping, or meteorology. Later, applications were found in many areas such as in the numerical solution of PDEs, artificial intelligence, learning theory, neural networks, signal processing, statistics (kriging), finance, and optimization. It should be pointed out that meshfree local regression methods have been used (independently) in statistics for more than 100 years. "Standard" multivariate approximation methods (splines or finite elements) require an underlying

mesh (e.g. triangulation) for the definition of basis functions or elements. This is very difficult in space dimensions greater than two [44].

Some historical landmarks for meshfree methods in approximation theory [44]:

- D. Shepard, Shepard functions, late 1960s (application, surface modelling).
- Rolland Hardy (Iowa State Univ.), multiquadrics (MQs), early 1970s (application, geodesy).
- Jean Meinguet (Universitè Catholique de Louvain, Louvain, Belgium), surface splines, late 1970s (mathematics).
- Richard Franke (NPG, Montery), in 1982 compared scattered data interpolation methods, and concluded MQs and TPs were the best. Franke conjectured interpolation matrix for MQs is invertible.
- Charles Micchelli (IBM), Interpolation of scattered data: Distance matrices and conditionally positive definite functions, 1986.

Advantages of meshfree methods

Meshfree methods have gained much attention in recent years. This is due to the following reasons:

- Many traditional numerical methods (finite differences, finite elements or finite volumes) have trouble with high-dimensional problems.
- Meshfree methods can often handle better the changes in the geometry of the domain of interest (e.g., free surfaces, moving particles and large deformations).
- Independence from a mesh is a great advantage since mesh generation is one of the most time consuming parts of any mesh-based numerical simulation.
- New generation of numerical tools.

Applications

- Original applications were in geodesy, geophysics, mapping, or meteorology.

- Later, many other application areas such as Numerical solution of PDEs in many engineering applications, Computer graphics, Sampling theory, Artificial intelligence, Machine learning or Statistical learning (neural networks or SVMs), Signal and image processing, Statistics (kriging), Finance, Optimization, etc.

3.2.2 Basis functions depending on data

- The basis functions of meshless methods noted by ϕ_i are dependent on the data sites x_i as suggested by Haar-Mairhuber-Curtis.
- The points x_i for which the basic function is shifted to form the basis functions, are usually referred as centers or knots.
- Technically, one could choose these centers different from the data sites. However, usually centers coincide with the data sites. This simplifies the analysis of the method, and is sufficient for many applications. In fact, relatively little is known about the case when centers and data sites differ.
- $\phi_i(x)$ are radially symmetric about their centers, for this reason we call these functions Radial Basis Functions (RBFs).

In 1968, R.L. Hardy [52] aimed to create a function capable of accurately representing a topographical curve. In his investigation, Hardy discovered that the data could be effectively depicted by a piecewise linear interpolating function [52]. He proposed that given a set of N distinct scattered data points $\{x_j\}_{j=0}^{N}$ and their corresponding measurements $\{f_j\}_{j=0}^{N}$, the following form would be adequate:

$$\phi_j(x) = |x - x_j|, \quad j = 0, 1, \ldots, N.$$

Hardy soon recognized that the absolute function had a jump in the first derivative at each source point. Hardy figured out that this problem could be solved by removing the absolute value basis function and replacing it with a function that is continuously differentiable. Hardy's function was $\sqrt{\epsilon^2 + r^2}$, where ϵ is an arbitrary non-zero constant [52]. Hardy applied the interpolation method using this function to multidimensional spaces. Note that the absolute value of the difference between two points in two dimensional space is the Euclidean distance between the two points; for example, $|x - x_j| = \sqrt{(x - x_j)^2}$ in one dimension. What Hardy created was an interpolating function based on translates of the Euclidean distance function in

two dimensions. Hence, given N distinct scattered data points $\{(x_j, y_j)\}_{j=0}^{N}$ and corresponding topographic measurements $\{f_j\}_{j=0}^{N}$ for $j = 0, 1, \ldots, N$, Hardy proposed the following basis function

$$\phi_{i,j}(x, y) = \sqrt{(x - x_j)^2 + (y - y_j)^2}. \tag{3.3}$$

To be exact $\phi(r) = \sqrt{x^2 + y^2}$. Also, as previously described in one dimension, the vertex of each cone is centered at one of the data points. Again, Hardy ran into the same problem as his one dimensional interpolating function. The problem was that function defined in equation (3.3) suffered from being piecewise continuous. He was unable to find a simple fix for this problem. Hardy proposed using a linear combination of circular hyperboloid basis functions (rotated hyperbola basis functions $\sqrt{\epsilon^2 + x^2}$ translated to be centered at each source point). The new form of equation (3.3) is

$$\phi_{i,j}(x, y) = \sqrt{\epsilon^2 + (x - x_j)^2 + (y - y_j)^2}.$$

Hardy discovered that the interpolation method based on the new function was an excellent method for approximating topographical information from sparse data points. Unlike the Fourier series, the new function did not suffer from large oscillations. Also, the function alleviated the problem associated with the polynomial series method (i.e. the polynomial series was unable to account for rapid variations of the topographical surface) [51]. Hardy named this new technique the multiquadric basis function (MQ).

Notice that the multiquadric basis function is also radially symmetric about its center. Because of this radial symmetry, the multiquadric kernel can be described as a Radial Basis Function. In other words, it is a basis function which depends only on the radial distance from its center. Since our basis functions depend only on distance. This leads us to the following definitions.

Definition 3.2.1. *A function $\Phi : \mathbb{R}^s \to \mathbb{R}$ is called **radial** provided there exists a univariate function $\phi : [0, \infty) \to \mathbb{R}$ such that*

$$\Phi(x) = \phi(r),$$

where $r = \|x\|$, and $\|\cdot\|$ is some norm on $\mathbb{R}^s$ -usually the Euclidean norm.

The last definition says that for a radial function Φ

$$\|x_1\| = \|x_2\| \Longrightarrow \Phi(x_1) = \Phi(x_2), \forall x_1, x_2 \in \mathbb{R}^s.$$

In other words, the value of Φ at any point at a certain fixed distance from the origin (or any other fixed center point) is constant. Thus, Φ is radially (or spherically) symmetric about its center. The definition shows that the Euclidean distance function is just a special case of a radial (basis) function; namely, with $\phi(r) = r$.

Definition 3.2.2. *RBF approximations are usually finite linear combinations of the translation of a radially symmetric basis function. The set of RBFs ϕ_i, is as follows*

$$\phi_i : \mathbb{R}^d \longrightarrow \mathbb{R}, \phi_i(x) = \phi\left(\|x - x_i\|\right),$$

where $\|.\|$ denote the Euclidean norm and x_i is the center of the RBF.

3.2.3 RBF interpolation problem

This method was proposed by Edward Kansa in 1990 [66], a professor at the University of California. It was used for the first time for polynomial interpolation problems.The method makes it possible to achieve high-order accuracy with nodes dispersed on a totally irregular geometry, employing a particularly simple algorithm compared to the classical methods used until this moment. Before Kansa's successful research, Hardy ([51], [52]) used the multiquadric function to interpolate multidimensional data and fit two-dimensional geographic surfaces, showing that the multiquadric function has a physical foundation as a consistent solution to the biharmonic potential problem. Buhmann and Michelli [24] have shown that the MQ interpolation sheme converges faster as the spatial dimension increases, and converges exponentially as the density of the nodes increases. Buhmann and Michelli [25] and Chui et al [29] have shown that MQ and other RBFs were prewavelets. Kansa intervened to solve partial differentiall equations of elliptic, parabolic or even hyperbolic type [67]. This intervention which modified the multiquadric function was very succesful. Finaly, in 1990 Hon et al [54] have improved the MQ method for solving varieties of nonlinear boundary problems, the most common of which is the Burgers equation.

The scattered data approximation problem is as follows: Given a set of N distinct data points $X = (x_1, x_2, \ldots, x_N)$ in $\mathbb{R}^N$ and a corresponding set of N values $(y_1, y_2, \ldots, y_N)$ sampled from an unknown function f such that $y_i = f(x_i)$. We can then choose a radial function ϕ and a set of centers

$(x_{c_1}, x_{c_2}, \ldots, x_{c_N})$ for some $N \in \mathbb{N}$, to obtain a basis $(\phi(\|. - x_{c_1}\|), \phi(\|.- x_{c_2}\|), \ldots, \phi(\|. - x_{c_N}\|))$.

This basis can then be used to construct an approximation σ of the function f. One option is to center an RBF on each data site. In that case, the approximation will be constructed from N radial basis functions, and there will be one basis function with $x_c = x_i$ for each $i = 1, 2, \ldots, N$.

The approximation σ is then constructed from a linear combination of those N RBFs, such that

$$\sigma(x) = \sum_{i=1}^{N} c_i \phi(\|x - x_i\|), \tag{3.4}$$

with: $r_i = \|x - x_i\|$. Then,

$$\begin{bmatrix} \phi(r_1) & \phi(r_2) & \cdots & \phi(r_N) \\ \phi(r_1) & \phi(r_2) & \cdots & \phi(r_N) \\ \vdots & \vdots & \ddots & \vdots \\ \phi(r_1) & \phi(r_2) & \cdots & \phi(r_N) \end{bmatrix} \begin{bmatrix} c_1 \\ c_2 \\ \vdots \\ c_N \end{bmatrix} = \begin{bmatrix} f_1 \\ f_2 \\ \vdots \\ f_N \end{bmatrix}$$

such that, $c = [c_1, c_2, \ldots, c_N]$ and $y = [f_1, f_2, \ldots, f_N]$ .The constants c_i are determined by ensuring that the approximation will exactly match the given data at the data points. This is accomplished by enforcing $s(x_i) = y_i = f_i, i = 1, \ldots N$, which produces the system of linear equations

$$Ac = y$$

The solution of the system requires that the matrix A is non-singular. The situation is favorable if we know in advance that the matrix is positive definite. Moroever we would like to characterize the class of functions ϕ for which the matrix is positive definite.

Positive-definite matrices and functions

Definition 3.2.3. *[44] A real symmetric matrix A is called positive semi-definite if its associated quadratic form $c^T Ac \geq 0$, that is*

$$\sum_{i=1}^{N} \sum_{j=1}^{N} c_i c_j A_{i,j} \geq 0 \tag{3.5}$$

for all $c = [c_1, \cdots, c_N]^{\mathrm{T}} \in \mathbb{R}^N$. If the quadratic form (3.5) is zero only for $c = 0$ then A is called positive definite.

Hence, if in (3.4) the basis ϕ_i generates a positive definite interpolation matrix, then we would always have a well-defined interpolation problem. In order to get such property, we need to introduce the class of positive definite functions.

Definition 3.2.4. *[44] A continuous complex valued function $\phi : \mathbb{R}^s \to \mathbb{C}$ is called positive semidefinite if, for all $N \in \mathbb{N}$, all sets of pairwise distinct points $X = \{x_1, \ldots, x_N\} \subset \mathbb{R}^s$ and $c \in \mathbb{C}^N$ the quadratic form is nonnegative:*

$$\sum_{i=1}^{N} \sum_{j=1}^{N} c_i \overline{c_j} \phi(x_i - x_j) \geq 0.$$

The function ϕ is then called positive definite if the quadratic form above is positive for any $c \in \mathbb{C}^N, c \neq 0$.

One of the most celebrated results on positive definite functions is their characterization in terms of Fourier transforms established by Bochner in 1932.

Theorem 3.2.1. *(Bochner)[17] A (complex-valued) function $\Phi \in C(\mathbb{R}^s)$ is positive definite on $\mathbb{R}^s$ if and only if it is the Fourier transform of a finite non-negative Borel measure μ on $\mathbb{R}^s$, i.e.*

$$\Phi(x) = \frac{1}{\sqrt{(2\pi)^s}} \int_{\mathbb{R}^s} e^{-ixy} d\mu(y), x \in \mathbb{R}^s.$$

Completely monotone functions

Definition 3.2.5. *[44](p.47) A function $\phi : [0, \infty) \to \mathbb{R}$ that is $\mathcal{C}[0, \infty) \cap C^\infty(0, \infty)$ and satisfies*

$$(-1)^k \phi^{(k)}(r) \geq 0, \quad \text{for } r > 0, \text{ and } k = 0, 1, 2, \ldots$$

is called completely monotone.

Here we enumerate some of the most important positive definite functions showing that they are completely monotone.

- The function $\phi(r) = \epsilon, \epsilon \geq 0$ is completely monotone on $[0, \infty)$.
- The function $\phi(r) = e^{-\epsilon r}, \epsilon \geq 0$ is completely monotone on $[0, \infty)$ since

$$(-1)^k \phi^{(k)}(r) = \epsilon^k e^{-\epsilon r} \geq 0, k = 0, 1, 2, \ldots$$

- The function $\phi(r) = \frac{1}{(1+r)^\beta}, \beta \geq 0$ is completely monotone on $[0, \infty)$ since $(-1)^k \phi^{(k)}(r) = (-1)^{2k} \beta(\beta+1)\ldots(\beta+k-1)(1+r)^{-\beta-k} \geq 0, k = 0, 1, 2, \ldots$

Theorem 3.2.2. *(Hausdorff-Bernstein-Widder)[117](p.91) A function* $\Phi : [0, \infty) \to \mathbb{R}$ *is completely monotone on* $[0, \infty)$ *if and only if it is the Laplace transform of a nonnegative finite Borel measure* ν*, i.e. it is of the form*

$$\Phi(r) = \int_0^\infty e^{-rt} d\nu(t)$$

Theorem 3.2.3. *(Schoenberg)[117](p.93) A function* ϕ *is completely monotone on* $[0, \infty)$ *if and only if* $\Phi = \phi(\|.\|_2^2)$ *is positive semi-definite on* $\mathbb{R}^s$ *for all* s*.*

Multiply monotone functions

This characterization allows to check when a function is positive definite and radial on $\mathbb{R}^d$ for some fixed d.

Definition 3.2.6. *[44](p.49) A function* $\phi : (0, \infty) \to \mathbb{R}$ *which is* $\mathcal{C}^{s-2}(0, \infty), s \geq 2$ *and for which* $(-1)^k \phi^{(k)}(r) \geq 0$*, non-increasing and convex for* $k = 0, 1, \ldots, s-2$ *is called* s *times monotone on* $(0, \infty)$*. In case* $s = 1$ *we only require* $\phi \in \mathcal{C}(0, \infty)$ *to be non-negative and non-increasing.*

Characterizing positive definite functions using a more comprehensible approach based on the definition of completely monotone and multiply monotone functions can be found in ([23],[44],[117]).

Conditionally positive definite functions

Definition 3.2.7. *[117](p.97) A continuous function $\Phi : \mathbb{R}^s \longrightarrow \mathbb{C}$ is said to be conditionally positive semi-definite of order m in $\mathbb{R}^s$, if*

$$\sum_{i=1}^{N}\sum_{j=1}^{N} c_i\overline{c_j}\phi\left(x_i - x_j\right) > 0, \tag{3.6}$$

for any set $X = \{x_1, \ldots, x_N\} \subset \mathbb{R}^s$ of N pairwise distinct points, and $c = (c_1, \ldots, c_N)^{\mathrm{T}} \subset \mathbb{C}^N$ such that

$$\sum_{k=1}^{N} c_k p\left(x_k\right) = 0,$$

for any complex-valued polynomial p of degree $\leq m-1$. The function Φ is then called conditionally positive definite of order m on $\mathbb{R}^s$ if the quadratic form (3.6) vanishes only when $c \equiv 0$.

The first important fact concerning conditionally positive (semi)-definite functions is their order. To this aim, the following important results hold.

- A function which is conditionally positive (semi)-definite of order m is also conditionally positive (semi)-definite of any order $s \geq m$.
- A function that is conditionally positive (semi)-definite of order m in $\mathbb{R}^s$ is also conditionally positive (semi)-definite of order m on $\mathbb{R}^k$ with $k \leq s$.

Theorem 3.2.4. *[117](p.99) Suppose Φ is conditionally positive definite of order 1 and that $\Phi(0) \leq 0$. Then the matrix $A \in \mathbb{R}^{N\times N}$, i.e. $A_{i,j} = \Phi\left(x_i - x_j\right)$, has one negative and $N-1$ positive eigenvalues. In particular it is invertible.*

The most used positive definite RBFs and conditionally positive definite RBFs are given in tables 3.3 and 3.4 respectively. The representations of multiquadric, gaussian, inverse multiquadric, inverse quadric and polyharmonic splines RBFs are given in figures 3.2.1 and 3.2.2.

Name	$\phi(r)$
Inverse Multiquadric (IMQ)	$\phi(r) = \frac{1}{\sqrt{r^2+\epsilon^2}}$
Gaussian Function (GS)	$\phi(r) = e^{-\epsilon r^2}$

Table 3.3 : Positive definite radial basis functions.

Name	$\phi(r)$	Order
Multiquadric (MQ)	$\phi(r) = (r^2+\epsilon^2)^k, k > 0, k \notin \mathbb{N}$	$\lceil k \rceil + 1$
Inverse Multiquadric (IMQ)	$\phi(r) = (r^2+\epsilon^2)^{-k}, k > 0, k \notin \mathbb{N}$	0
Polyharmonic spline	$\phi(r) = r^{2k-1}, k \in \mathbb{N}$	$\lceil k/2 \rceil + 1$
Polyharmonic spline	$\phi(r) = r^{2k}\ln(r), k \in \mathbb{N}$	$\lceil k/2 \rceil + 1$
Thin Plate Spline (TPS)	$\phi(r) = r^2\ln(r)$	2

Table 3.4 : Conditionally positive definite radial basis functions, where $\lceil k \rceil$ denotes the nearest integers less than or equal to k, and $\mathbb{N}$ the natural numbers, ϵ a positive constant which is known as the shape parameter .

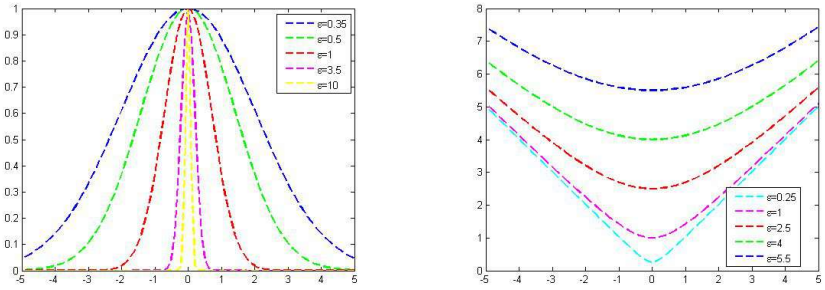

Figure 3.2.1: Graph of gaussian RBF (left), multiquadric RBF (right), for a center $x = 0$, with different values of shape parameter.

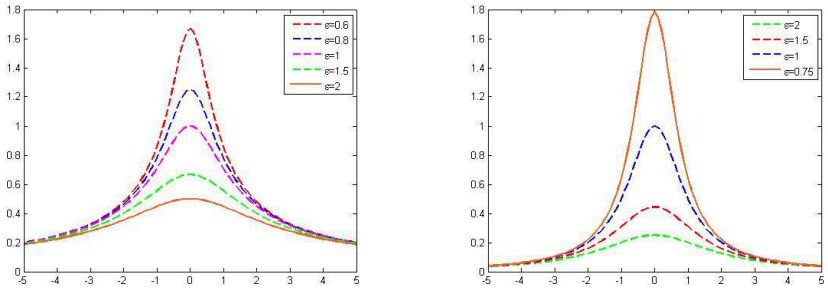

Figure 3.2.2: Graph of inverse multiquadric RBF (left), inverse quadric RBF (right), for a center $x = 0$, with different values of shape parameter.

3.3 Compactly supported radial basis functions

Here we introduce the concept of compactly supported radial basis functions CSRBFs. Then we explain a popular family of them that we will use in the following chapter through some applications.

After successful studies and tests for the result of partial differential equations, such as the resolution of hydrodynamic equations by Hon et al [55], the numerical results demonstrated that the MQ diagrams are more assuring than the finite element method. However, the MQ method requires solving a linear system with a full matrix, which could make the method cumbersome and very expensive once you have to do hundreds of collocation points. To overcome this problem, researchers have developed a sheme based on radial basis functions with compact support (CSRBFs). The compactly supported radial basis functions can cover the global schemes that the simple RBF methods are weak to solve as in the case of the badly conditioned matrices [55],[56].

The accuracy of the RBFs method depends on the value of the shape parameter which is still an unsolved problem, also the resulting interpolation matrix is dense and highly ill conditioned. So it was suggested the use of compactly supported radial basis functions which can reduce the resultant full matrix to a sparse one, also the operation of the banded matrix system could reduce the ill-conditioning of the resultant coefficient matrix when using the global radial basis functions [56].

We need the following theorem to justify the need for Compactly Supported Radial Basis Functions **CSRBFs**.

Theorem 3.3.1. *[44] (P.35) There are no oscillatory univariate continuous functions that are strictly positive definite and radial on $\mathbb{R}^s$ for all s. Moreover, there are no compactly supported univariate continuous functions that are strictly positive definite and radial on $\mathbb{R}^s$ for all s.*

Theorem 3.3.2. *[44] (P.75) Assume that the complex-valued function $\Phi \in C(\mathbb{R}^s)$ has compact support. If Φ is strictly conditionally positive definite of (minimal) order m, then m is necessarily zero, i.e., Φ is already strictly positive definite.*

As we see in the last theorem (3.3.2), compactly supported functions Φ that are truly strictly conditionally positive definite of order $m > 0$ do not exist. The compact support automatically ensures that Φ is strictly positive definite. An observation from the theorem (3.3.1) is that compactly supported radial functions can be strictly positive definite on $\mathbb{R}^s$ only for a fixed maximal s-value. It is not possible for a function to be strictly positive definite and radial on $\mathbb{R}^s$ for all s and also have a compact support.

According to Bochner's work [17], a function is strictly positive definite and radial on $\mathbb{R}^s$ if its s-variate Fourier transform is non-negative.

The Bessel function $\mathcal{J}$ of the first kind of order $v \in \mathbb{C}$ can be expressed as follow

$$J_\nu := \sum_{k=0}^{\infty} \frac{(-1)^k (z/2)^{2k+v}}{k!\Gamma(k+v+1)}, \text{ for } z \in \mathbb{C}\backslash\{0\}.$$

such that the Γ-function is given as follow

$$\Gamma(z) := \lim_{n \longrightarrow \infty} \frac{n! n^z}{z(z+1)\dots(z+n)}, \text{ for } z \in \mathbb{C}.$$

Theorem 3.3.1. *[117](p.119) Suppose $\Phi \in L^1(\mathbb{R}^s) \cap C(\mathbb{R}^s)$ is radial, i.e. $\Phi = \phi(\|.\|_2), x \in \mathbb{R}^s$. Then its Fourier transform $\widehat{\Phi}$ is also radial, i.e. $\widehat{\Phi} = \mathcal{F}_s(\|.\|_2)$ with*

$$\widehat{\Phi}(x) = \mathcal{F}_s \phi(r) = r^{-(s-2)/2} \int_0^\infty \phi(t) t^{s/2} \mathcal{J}_{(s-2)/2}(rt) dt.$$

3.3.1 Operators for Radial Functions and Dimension Walks

Schaback and Wu [101] defined an integral operator and its inverse differential operator, and discussed an entire calculus for how these operators act on radial functions. These operators will facilitate the construction of compactly supported radial functions.

Definition 3.3.3. *[117](p.121) Let ϕ be given such that $t \to t\phi(t) \in L^1[0,\infty)$, then we define*

$$(\mathcal{I}\phi)(r) = \int_r^{+\infty} t\phi(t)dt, r \geq 0$$

For even $\phi \in C^2(\mathbb{R})$ we define

$$(\mathcal{D}\phi)(r) = -\frac{1}{r}\phi'(r), r \geq 0.$$

In both cases the resulting functions are to be interpreted as even functions using even extension.

Theorem 3.3.2. *[117](p.121-122)*

1. *Both $\mathcal{D}$ and $\mathcal{I}$ preserve compact support, i.e., if ϕ has compact support, then so do $\mathcal{D}\phi$ and $\mathcal{I}\phi$.*

2. *If $\phi \in C(\mathbb{R})$ and $t \to \phi(t) \in L^1[0,\infty)$, then $\mathcal{D}\mathcal{I}\phi = \phi$.*

3. *If $\phi \in C^2(\mathbb{R})$ and $\phi' \in L^1[0,\infty)$, then $\mathcal{I}\mathcal{D}\phi = \phi$.*

4. *If $t \to t^{s-1}\phi(t) \in L^1[0,\infty)$ and $s \geq 3$, then $\mathcal{F}_s(\phi) = \mathcal{F}_{s-2}(\mathcal{I}\phi)$.*

5. *If $\phi \in C^2(\mathbb{R})$ is even and $t \to t^s\phi'(t) \in L^1[0,\infty)$, then $\mathcal{F}_s\phi = \mathcal{F}_{s+2}(\mathcal{D}\phi)$.*

The operators $\mathcal{I}$ and $\mathcal{D}$ allow us to express s-variate Fourier transforms as $(s-2)$ or $(s+2)$-variate Fourier transforms, respectively.

3.3.2 Wendland's Compactly Supported Functions

In [117] Wendland constructed a popular family of compactly supported radial functions by starting with the truncated power function which we know to be strictly positive definite and radial on $\mathbb{R}^s$ for $s \leq 2l-1$, and then walking through dimensions by repeatedly applying the operator $\mathcal{I}$.

Definition 3.3.4. *[117](p.128) With $\phi_l(r) = (1-r)_+^l$ we define*

$$\phi_{s,k} = \mathcal{I}^k \phi_{\lfloor s/2 \rfloor + k + 1}.$$

It turns out that the functions $\phi_{s,k}$ are all supported on $[0,1]$ and have a polynomial representation there.

Theorem 3.3.3. *[117](p.128) The functions $\phi_{s,k}$ are strictly positive definite and radial on $\mathbb{R}^s$ and are of the form*

$$\phi_{s,k}(r) = \begin{cases} p_{s,k}(r), & \text{if } r \in [0,1] \\ 0, & \text{if } r > 1 \end{cases}$$

with a univariate polynomial $p_{s,k}$ of degree $\lfloor s/2 \rfloor + 3k + 1$. Moreover, $\phi_{s,k} \in C^{2k}(\mathbb{R})$ are unique up to a constant factor, and the polynomial degree is minimal for given space dimension s and smoothness $2k$.

Wendland gave recursive formulas for the functions $\phi_{s,k}$ for all s, k. The abbreviation SPD means striclty positive definite.

Example 3.3.5. *Wendland's compactly supported functions $\phi_{s,k}$, for $k = 0,1,2,3$, are written in the following form*

- $\phi_{s,0}(r) = (1-r)_+^{\lfloor s/2 \rfloor + 1}$
- $\phi_{s,1}(r) \doteq (1-r)_+^{l+1}[(l+1)r + 1]$
- $\phi_{s,2}(r) \doteq (1-r)_+^{l+2}\left[(l^2+4l+3)\,r^2 + (3l+6)r + 3\right]$
- $\phi_{s,3}(r) \doteq (1-r)_+^{l+3}\left[(l^3+9l^2+23l+15)\,r^3 + (6l^2+36l+45)\,r^2 + (15l+45)r + 15\right]$,

where $l := \lfloor s/2 \rfloor + k + 1$, *and the symbol* $\doteq$ *denotes equality up to a multiplicative positive constant.*

Example 3.3.6. *For* $s = 3$ *we get some of the most commonly used functions as*

- $\phi_{3,0}(r) = (1-r)_+^3 \in C^0 \cap SPD(\mathbb{R}^3)$
- $\phi_{3,1}(r) \doteq (1-r)_+^4 [4r+1] \in C^2 \cap SPD(\mathbb{R}^3)$
- $\phi_{3,2}(r) \doteq (1-r)_+^6 [35r^2 + 18r + 3] \in C^4 \cap SPD(\mathbb{R}^3)$
- $\phi_{3,3}(r) \doteq (1-r)_+^8 [32r^3 + (6l^2 + 36l + 45) r^2 + (15l + 45)r + 15] \in C^6 \cap SPD(\mathbb{R}^3)$.

Graph (3.3.3) shows three of Wendland's Compactly Supported Functions.

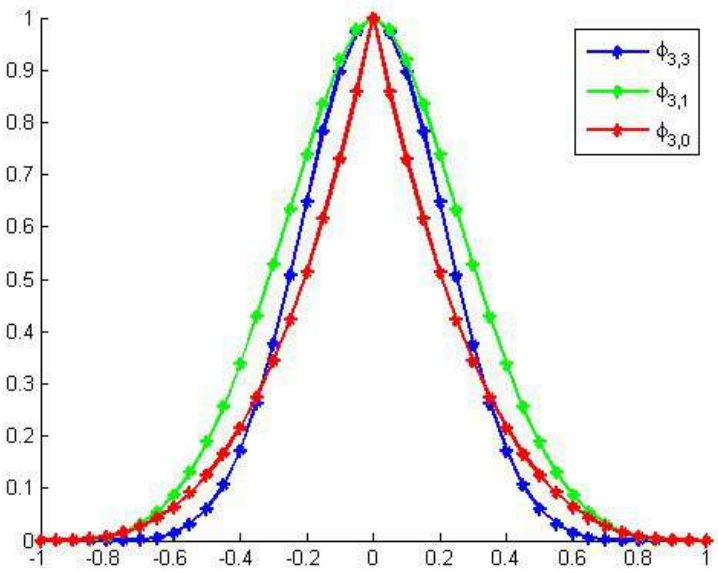

Figure 3.3.3: Graph of Wendland's CSRBFs for $s = 3$.

Furthermore, in the cited references ([118] and [22]), one can explore additional families of Compactly Supported Radial Basis Functions, that

were suggested by Wu and Buhmann, expanding the understanding of this class of functions beyond the context discussed earlier.

Chapter 4

Numerical solution of Integral equations by RBF's

4.1 Introduction

A considerable large amount of research literature and books on the theory and applications of Volterra's integral equations have emerged over many decades since the apparition of Volterra's book "Leçons sur les équations intégrales et intégro-différentielles" [110] in 1913.

The applications include elasticity, plasticity, semi-conductors, scattering theory, seismology, heat and mass conduction or transfer, metallurgy, fluid flow dynamics, chemical reactions, population dynamics, and oscillation theory, among many others (see for example [31]). Other important references more related with the numerics of this type of equation are [11, 26].

In fact, Volterra integral equations (VIEs) appear naturally when we try to transform an initial value problem into integral form, so that the solution of this integral equation is usually much easier to obtain than the original initial value problem. In the same way, some nonlinear Volterra integral equations are equivalent to an initial-value problem for a system of ordinary differential equations (ODEs). So, some authors (like for example [103]) have sought to exploit this connection for the numerical solution of the integral equations as well, since very effective ODE codes are widely available.

Volterra integral equations arise in many usual applications of technology, engineering and science in general: as in population dynamics, the spread of epidemics, some Dirichlet problems in potential theory, electrostatics, mathe-

matical modeling of radioactive equilibrium, the particle transport problems of astrophysics and reactor theory, radiative energy and/or heat transfer problems, other general heat transfer problems, oscillation of strings and membranes, the problem of momentum representation in quantum mechanics, etc. However, many other complex problems of mathematics, chemistry, biology, astrophysics and mechanics, can be expressed in the terms of Volterra integral equations. Moreover, some practical problems, where impulses arise naturally (like in population dynamics or many biological applications) are caused by some control system (like electric circuit problems and simulations of semiconductor devices) can be modeled by a differential equation, an integral equation, an integro-differential equation, or a system of these equations all combined.

The systems of integral and/or integro-differential equations are usually difficult to solve analytically, in particular systems of Volterra integral nonlinear equations or with variable coefficients; so a numerical method is often needed. In such cases, it is required to approximate the solutions; and many different numerical techniques have been developed and presented during decades of research, with appropriate combinations of numerical integration and interpolation procedures (see the references [11, 20], among others).

In order to approximate numerically the solution of general integral equations, the predominant technique have been the use of some kind of piecewise constant basis functions (PCBFs) (see for example [21], among many others); Chebyshev polynomial ([40] and others). However, after a long period of time many other techniques have attracted much attention recently; like wavelets theory, started with the introduction of Haar function in 1910, and from 1990's (see [33]) also many wavelet type methods have been applied for solving integral equations. Haar wavelets, despite its relative simplicity, have many valued properties: as its compact support and orthogonality properties. So they can be used for the solution of differential and integro-differential equations related with signal and image processing, for example. They have been also used to solve linear and nonlinear integral equations by Aziz et. al. [9], Babolian et. al. [10], Lepik [77], Maleknejad et al. [82], Farshid Mirzaae [85], among others. More recently, several numerical methods based on different triangular type and delta orthogonal functions were designed for approximating the solution of integral and/or integro-differential Volterra equations (see for example [87, 34, 95], and the references therein). All these publications have demonstrated and revealed that these techniques based on PCBF and wavelets are effective to obtain the solution of such integral equations.

Particularly, systems of linear integral equations, and their exact or approximate solutions, are of great importance in science and engineering.

There are several numerical methods for solving systems of linear Volterra integral equations of the second kind, and they have been often solved by classical numerical and analytical methods: such as Galerkin and Finite Element methods, collocation and spectral methods, Taylor or Power series and expansion methods, transforming the equations into a linear or nonlinear system of algebraic equations, and so on. However, new methods also have been applied to solve them, like the homotopy perturbation method [46], Adomian decomposition method (and many others) [112], use of Legendre wavelets [120] or hybrid Legendre and block pulse functions [81], Chebyshev polynomials [39, 121], etc. Berenguer et al. [13, 14] have solved them with the aid of a combination of analytical methods and bi-orthogonal systems in Banach spaces, Sahn et al. [32] have used Bessel polynomials method, Malnekad et al. [87] have employed delta basis functions (DBFs), Balakumar et al. [12] have applied the block-pulse functions method, Li-Hong et al. [119] have applied reproducing kernel method. Furthermore, there are also expansion methods for integral equations such as El-gendi's and Wolfe's methods (see for example [35]). Additionally, the approximate solutions of systems of integral equations that usually appear in problems of physics, biology and engineering are based on numerical integration methods: such as Euler–Chebyshev or Runge–Kutta methods (see for example [109]).

Concerning many other possible techniques to solve these types of integral equations, Draidi and Qatanani [37] implemented a product Nystrom and sinc-collocation methods to solve Volterra integral equations with Carleman kernel; also Issa, Qatanani and Daraghmeh [61] used a Taylor expansion and the variational iteration methods to give an approximate solution of Volterra integral equations of the second kind. Aggarwal et al. [1] and Chauhan [27] used different integral transformations for obtaining the solutions of VIEs of second kind. Mahgoub [86] solved constant coefficient linear differential equations by defining the called Sawi transformation, but many other authors exploited this idea, or other appropriate transforms, to deal with these types of integral or integro-differential equations.

Next, we are going to cite the most recent references from the last 3 or 4 years. In [60] the authors present an approximation solution of system of Volterra integral equations of second kind in an analytical way, using an Adomian decomposition method in Mathematica. In [57] the authors propose a numerical algorithm based on Monte Carlo method for approximating solutions of the system of Volterra integral equations. In [69] the authors develop a numerical technique for the solution of 2D Volterra integral equations based on a discretization method by using two-dimensional Bernstein's approximations. In [2] the authors discussed the solution of linear Volterra integral equations of second kind using Mohand transform. In [90] the authors pro-

pose Bernstein polynomials to present effective solution for the second kind linear Volterra integral equations with delay. In [68] the author presents a method to solve numerically Volterra integral equations of the first kind with separable kernels.

In this chapter, we explore some practical applications of radial basis functions. The initial section introduces the fundamental concept of integral equations, followed by a comprehensive classification based on linearity, homogeneity, and the integration domain. Subsequently, we provide a numerical solution to systems of linear Volterra integral equations, employing radial basis functions of Wendland's type. The ensuing section addresses the numerical approximation of a solution to a linear Volterra integro-differential problem, utilizing compactly supported radial basis functions of Wendland's type. It is noteworthy that the outcomes presented in these sections have been disseminated through published articles.

4.2 Integral equations

In this section, we explore the concept of integral equations. We'll look at how these equations can be classified based on linearity, homogeneity and the integration domain.

Definition 4.2.1. *[107] An integral equation is one in which function to be determined appears under the integral sign. The most general form of an integral equation is*

$$h(t)x(t) = f(t) + \int_a^{b(t)} K(t, s, x(s))ds$$

*for all $t \in [a, b]$ in which, $x(t)$ is the function to be determined, $K(t, s)$ is known and is called the **Kernel** of the integral equation and $h(t), f(t)$ and $b(t)$ are known functions.*

There are different classification methods for integral equations [107]:

- Based on **linearity**, one can divide integral equations into:

    1. **linear** integral equations if the unknown function $x(t)$ and its integrals appear in linear form. For example

$$x(t) = f(t) + \int_a^{b(t)} K(t, s)x(s)ds.$$

2. **nonlinear** integral equations if $x(t)$ or any of its integrals appear nonlinearly in the equation. For example

$$x(t) = f(t) + \int_a^{b)} K(t,s)cos(x(s))ds.$$

- Based on **homogeneity**, integral equations can be classified into:

1. homogenous if the known function $f(t)$ is identically zero. For example

$$x(t) = \int_a^{b(t)} K(t,s)x(s)ds.$$

2. inhomogenous if the known function $f(t)$ is nonzero.

- In classifying integral equations we say, very roughly, that those integral equations in which the integration domain varies with the independent variable in the equation are **Volterra** integral equations; and those in which the integration domain is fixed are **Fredholm** integral equations.

Definition 4.2.2. *[6] A **Fredholm** integral equation is one of the form:*

$$h(t)x(t) = f(t) + \int_a^b K(t,s,x(s))ds$$

for all $t \in [a,b]$.

That is, $b(t) = b$ *in this case, or we can say that in Fredholm integral equation both lower and upper limits are constant.*

Definition 4.2.3. *[6] A **Volterra** integral equation is one of the form:*

$$h(t)x(t) = f(t) + \int_a^t K(t,s,x(s))ds \tag{4.1}$$

for all $t \in [a,b]$.

That is, in Volterra equation $b(t) = t$.

Integral equations can be thought of as generalizations of

$$x'(t) = f(t,x(t)), t \geq a, x(a) = x_0$$

an initial value problem for ordinary differential equations. This equation is equivalent to the integral equation

$$x(t) = x_0 + \int_a^t f(s, x(s))ds, t \geq a$$

which is a special case of (4.1).

A **linear Volterra** integral equation is one of the form:

$$h(t)x(t) = f(t) + \int_a^t K(t, s)x(s)ds$$

for all $t \in [a, b]$.

There are two kinds of a linear Volterra integral equation [6]:

1. If $h(t) = 0$, the above equation reduces to

$$-f(t) = \int_a^t K(t, s)x(s)ds$$

This equation is called Volterra integral equation of **first kind.**

2. If $h(t) = 1$, the above equation reduces to

$$x(t) = f(t) + \int_a^t K(t, s)x(s)ds$$

This equation is called Volterra integral equation of **second kind.**

4.3 Numerical Solution of LVIES's of Second Kind by RBFs

Volterra integral equations find applications across various fields including technology, engineering, and science such as population dynamics, epidemics spread, electrostatics, chemistry, biology, and astrophysics. They are also used in mathematical modeling of radioactive equilibrium, particle transport problems in astrophysics and reactor theory, and radiative energy/heat transfer problems. Additionally, they are applicable in electric circuit problems, simulations of semiconductor devices, oscillation of strings and membranes, momentum representation in quantum mechanics, and certain Dirichlet problems in potential theory. (See, for example, [104], [78], and [110].)

In this section, we present specific variational methods used to study and approximate systems of linear Volterra integral equations with Radial Basis Functions (RBFs) of Wendland type. Wendland functions, being compactly supported radial basis functions, simplify calculations. However, determining the actual functions for software implementation often requires extensive manual or symbolic calculations (refer, for instance, to [16]). Despite the availability of just a few articles on these techniques (such as [4], [43], [83], [111], and [122]), we believe there is ample scope for further investigation in this area.

Our goal in this section is to devise an appropriate approach procedure that is capable of solving this type of problem in a precise and efficient way. We consider then the linear Volterra equations system of the second kind as follows (see for example [110]):

$$\boldsymbol{x}(t) = \boldsymbol{f}(t) + \int_0^t \boldsymbol{k}(t,s)\boldsymbol{x}(s)ds, \quad 0 \leq s \leq t \leq 1, \tag{4.2}$$

where

$$\begin{aligned} \boldsymbol{x}(t) &= (x_1(t), \ldots, x_n(t))^\top, \\ \boldsymbol{f}(t) &= (f_1(t), \ldots, f_n(t))^\top, \\ \boldsymbol{k}(t,s) &= (k_{ij}(t,s))_{1\leq i,j\leq n}. \end{aligned}$$

We assume that (4.2) has a unique continuous solution for appropriate functions f. In any case, the equations system (4.2) can be re-written in operator form as an equation of second kind

$$\boldsymbol{f} = (I - K)\boldsymbol{x},$$

where K is an integral operator and I denotes the identity operator. It is usual to impose certain assumptions on compactness on the operator K (see [7], Section 2.8.1) in order to establish the existence and uniqueness of the solution of (4.2), that we will assume throughout this chapter.

Moreover, in [75] the authors proposed another method to solve second kind Fredholm integral equation systems, but the discrete functional space chosen in that article has been the space of spline functions. While at first glance it might seem that both works are similar, especially in the way they are presented, the two methods are totally different, not only be the fact that the discretization spaces are different (so we have adapted the notations accordingly), while the proofs (except the very preliminary ones, that can be also adapted), of the convergence results, are completely different, due to their greater complexity.

4.3.1 Discretization Space

For the remainder of the chapter, we are going to consider a space of finite dimension, where we will formulate and solve a discrete approximation problem. The discrete functional space we have chosen is the radial basis functions space with compact support, namely the radial basis function space generated by the Wendland functions (see [115]).

Definition 4.3.1. *Given a continuous function $\phi : \mathbb{R}_0^+ \to \mathbb{R}$, a subset $\Omega \subset \mathbb{R}^d$, $d \geq 1$, and a point $\boldsymbol{\xi} \in \Omega$, the radial function defined on Ω from the function ϕ with center $\boldsymbol{\xi}$ is the continuous function $\boldsymbol{\Phi}_{\boldsymbol{\xi}} : \Omega \to R$ given by*

$$\boldsymbol{\Phi}_{\boldsymbol{\xi}}(\boldsymbol{x}) = \phi(\langle \boldsymbol{x} - \boldsymbol{\xi} \rangle_d).$$

Then $\boldsymbol{\Phi}_{\boldsymbol{\xi}}$ only depends of the distance to $\boldsymbol{\xi}$.

Definition 4.3.2. *Given a centers set $\Xi = \{\boldsymbol{\xi}_1, \ldots, \boldsymbol{\xi}_N\}$ the linear space generated by the functions*

$$\{\phi(\langle \cdot - \boldsymbol{\xi}_1 \rangle_d), \ldots, \phi(\langle \cdot - \boldsymbol{\xi}_N \rangle_d)\}$$

is called a radial basis functions space.

Definition 4.3.3. *For a function $\boldsymbol{u} \in C([0,1]; \mathbb{R}^n)$, the radial basis function interpolating $\boldsymbol{u}$ on a set of distinct centers $\boldsymbol{T}_N = \{t_1, \ldots, t_N\} \subset [0,1]$ is given by*

$$\boldsymbol{s}_{\boldsymbol{u},\boldsymbol{T}_N}(t) = \sum_{i=1}^{N} \boldsymbol{\alpha}_i \phi(|t - t_i|), \quad t \in [0,1],$$

where $\phi : \mathbb{R}_0^+ \to \mathbb{R}$ is a continuous function and the coefficients $\boldsymbol{\alpha}_1, \ldots, \boldsymbol{\alpha}_N \in \mathbb{R}^n$ are determined by the interpolation conditions

$$\boldsymbol{s}_{\boldsymbol{u},\boldsymbol{T}_N}(t_i) = \boldsymbol{u}(t_i), \quad 1 \leq i \leq N.$$

In his work [115], H. Wendland introduced a family of compactly supported radial basis functions, as detailed in Section 3.3.

For the remainder of this section we suppose $0 \leq k \leq N-1$, and we take $\phi = \phi_{1,k}$ in Definition 4.3.3.

Table 4.1 shows the Wendland functions $\phi_{1,k}$ for $k = 0, 1, 2$, and its continuity order.

Table 4.1 : Wendland functions $\phi_{1,k}$ for $k = 0, 1, 2$ and its continuity order.

k	**Wendland function**	**Continuity order**
$k=0$	$\phi_{1,0}(r) = (1-r)_+$	C^0
$k=1$	$\phi_{1,1}(r) \doteq (1-r)_+^3(3r+1)$	C^2
$k=2$	$\phi_{1,2}(r) \doteq (1-r)_+^5(8r^2+5r+1)$	C^4

Let

$$h = \sup_{t\in[0,1]} \min_{1\leq i\leq N} |t - t_i|. \tag{4.3}$$

From ([115], Theorem 2.1) we can affirm that $\phi_{1,k} \in C^{2k}([0,1])$ and the corresponding native space is $H^{k+1}([0,1])$. Finally, from ([115], Theorem 2.1) and ([116], Theorem 4.1) we conclude that there exists $C > 0$ such that

$$\|\boldsymbol{u} - \boldsymbol{s}_{\boldsymbol{u},\boldsymbol{T}_N}\|_{L_\infty((0,1);\mathbb{R}^n)} \leq C\|\boldsymbol{u}\|_{k+1} h^{k+\frac{1}{2}}, \quad \forall\, \boldsymbol{u} \in H^{k+1}([0,1];\mathbb{R}^n),$$

and

$$|\boldsymbol{u} - \boldsymbol{s}_{\boldsymbol{u},\boldsymbol{T}_N}|_j \leq Ch^{k+1-j}\|\boldsymbol{u}\|_{k+1}, \quad 0 \leq j \leq k+1, \quad \forall\, \boldsymbol{u} \in H^{k+1}([0,1];\mathbb{R}^n). \tag{4.4}$$

Let S_N be the space of the restrictions of functions on $[0,1]$ of the functional space generated by the radial basis functions $\{\phi_{1,k}(|\cdot - t_1|), \ldots, \phi_{1,k}(|\cdot - t_N|)\}$ and $\boldsymbol{S}_N = (S_N)^n$. Then $\boldsymbol{S}_N \subset H^{k+1}((0,1);\mathbb{R}^n) \cap C^{2k}([0,1];\mathbb{R}^n)$.

4.3.2 Formulation of the Problem

We can define the operator $\rho:\ H^{k+1}((0,1);\mathbb{R}^n) \to \mathbb{R}^{N,n}$ given by

$$\rho\boldsymbol{v} = ((I-K)\boldsymbol{v}(t_i))_{1\leq i\leq N}.$$

Let assume that $\boldsymbol{f} \in H^{k+1}((0,1);\mathbb{R}^n)$, and consider the affine variety $\boldsymbol{H}_N = \{\boldsymbol{u} \in \boldsymbol{S}_N :\ \rho\boldsymbol{u} = (\boldsymbol{f}(t_i))_{1\leq i\leq N}\}$ and the linear subspace $\boldsymbol{H}_N^0 = \{\boldsymbol{u} \in \boldsymbol{S}_N :\ \rho\boldsymbol{u} = \boldsymbol{0} \in \mathbb{R}^{N,n}\}$.

Proposition 4.3.4. *The set $\boldsymbol{H}_N$ is a nonempty closed bounded convex subset of $\boldsymbol{S}_N$. Moreover it is an affine variety associated with the linear subspace $\boldsymbol{H}_N^0$.*

Proof. By adapting the notations, as in the proof of Proposition 4.1 of [75]. □

Lemma 4.3.5. *The application $\ll \cdot, \cdot \gg$: $H^{k+1}((0,1);\mathbb{R}^n)\times H^{k+1}((0,1);\mathbb{R}^n) \to \mathbb{R}$ defined by*

$$\ll \boldsymbol{u}, \boldsymbol{v} \gg = \langle \rho\boldsymbol{u}, \rho\boldsymbol{v}\rangle_{N,n} + ((I-K)\boldsymbol{u}, (I-K)\boldsymbol{v})_{k+1}$$

is an inner product on $H^{k+1}((0,1);\mathbb{R}^n)$ and its associated norm, given by $[[\boldsymbol{u}]] = \ll \boldsymbol{u}, \boldsymbol{u} \gg^{\frac{1}{2}}$, is equivalent to the usual Sobolev norm $\| \cdot \|_{k+1}$.

Proof. By adapting the notations as in the proof of Lemma 4.2 of [75] and using ([7], Theorem 7.3.12) the proof can be obtained. □

Definition 4.3.6. *We say that $\boldsymbol{u}_N \in \boldsymbol{H}_N$ is an approximating radial basis function relative to $\boldsymbol{T}_N$, ρ and $\boldsymbol{f}$ if $\boldsymbol{u}_N$ is a solution of the following minimization problem:*

$$\text{Find } \boldsymbol{u}_N \in \boldsymbol{H}_N \text{ such that } \forall\, \boldsymbol{v} \in \boldsymbol{H}_N, \quad J(\boldsymbol{u}_N) \leq J(\boldsymbol{v}), \tag{4.5}$$

where $J : H^{k+1}((0,1);\mathbb{R}^n) \to \mathbb{R}$ is given by

$$J(\boldsymbol{v}) = |(I-K)\boldsymbol{v}|_{k+1}^2.$$

Theorem 4.3.1. *Problem (4.5) has a unique solution $\boldsymbol{u}_N \in \boldsymbol{H}_N$ which is the unique solution of the variational problem*

$$\forall\, \boldsymbol{v} \in \boldsymbol{H}_N^0, \quad ((I-K)\boldsymbol{u}_N, (I-K)\boldsymbol{v})_{k+1} = 0. \tag{4.6}$$

Proof. From Proposition 4.3.4 and ([7], Theorem 3.4.3) we can deduce that there exists a unique $\boldsymbol{u}_N \in \boldsymbol{H}_N$, which is the projection of $\mathbf{0}$ on $\boldsymbol{H}_N$ such that

$$[[\boldsymbol{u}_N]] \leq [[\boldsymbol{v}]],\ \forall\, \boldsymbol{v} \in \boldsymbol{H}_N$$

and verifying

$$\forall\, \boldsymbol{w} \in \boldsymbol{H}_N, \quad \ll -\boldsymbol{u}_N, \boldsymbol{w} - \boldsymbol{u}_N \gg \leq 0,$$

that is

$$\forall \boldsymbol{v} \in \boldsymbol{H}_N^0, \quad \ll -\boldsymbol{u}_N, \boldsymbol{v} \gg \leq 0$$

and, taking into account that $\boldsymbol{H}_N^0$ is a vector space, we obtain that

$$\forall \boldsymbol{v} \in \boldsymbol{H}_N^0, \quad \ll \boldsymbol{u}_N, \boldsymbol{v} \gg = 0.$$

Therefore (4.6) holds. Finally, $\boldsymbol{u}_N$ is the unique solution of (4.5) since $J(\boldsymbol{v}) = [[\boldsymbol{v}]]^2 - \langle \rho \boldsymbol{f} \rangle_{N,n}^2$, for any $\boldsymbol{v} \in \boldsymbol{H}_N$. □

Theorem 4.3.2. *There exists a unique $\lambda \in \mathbb{R}^{N,n}$ such that*

$$\forall\, \boldsymbol{v} \in \boldsymbol{S}_N, \quad ((I-K)\boldsymbol{u}_N, (I-K)\boldsymbol{v})_{k+1} + \langle \lambda, \rho \boldsymbol{v} \rangle_{N,n} = 0, \tag{4.7}$$

where $\boldsymbol{u}_N$ is the unique solution of (4.6).

Proof. For $i = 1, \ldots, N$, let us consider $\varphi_i \in S_N$ the unique radial basis function determined by the interpolation conditions

$$\varphi_i(t_j) = \delta_{ij},\ \forall\, j = 1, \ldots N.$$

Let take $\boldsymbol{v} \in \boldsymbol{S}_N$, and we consider the function

$$\boldsymbol{w} = \boldsymbol{v} - \sum_{i=1}^{N} (I-K)\boldsymbol{v}(t_i)\varphi_i,$$

then

$$(I-K)\boldsymbol{w}(t_j) = (I-k)\boldsymbol{v}(t_j) - \sum_{i=1}^{N} (I-K)\boldsymbol{v}(t_i)\varphi_i(t_j) = 0,\ \forall\, j = 1, \ldots, N;$$

that is $\rho\boldsymbol{w} = \mathbf{0} \in \mathbb{R}^{N,n}$, and in fact $\boldsymbol{w} \in \boldsymbol{H}_N^0$. Thus, from Theorem 4.3.1, we have

$$((I-K)\boldsymbol{u}_N, (I-K)\boldsymbol{w})_{k+1} = 0. \tag{4.8}$$

We notice $\Pi_\ell : \mathbb{R}^n \to \mathbb{R}$, for $\ell = 1, \ldots, n$, the projection application given by $\Pi_\ell(x_1, \ldots, x_n) = x_\ell$.

Then, for $i = 1, \ldots, N$, it is verified that

$$\begin{aligned}((I-K)\boldsymbol{u}_N, (I-K)\boldsymbol{v}(t_i)\varphi_i)_{k+1} &= \sum_{\ell=1}^{n} (\Pi_\ell((I-K)\boldsymbol{u}_N, \Pi_\ell((I-K)\boldsymbol{v}(t_i)\varphi_i))_{k+1} \\ &= \sum_{\ell=1}^{n} \Pi_\ell((I-K)\boldsymbol{v}(t_i)) \left(\Pi_\ell((I-K)\boldsymbol{u}_N, \varphi_i\right)_{k+1}.\end{aligned}$$

Let denote $\lambda_{i\ell} = -\left(\Pi_\ell((I-K)\boldsymbol{u}_N, \varphi_i\right)_{k+1} \in \mathbb{R}$ and $\lambda = (\lambda_{i\ell})_{\substack{1\le i\le N \\ 1\le \ell\le n}} \in \mathbb{R}^{N,n}$. Then

$$\begin{aligned}&((I-K)\boldsymbol{u}_N, (I-K)\boldsymbol{w})_{k+1} = \\ &((I-K)\boldsymbol{u}_N, (I-K)\boldsymbol{v})_{k+1} - \sum_{i=1}^{N} ((I-K)\boldsymbol{u}_N, (I-K)\boldsymbol{v}(t_i)\varphi_i)_{k+1} = \\ &((I-K)\boldsymbol{u}_N, (I-K)\boldsymbol{v})_{k+1} + \sum_{i=1}^{N}\sum_{\ell=1}^{n} \Pi_\ell((I-K)\boldsymbol{v}(t_i))\lambda_{i\ell} = \\ &((I-K)\boldsymbol{u}_N, (I-K)\boldsymbol{v})_{k+1} + \langle\lambda, \rho\boldsymbol{v}\rangle_{N,n}.\end{aligned}$$

From (4.8), we conclude that there exists $\lambda = (-(\Pi_\ell((I-K)\boldsymbol{u}_n), \varphi_i)_{k+1})_{\substack{1\le i\le N \\ 1\le \ell\le n}} \in \mathbb{R}^{N,n}$ such that

$$((I-K)\boldsymbol{u}_N, (I-K)\boldsymbol{v})_{k+1} + \langle\lambda, \rho\boldsymbol{v}\rangle_{N,n} = 0$$

and (4.7) holds.

The uniqueness of λ is immediate. □

4.3.3 Convergence Result

Assume that $\boldsymbol{f} \in H^{k+1}((0,1);\mathbb{R}^n)$ and $\boldsymbol{k} \in H^k((0,1)\times(0,1);\mathbb{R}^{n,n})$, then there exists a unique solution $\boldsymbol{x} \in H^{k+1}((0,1);\mathbb{R}^n)$ of (4.2). Moreover, the following convergence result is verified.

Theorem 4.3.3. *Suppose given* $\boldsymbol{f} \in H^{k+1}((0,1);\mathbb{R}^n)$ *and* $\boldsymbol{k} \in H^k((0,1)\times(0,1);\mathbb{R}^{n,n})$. *Let denote* $\boldsymbol{x} \in H^{k+1}((0,1);\mathbb{R}^n)$ *the unique solution of (4.2) and* $\boldsymbol{u}_N \in \boldsymbol{H}_N$ *the unique solution of (4.5). Suppose that the hypothesis (4.3) holds, where h is mentioned. Then, one has*

$$\lim_{h\to 0} \|\boldsymbol{u}_N - \boldsymbol{x}\|_k = 0.$$

Proof. Let $\boldsymbol{s}_{\boldsymbol{x},\boldsymbol{T}_N}$ be the interpolating radial basis function of $\boldsymbol{x}$ on $\boldsymbol{T}_N$ from the Wendland function $\phi_{1,k}$, then $\boldsymbol{s}_{\boldsymbol{x},\boldsymbol{T}_N} \in \boldsymbol{S}_N$. Thus $J(\boldsymbol{u}_N) \leq J(\boldsymbol{s}_{\boldsymbol{x},\boldsymbol{T}_N})$, that also implies that

$$|(I-K)\boldsymbol{u}_N|_{k+1} \leq |(I-K)\boldsymbol{s}_{\boldsymbol{x},\boldsymbol{T}_N}|_{k+1}.$$

In this case, we have

$$[[(I-K)\boldsymbol{u}_N]] \leq [[(I-K)\boldsymbol{s}_{\boldsymbol{x},\boldsymbol{T}_N}]].$$

From this, and that the operator $(I-K)$ is linear and compact in the finite-dimensional space $\boldsymbol{S}_N$, and thus bijective, we can deduce that there exists $C_1 > 0$ verifying

$$\|\boldsymbol{u}_N\|_{k+1} \leq C_1 \|\boldsymbol{s}_{\boldsymbol{x},\boldsymbol{T}_N}\|_{k+1}. \tag{4.9}$$

Taking into account (4.4), it is verified that there exists $C_2 > 0$ such

$$\|\boldsymbol{s}_{\boldsymbol{x},\boldsymbol{T}_N}\|_{k+1} \leq C_2 \|\boldsymbol{x}\|_{k+1}.$$

and, from here and (4.9) we obtain that there exists $C > 0$ such that

$$\|\boldsymbol{u}_N\|_{k+1} \leq C \|\boldsymbol{x}\|_{k+1}.$$

Thus, the family $(\boldsymbol{u}_N)_{N\in\mathbb{N}}$ is bounded in $H^{k+1}((0,1);\mathbb{R}^n)$, and consequently

there exists a sequence $(\boldsymbol{u}_{N_\ell})_{\ell\in\mathbb{N}}$ extracted from this family, and an element $\boldsymbol{x}^* \in H^{k+1}((0,1);\mathbb{R}^n)$ such that

$$\boldsymbol{x}^* = \lim_{\ell\to+\infty} \boldsymbol{u}_{N_\ell} \text{ weakly in } H^{k+1}((0,1);\mathbb{R}^n). \tag{4.10}$$

Suppose that $\boldsymbol{x}^* \neq \boldsymbol{x}$; then, from the continuous injection of $H^{k+1}((0,1);\mathbb{R}^n)$ into $C([0,1];\mathbb{R}^n)$, there exists $\gamma > 0$ and a nonempty interval $\omega \subset [0,1]$ such that

$$\forall\, t \in \omega, \quad \langle \boldsymbol{x}^* - \boldsymbol{x}\rangle_n > \gamma.$$

As this injection is compact, from (4.10)

$$\exists \ell_0 \in \mathbb{N},\ \forall\, \ell \geq \ell_0,\ \langle \boldsymbol{u}_{N_\ell}(t) - \boldsymbol{x}^*(t)\rangle_n \leq \frac{\gamma}{2}.$$

Thus, for any $\ell \geq \ell_0$ and $t \in \omega$ it is verified

$$\langle \boldsymbol{u}_{N_\ell}(t) - \boldsymbol{x}(t)\rangle_n \geq \langle \boldsymbol{x}^*(t) - \boldsymbol{x}(t)\rangle_n - \langle \boldsymbol{u}_{N_\ell}(t) - \boldsymbol{x}^*(t)\rangle_n > \frac{\gamma}{2}. \tag{4.11}$$

On the other hand, as we are taking $h \to 0$ along the whole process, using the density condition (4.3) we can assure that there exists $\ell \in \mathbb{N}$ and $t^*_\ell \in \omega$ such that $t^*_\ell \in T_{N_\ell} \cap \omega$ and thus

$$(I - K)\boldsymbol{u}_{N_\ell}(t^*_\ell) = (I - K)\boldsymbol{x}(t^*_\ell).$$

The operator $I - K$, considering the hypotheses taken from the beginning, it is also a bijection in $C((0,1);\mathbb{R}^n)$, and thus $\boldsymbol{u}_{N_\ell}(t^*_\ell) = \boldsymbol{x}(t^*_\ell)$, which is a contradiction with (4.11). Thus $\boldsymbol{x}^* = \boldsymbol{x}$.
For any $\ell \in \mathbb{N}$ it is verified

$$\|\boldsymbol{u}_{N_\ell} - \boldsymbol{x}\|_k^2 = \|\boldsymbol{u}_{N_\ell}\|_k^2 + \|\boldsymbol{x}\|_k^2 - 2(\boldsymbol{u}_{N_\ell}, \boldsymbol{x})_k.$$

Then, from (4.10) and the compact inclusion of $H^{k+1}((0,1);\mathbb{R}^n)$ into $H^k((0,1);\mathbb{R}^n)$ (see for example [7]), one has

$$\lim_{\ell\to+\infty} \|\boldsymbol{u}_{N_\ell} - \boldsymbol{x}\|_k = 0. \tag{4.12}$$

Suppose now that $\|\boldsymbol{u}_N - \boldsymbol{x}\|_k$ does not tend to 0 as h tends to 0; in this case, it would exist $\alpha > 0$, and a sequence $(\boldsymbol{u}_{N'_\ell})_{\ell\in\mathbb{N}}$ such that

$$\forall\, \ell \in \mathbb{N},\ \|\boldsymbol{u}_{N'_\ell} - \boldsymbol{x}\|_k > \alpha. \tag{4.13}$$

However, the sequence $(\boldsymbol{u}_{N'_\ell})_{\ell\in\mathbb{N}}$ is bounded in $H^{k+1}((0,1);\mathbb{R}^n)$ and then, by reasoning as above, we deduce that from this sequence we can extract a subsequence convergent to $\boldsymbol{x}$ in $H^k((0,1);\mathbb{R}^n)$, what contradicts (4.13). Thus

$$\lim_{h\to 0} \|\boldsymbol{u}_N - \boldsymbol{x}\|_k = 0.$$

□

Corollary 4.3.7. *Under the conditions of Theorem 4.3.3 one has*

$$\lim_{h\to 0} \|\boldsymbol{f} - (I-K)\boldsymbol{u}_N\|_k = 0.$$

Proof. From Theorem 4.3.3 and the continuity of the operator $I-K$ we have

$$\lim_{h\to 0}(I-K)\boldsymbol{u}_N = (I-K)\boldsymbol{x} = \boldsymbol{f} \text{ in } H^k((0,1);\mathrm{R}^n).$$

Then, from here the result is obtained. □

4.3.4 Computation

Let us compute the unique solution of (4.7). The solution of problem (4.6) can be expressed by

$$\boldsymbol{u}_N = \sum_{i=1}^{N} \boldsymbol{\alpha}_i \phi_{1,k}(|\cdot - t_i|),$$

with $\boldsymbol{\alpha}_1, \ldots, \boldsymbol{\alpha}_N \in \mathbb{R}^n$.
Consider the basis $\{\boldsymbol{B}_1, \ldots, \boldsymbol{B}_{Nn}\}$ of the space $\boldsymbol{S}_N$ given, for $\ell = 1, \ldots Nn$, by

$$\boldsymbol{B}_\ell(t) = \phi_{1,k}(|t - t_i|)\boldsymbol{e}_j,$$

being $i = quotient(\ell - 1, n) + 1$ and $j = \ell - (i-1)n$.
Then, the solution of (4.6) can be expressed by

$$\boldsymbol{u}_N = \sum_{\ell=1}^{Nn} \alpha_\ell \boldsymbol{B}_\ell,$$

with $\alpha_1, \ldots, \alpha_{Nn} \in \mathbb{R}$.
By replacing in (4.7), we have

$$\sum_{\ell=1}^{Nn} \alpha_\ell \left((I-K)\boldsymbol{B}_\ell, (I-K)\boldsymbol{v}\right)_{k+1} + \langle \lambda, \rho \boldsymbol{v} \rangle_{N,n} = 0, \ \forall\, \boldsymbol{v} \in \boldsymbol{S}_N,$$

subject to the restrictions

$$\sum_{\ell=1}^{Nn} \alpha_\ell (I-K)\boldsymbol{B}_\ell(t_i) = \boldsymbol{f}(t_i), \quad i = 1, \ldots, N.$$

Taking $\boldsymbol{v} = \boldsymbol{B}_j$, for $j = 1, \ldots, Nn$, we obtain a linear system of order $2Nn$ with unknowns $\alpha_1, \ldots, \alpha_{Nn}, \lambda_1, \ldots, \lambda_{Nn} \in \mathbb{R}$, that can be expressed in matrix form as follows:

$$\begin{pmatrix} \mathcal{C} & \mathcal{D} \\ \mathcal{D}^\top & 0 \end{pmatrix} \begin{pmatrix} \boldsymbol{\alpha} \\ \boldsymbol{\lambda} \end{pmatrix} = \begin{pmatrix} \boldsymbol{0} \\ \boldsymbol{F} \end{pmatrix},$$

with

$$\begin{aligned} &\mathcal{C} = \left(\left((I-K)\boldsymbol{B}_\ell, (I-K)\boldsymbol{B}_j\right)_{k+1}\right)_{\substack{1 \le \ell \le Nn \\ 1 \le j \le Nn}}, \\ &\mathcal{D} = (d_{ij})_{\substack{1 \le i \le Nn \\ 1 \le j \le Nn}}, \\ &\boldsymbol{\alpha} = (\alpha_1, \ldots, \alpha_{Nn})^\top, \quad \boldsymbol{\lambda} = (\lambda_1, \ldots, \lambda_{Nn})^\top, \\ &\boldsymbol{F} = (f_i)_{1 \le i \le Nn}, \end{aligned}$$

being, for $i = 1 \ldots, Nn$ and $j = 1, \ldots, Nn$,

$$d_{ij} = \Pi_\ell((I-K)\boldsymbol{B}_r(t_s)),$$

with $r = quotient(i-1, n) + 1$, $s = quotient(j-1, n) + 1$, $\ell = j - (s-1)n$ and for $i = 1, \ldots, Nn$,

$$f_i = \Pi_\ell(\boldsymbol{f}(t_s)),$$

with $s = quotient(i-1, n)$ and $\ell = i - (s-1)n$.

4.3.5 Numerical Examples

To check the validity of the described method for approximating the solution of Problem (4.2) we present some numerical experiments.
In order to show the accuracy of the method, we have computed two relative error estimations, given by the expressions

$$E_1 = \frac{1}{1000}\sum_{i=1}^{1000}\langle \boldsymbol{f}(a_i) - (I-K)\boldsymbol{u}_N(a_i)\rangle_n,$$

which estimates how close $\boldsymbol{u}_N$ is to the solution of (4.2) and

$$E_2 = \sqrt{\frac{\sum_{i=1}^{1000}\langle \boldsymbol{u}_N(a_i) - \boldsymbol{x}(a_i)\rangle_n^2}{\sum_{i=1}^{1000}\boldsymbol{x}(a_i)\rangle_n^2}},$$

which is an approximation of the relative error of $\boldsymbol{u}_N$ with respect to $\boldsymbol{x}$ in $L^2((0,1);\mathrm{R}^n)$ being $\{a_1,\ldots,a_{1000}\}\subset[0,1]$ thousand distinct random points. From Theorem 4.3.3 and Corollary 4.3.7, these relative error estimations E_1 and E_2 tend to 0 as h tends to 0.
Moreover, in all the examples, the discrete space that we use to calculate the approximated solution $\boldsymbol{u}_N$ is the radial basis function space constructed from the Wendland function $\phi_{1,1}$ and the centers set $\boldsymbol{T}_N = \{t_i = \frac{i}{N},\ i = 0,\ldots,N\}$.
In order to compute the numerical integrals, we have employed the following quadrature formula (see [99])

$$\begin{aligned}\int_a^b g(t)dt \;\approx\; &\sum_{i=6}^{n-3} g(\xi_i) + h\left(\frac{206}{1575}(g(\xi_1)+g(\xi_{n+2}) + \frac{107}{128}(g(\xi_2)+g(\xi_{n+1}))+\right.\\ &\frac{6019}{5760}(g(\xi_3)+g(\xi_n)) + \frac{9467}{9600}(g(\xi_4)+g(\xi_{n-1}))+\\ &\left.\frac{13469}{13440}(g(\xi_5)+g(\xi_{n-2}))\right),\end{aligned}$$

where $h = \dfrac{b-a}{n}$ and

$$\xi_1 = a, \quad \xi_{n+2} = b, \quad \xi_i = a + \frac{2i-1}{2}h,\ i = 2,\ldots,n+1.$$

This formula has an error order of $O(h^6)$ for $g \in C^6([a,b])$.

Example 4.3.8. *We consider the following Volterra equation system of order* 2

$$\begin{cases} x_1(t) - \int_0^t ((t-s)^3 x_1(s) + (t-s)^2 x_2(s))ds = t - \dfrac{t^5}{12}, \\ x_2(t) - \int_0^t ((t-s)^4 x_1(s) + (t-s)^3 x_2(s))ds = t^2 - \dfrac{t^6}{20}. \end{cases}$$

The exact solution is

$$x_1(t) = t, \quad x_2(t) = t^2.$$

Table 4.2 shows the relative error estimations for distinct values of N.

Table 4.2 : Computed relative error estimations for Example 4.3.8 from some values of N

N	E_1	E_2
5	2.1868×10^{-2}	3.1058×10^{-2}
10	3.6034×10^{-3}	4.8048×10^{-3}
20	6.2683×10^{-4}	8.2990×10^{-4}
30	2.0727×10^{-4}	3.0254×10^{-4}
40	1.0215×10^{-4}	1.2509×10^{-4}
50	6.4520×10^{-5}	9.2824×10^{-5}

Example 4.3.9. *We consider the following Volterra equation system of order* 2

$$\begin{cases} x_1(t) - \int_0^t (e^{t-s} x_1(s) + e^{t+s} x_2(s))ds = e^t(1-2t), \\ x_2(t) - \int_0^t (-e^{t-s} x_1(s) + e^{t+s} x_2(s))ds = e^{-t}. \end{cases}$$

The exact solution is

$$x_1(t) = e^t, \quad x_2(t) = e^{-t}.$$

Table 4.3 shows the relative error estimations for distinct values of N.

Table 4.3 : Computed relative error estimations for Example 4.3.9 from some values of N

N	E_1	E_2
5	3.0586×10^{-2}	2.5854×10^{-2}
10	6.4473×10^{-3}	3.7229×10^{-3}
20	1.1610×10^{-3}	6.3689×10^{-4}
30	4.4048×10^{-4}	2.2905×10^{-4}
40	1.5159×10^{-4}	1.1068×10^{-4}
50	9.9079×10^{-5}	6.3629×10^{-5}

Example 4.3.10. *We consider the following Volterra equation system of order* 3

$$\begin{cases} x_1(t) - \int_0^t (x_1(s) + tx_3(s))ds = -t + t^2, \\ x_2(t) - \int_0^t ((t+s)x_1(s) + x_2(s) + (t-s)x_3(s))ds = 1 - t - \dfrac{t^4}{2}, \\ x_3(t) - \int_0^t ((-t-s)x_1(s) - x_2(s) + (-t+s)x_3(s))ds = -t - t^2 + \dfrac{t^4}{2}. \end{cases}$$

The exact solution is

$$x_1(t) = t^2, \quad x_2(t) = 1, \quad x_3(t) = -t^2.$$

Table 4.4 shows the relative error estimations for distinct values of N.

Table 4.4 : Computed relative error estimations for Example 4.3.10 from some values of N

N	E_1	E_2
5	2.0024×10^{-2}	3.5705×10^{-2}
10	2.4457×10^{-3}	5.2296×10^{-3}
20	2.9878×10^{-4}	7.5222×10^{-4}
30	7.5462×10^{-5}	2.6518×10^{-4}
40	2.6133×10^{-5}	1.1834×10^{-4}
50	1.0932×10^{-5}	7.1453×10^{-5}

4.4 Linear Volterra integro-differential equations

In this section, we propose a specific variational method for the numerical approximation of the solution of a linear Volterra integro-differential problem. The proposed method is based on the minimization of a suitable functional in a finite-dimensional space generated by a finite Wendland's type radial basis functions (RBFs) set.

4.4.1 Wendland radial basis functions

We consider the same functions $\phi_{1,k}$ for $k = 0, 1, 2$ listed in table 4.1 in the previous section.
Consider

$$h = \sup_{t \in I} \min_{1 \le i \le N} |t - t_i|. \tag{4.14}$$

From [115, Theorem 2.1 and Theorem 2.2] we can prove the following results.

Theorem 4.4.1. *The function $\phi_{1,n}$ belongs to $C^{2n}(\mathbb{R})$ and the corresponding native space coincides with the Sobolev space $H^{n+1}(\mathbb{R})$. Moreover, if $\hat{\phi}_{1,n}$ is the Fourier transform of the function $\phi_{1,n}(|\cdot|)$ then there exist constants K_1*

and K_2 such that

$$K_1(1+t^2)^{-n-1} \leq \hat{\phi}_{1,n}(|t|) \leq K_2(1+t^2)^{-n-1}, \quad \forall\, t \in \mathbb{R}. \tag{4.15}$$

Theorem 4.4.2. *For all $u \in H^{n+1}(I)$, let s_{u,T_N} be the radial basis function interpolating u on T_N from the Wendland function $\phi_{1,n}$. Then, there exists $C > 0$ such that*

$$\|u - s_{u,T_N}\|_{L_\infty(I)} \leq C\|u\|_{n+1} h^{n+\frac{1}{2}}, \quad \forall\, u \in H^{n+1}(I). \tag{4.16}$$

Finally, from (4.15) and [Theorem 4.1] in [116] we conclude the following result.

Theorem 4.4.3. *There exists a real number $C > 0$ and a integer $N_0 > 0$ such that for all $N \geq N_0$ one has*

$$|u - s_{u,T_N}|_j \leq Ch^{n+1-j}\|u\|_{n+1}, \quad 0 \leq j \leq n+1, \quad \forall\, u \in H^{n+1}(I). \tag{4.17}$$

Let be $r \in \mathbb{N}$ with $r \geq n$ and let S_N be the space of the restrictions of functions on I of the functional linear space generated by the radial basis functions $\{\phi_{1,r}(|\cdot - t_1|), \ldots, \phi_{1,r}(|\cdot - t_N|)\}$. Then $S_N \subset H^{n+1}(I) \cap C^{2n}(I)$.

4.4.2 Formulation of the problem

Consider the Volterra integro-differential problem: Find $u \in H^{2n}(I)$ such that

$$\begin{cases} Du(t) = f(t) + \displaystyle\int_a^t k(t,s)u(s)ds, & a \leq t \leq b, \\ d^i u(a) = y_1^i, \quad d^i u(b) = y_2^i, & 0 \leq i \leq n-1, \end{cases} \tag{4.18}$$

where $k \in C(I \times I)$, $f \in C(I)$ and $y_1^i,\ y_2^i \in \mathbb{R}$, for $i = 0, \ldots, n-1$, are given. In the remainder of this section, we suppose that Problem (4.18) has a unique solution $x \in H^{2n}(I)$.
Then, Problem (4.18) is equivalent to the problem: Find $u \in H^{2n}(I)$ such that

$$\begin{cases} (D - \Lambda)u = f, \\ d^i u(a) = y_1^i, \quad d^i u(b) = y_2^i, \quad 0 \leq i \leq n-1, \end{cases} \tag{4.19}$$

and $x = (D-\Lambda)^{-1}(f)$, verifying $d^i x(a) = y_1^i, \quad d^i x(b) = y_2^i$, for $0 \leq i \leq n-1$, is the unique solution of Problem (4.18).
Suppose $N > 2n+2$ and let $\rho : H^n(I) \to \mathbb{R}^{N-2n}$ be the operator given by

$$\rho v = ((D-\Lambda)v(t_{i+n}))_{1\leq i\leq N-2n}.$$

For $i = 1, \ldots, 2n$, let φ_i be the linear form in $H^n(I)$ given by

$$\varphi_i(v) = \begin{cases} d^{i-1}v(a) \text{ if } i = 1, \ldots, n, \\ d^{i-n-1}v(b) \text{ if } i = n+1, \ldots, 2n, \end{cases}$$

and consider the operator $\tau : H^n(I) \to \mathbb{R}^{2n}$ given by

$$\tau u = (\varphi_i(v))_{1\leq i\leq 2n},$$

the vector $y = (y_1, \ldots, y_n) \in \mathbb{R}^{2n}$, being

$$y_i = \begin{cases} y_{i-1}^1 \text{ if } i = 1, \ldots, n, \\ y_{i-n-1}^2 \text{ if } i = n+1, \ldots, 2n, \end{cases}$$

the vector $F = (f(t_{i+n}))_{1\leq i\leq N-2n} \in \mathbb{R}^{N-2n}$, the affine variety $K_N = \{u \in S_n \,:\, \rho u = F\}$ and the linear subspace $K_N^0 = \{u \in S_N \,:\, \rho u = 0\}$.

Lemma 4.4.4. *The set K_N is a nonempty closed convex subset of S_N. Moreover it is an affine variety associated with the linear subspace K_N^0.*

Proof. Let $x \in H^{2n}(I)$ the unique solution of Problem (4.18), then there exists a unique $u_0 \in S_N$ such that

$$u_0(t_i) = \begin{cases} 0, & \text{if } i = 1, \ldots, n, \text{ or } i = N-n+1, \ldots, N, \\ x(t_i), & \text{if } i = n+1, \ldots, N-n. \end{cases}$$

Then $\rho u_0 = \rho x = F$ and thus $u_0 \in K_N$ and K_N is a nonempty set.
The remainder of the proof is immediate. □

Lemma 4.4.5. *For $\varepsilon > 0$, the application $<< \cdot, \cdot >>$: $H^{n+1}(I) \times H^{n+1}(I) \to \mathbb{R}$ defined by*

$$<< u, v >> = \langle \tau u, \tau v \rangle_{2n} + \varepsilon (u, v)_{n+1} \tag{4.20}$$

is an inner product on $H^{n+1}(I)$ and its associated norm, given by $[[u]] = << u, u >>^{1/2}$, is equivalent to the usual Sobolev norm $\|u\|_{n+1}$.

Proof. Is similar to the proof of [49, Lemma 1]. □

Definition 4.4.6. *We say that $u_N \in K_N$ is an approximating radial basis function of Problem (4.18) relative to $\phi_{1,n}$, T_N, ε, F and y if u_N is a solution of the following minimization problem: Find $u_N \in K_N$ such that*

$$\forall\, v \in K_N,\ \langle \tau u_N - y\rangle_{2n}^2 + \varepsilon |u_N|_{n+1}^2 \leq \langle \tau v - y\rangle_{2n}^2 + \varepsilon |v|_{n+1}^2. \tag{4.21}$$

Theorem 4.4.7. *Problem (4.21) has a unique solution $u_N \in K_N$ which is the unique solution of the following variational problem:*

$$\forall\, v \in K_N^0,\ \langle \tau u_N, \tau v\rangle_{2n} + \varepsilon (u_N, v)_{n+1} = \langle y, \tau v\rangle_{2n}. \tag{4.22}$$

Proof. The application $<<\ \cdot, \cdot\ >>$ is a coercive bilinear and symmetric form on $H^{n+1}(I) \times H^{n+1}(I)$.

Let $\varphi(v) = \langle y, \tau v\rangle_{2n}$, which is clearly a linear and continuous operator on $H^{n+1}(I)$. So, by applying Stampacchia Theorem [19, Theorem 5.6] we conclude that there exists a unique $u_N \in K_N$ such that $<< u_N, w - u_N >> \geq \varphi(w - u_N)$ for all $w \in K_N$, which implies that $<< u_N, v >> \geq \varphi(v)$ for all $v \in K_N^0$.

As K_N^0 is a linear subspace, if $v \in K_N^0$ verifies that $-v \in K_N^0$, then it follows that $<< u_N, v >> = \varphi(v)$, for any $v \in K_N^0$. Furthermore, u_N is the minimum in K_N of the functional $\phi(v) = \frac{1}{2} << v, v >> - \varphi(v)$, that is equivalent to Problem (4.22). □

Theorem 4.4.8. *There exists one and only one $(N-2n+1)$-tuple $(u_N, \lambda) \in S_N \times \mathbb{R}^{N-2n}$ such that*

$$\forall\, v \in S_N,\ \langle \tau u_N, \tau v\rangle_{2n} + \varepsilon (u_N, v)_{n+1} + \langle \lambda, \rho v\rangle_{N-2n} = \langle y, \tau v\rangle_{2n}, \tag{4.23}$$

where u_N is the unique solution of (4.22).

Proof. For any $i = 1, \ldots, N$, let $p_i \in \mathbb{P}_{N-1}(I)$ the interpolating Lagrange polynomial such that $p_i(t_j) = \delta_{ij}$, for $i = 1, \ldots, N$, and let $\omega_i = (D-\Lambda)^{-1} p_i$, with $\tau\omega_i = y$. Finally, let $s_i \in S_N$ be the Wendland basis function associated with T_N and ω_i.

Then $(D-\Lambda)s_i(t_j) = (D-\Lambda)\omega_i(t_j) = p_i(t_j) = \delta_{ij}$, for any $j = 1, \ldots N$.

For any $v \in K_N$, let $w \in K_N$ given by

$$w(t) = v(t) - \sum_{j=n+1}^{N-n} (D-\Lambda)v(t_j)s_j(t).$$

Then, for any $i = n+1, \ldots, N-n$ we have

$$(D-\Lambda)w(t_i) = (D-\Lambda)v(t_i) - \sum_{j=n+1}^{N-n} (D-\Lambda)v(t_j)(D-\Lambda)s_j(t_i) =$$
$$(D-\Lambda)v(t_i) - (D-\Lambda)v(t_i) = 0.$$

Hence we deduce that $w \in K_N^0$ and, from Theorem 4.4.7,

$$\langle \tau u_N, \tau w\rangle_{2n} + \varepsilon(u_N, w)_{n+1} = \langle y, \tau w\rangle_{2n},$$

that is

$$\langle \tau u_N, \tau v\rangle_{2n} - \sum_{j=n+1}^{N-n} (D-\Lambda)v(t_j)\langle \tau u_N, \tau s_j\rangle_{2n} +$$
$$\varepsilon(u_N, v)_{n+1} - \varepsilon \sum_{j=n+1}^{N-n} (D-\Lambda)v(t_j)(u_N, s_j)_{n+1} =$$
$$\langle y, \tau v\rangle_{2n} - \sum_{j=n+1}^{N-n} (D-\Lambda)v(t_j)\langle y, \tau s_j\rangle_{2n}.$$

Here we have

$$\langle \tau u_N, \tau v\rangle_{2n} + \varepsilon(u_n, v)_{n+1} +$$
$$\sum_{j=n+1}^{N-n} \left(\langle y - \tau u_N, \tau s_j\rangle_{2n} - \varepsilon(u_N, s_j)_{n+1}\right)(D-\Lambda)v(t_j) = \langle y, \tau v\rangle_{2n}.$$

Taking $\lambda = \left(\langle y - \tau u_N, \tau s_j\rangle_{2n} - \varepsilon(u_N, s_j)_{n+1}\right)_{n+1 \le j \le N-n}$ we obtain (4.23).

The uniqueness of λ is immediate. □

4.4.3 Computation of the numerical solution

The solution of Problem (4.22) can be expressed by

$$u_N = \sum_{j=1}^{N} \alpha_j \phi_{1,r}(|\cdot - t_j|),$$

with $\alpha_1, \ldots, \alpha_N \in \mathbb{R}$.
By replacing in (4.23) we have

$$\begin{aligned} &\langle \tau(\sum_{j=1}^{N} \alpha_j \phi_{1,r}(|\cdot - t_j|), \tau v\rangle_{2n} + \varepsilon(\sum_{j=1}^{N} \alpha_j \phi_{1,r}(|\cdot - t_j|), v)_{n+1} + \\ &\langle \lambda, F\rangle_{N-2n} = \langle y, \tau v\rangle_{2n}, \quad \forall\, v \in S_N, \end{aligned}$$

subject to the restrictions

$$\sum_{j=1}^{N} \alpha_j (D - \Lambda)\phi_{1,r}(|t_i - t_j|) = f(t_i), \quad i = n+1, \ldots, N-n.$$

Taking $v = \phi_{1,r}(|\cdot - t_i)$, for $i = 1, \ldots, N$, we obtain a linear system of order $2N - 2n$ with unknowns $\alpha_1, \ldots, \alpha_N \in \mathbb{R}$, $\lambda \in \mathbb{R}^{N-2n}$, which can be expressed in matrix form as follows

$$\begin{pmatrix} \mathcal{C} & \mathcal{D} \\ \mathcal{D}^\top & 0 \end{pmatrix} \begin{pmatrix} \alpha \\ \lambda \end{pmatrix} = \begin{pmatrix} G \\ F \end{pmatrix},$$

with

$$\begin{aligned} &\mathcal{C} = \mathcal{A}\mathcal{A}^\top + \varepsilon \mathcal{R}, \\ &\mathcal{A} = (\varphi_j(\phi_{1,r}(|\cdot - t_i|)))_{\substack{1 \le i \le N \\ 1 \le j \le 2n}} \\ &\mathcal{R} = ((\phi_{1,r}(|\cdot - t_i|), \phi_{1,r}(|\cdot - t_j|)n + 1)_{1 \le i,j \le N}, \\ &\mathcal{D} = ((D - \Lambda)(\phi_{1,r}(|t_j - t_i|)))_{\substack{1 \le i \le N \\ n+1 \le j \le N-n}} \\ &G = \mathcal{A} y \end{aligned}$$

and $\alpha = (\alpha_1, \ldots, \alpha_N)^\top$.

4.4.4 Convergence results

Theorem 4.4.9. *Let denote $x \in H^{2n}(I)$ the unique solution of Problem (4.18) and $u_N \in S_N$ the unique solution of Problem (4.21). Suppose that the*

hypothesis (4.14) holds and moreover

$$\varepsilon = O(1), \quad N \to +\infty, \tag{4.24}$$

$$\frac{h^2}{\varepsilon} = o(1), \quad N \to +\infty. \tag{4.25}$$

Then, one has

$$\lim_{N\to+\infty} \|u_N - x\|_n = 0. \tag{4.26}$$

Proof. Let $s_{x,T_N} \in S_N$ be the interpolating radial basis function of x on T_N from the Wendland function $\phi_{1,r}$. Then

$$\langle \tau u_N - y\rangle_{2n}^2 + \varepsilon |u_N|_{n+1}^2 \leq \langle \tau s_{x,T_N} - y\rangle_{2n}^2 + \varepsilon |s_{x,T_N}|_{n+1}^2. \tag{4.27}$$

From (4.21) and (4.17) there exists $C > 0$ and $N_0 \in \mathbb{N}$ such that for $N \geq N_0$ one has

$$\langle \tau s_{x,T_N} - y\rangle_{2n}^2 \leq Ch^2 \|x\|_{n+1}^2 \text{ and } |s_{x,T_N}|_{n+1}^2 \leq C\|x\|_{n+1}^2.$$

Thus, from (4.27), one has

$$|u_N|_{n+1}^2 \leq C(\frac{h^2}{\varepsilon} + 1)\|x\|_{n+1}^2 \text{ and } \langle \tau u_N\rangle_{2n}^2 \leq C(h^2 + \varepsilon)\|x|_{n+1}^2 + \langle y\rangle_{2n}^2. \tag{4.28}$$

We conclude, from (4.24)–(4.28), that there exists $C > 0$ and $N_0 \in \mathbb{N}$ such that

$$\langle \tau u_N\rangle_{2n}^2 + |u_N|_{n+1}^2 \leq C, \quad \forall\, N \geq N_0.$$

Finally, from Lemma 4.4.5, we conclude that there exists $C > 0$ and $N_0 \in \mathbb{N}$ such that

$$\|u_N\|_{n+1} \leq C, \quad \forall\, N \geq N_0.$$

Hence, the family $(u_N)_{N\geq N_0}$ is bounded in $H^{n+1}(I)$ and consequently there

exists a sequence $(u_{N_\ell})_{\ell\in\mathbb{N}}$ extracted from this family and an element $x^* \in H^{n+1}(I)$ such that

$$x^* = \lim_{\ell\to+\infty} u_{N_\ell} \text{ weakly in } H^{n+1}(I). \tag{4.29}$$

From here the proof is analogous to the proof of [49, Theorem 4]

□

Corollary 4.4.10. *Under the conditions of Theorem 4.4.9 one has*

$$\lim_{N\to+\infty} \|f - (D-\Lambda)u_N\|_0 = 0.$$

Proof. From Theorem 4.4.9 and the continuity of the operator $D-\Lambda$ we have

$$\lim_{N\to+\infty} (D-\Lambda)u_N = (D-\Lambda)x = f \text{ in } L^2(I).$$

Then, from here the result is obtained. □

4.4.5 Numerical Examples

We present some numerical examples by computing an approximating solution of Problem (4.17) in order to verify the validity of the described method. To this end, in each case, we have computed two error estimations, given by the expressions

$$E_1 = \frac{1}{3000}\sum_{i=1}^{3000} |f(a_i) - (D-\Lambda)u_N(a_i)|,$$

and

$$E_2 = \sqrt{\frac{\sum_{i=1}^{3000}(u_N(a_i) - x(a_i))^2}{\sum_{i=1}^{3000} x(a_i)^2}},$$

which estimate how close u_N is to the solution of (4.17) and an approximation of the relative error of u_N with respect to this exact solution in $L^2(I)$,

respectively, being $\{a_1, \ldots, a_{3000}\} \subset I$ a distinct random points set.
From Theorem 4.4.9 and Corollary 4.4.10, these relative error estimations E_1 and E_2 tend to 0 as N tends to $+\infty$.
Moreover, in all the examples, we have taken $\varepsilon = 10^{-9}$, $r = 2$ and the centers set is $\boldsymbol{T}_N = \{t_i = a + \dfrac{b-a}{N} i,\ i = 0, \ldots, N\}$.
In order to compute the numerical integrals, we have used the composite Simpson 1/3 rule for $\max\{N + 1, 50\}$ equidistant knots.

Example 4.4.11. *We consider* $[a, b] = [0, 1]$ *and the following Volterra integro-differential problem of order* 2

$$\begin{cases} -u''(t) - \displaystyle\int_0^t (s-t)u(s)ds = -1 - t, \quad 0 < t < 1 \\ u(0) = 1, \quad u(1) = e. \end{cases}$$

The exact solution is

$$u(t) = e^t.$$

Table 4.5 shows the relative error estimations for distinct values of N.

N	E_1	E_2
10	2.7218×10^{-1}	8.1013×10^{-3}
20	6.1951×10^{-2}	1.4603×10^{-3}
40	1.6277×10^{-2}	3.5987×10^{-4}
80	6.2561×10^{-3}	1.4030×10^{-4}
160	1.0771×10^{-3}	6.0484×10^{-5}
320	4.5853×10^{-4}	3.0030×10^{-5}

Table 4.5 : Computed relative error estimations for Example 1 from some values of N.

Example 4.4.12. *We consider* $[a, b] = [0, 1]$ *the following Volterra integro-differential problem of order* 2

$$\begin{cases} -u''(t) + u(t) - \displaystyle\int_0^t -t\tan(s)u(s)ds = t + (2-t)\cos t, \quad 0 < t < 1 \\ u(0) = 1, \quad u(1) = \cos 1. \end{cases}$$

The exact solution is

$$u(t) = \cos t.$$

Table 4.6 shows the relative error estimations for distinct values of N.

N	E_1	E_2
10	7.1910×10^{-2}	3.5985×10^{-3}
20	2.0539×10^{-2}	5.4592×10^{-4}
40	5.0931×10^{-3}	5.6814×10^{-5}
80	1.3689×10^{-3}	1.9949×10^{-5}
160	4.9810×10^{-4}	9.9007×10^{-6}
320	6.8934×10^{-5}	4.9236×10^{-6}

Table 4.6 : Computed relative error estimations for Example 2 from some values of N.

Example 4.4.13. *We consider* $[a, b] = [0, \pi]$ *and the following Volterra integro-differential problem of order* 2

$$\begin{cases} -u''(t) + \sin t\, u(t) - \displaystyle\int_0^t (-\cos t - \cos s)u(s)ds = \\ \dfrac{t}{2} + \cos(t) + \dfrac{5}{2}\sin(t)\cos(t), \quad 0 < t < \pi \\ u(0) = 1, \quad u(\pi) = -1. \end{cases}$$

The exact solution is

$$u(t) = \cos t.$$

Table 4.7 shows the relative error estimations for distinct values of N.

N	E_1	E_2
20	1.0101×10^{-1}	1.0072×10^{-2}
40	3.0369×10^{-2}	5.4190×10^{-3}
80	8.4776×10^{-3}	1.0948×10^{-3}
160	1.5010×10^{-3}	7.2447×10^{-4}
320	5.5338×10^{-4}	5.1316×10^{-4}

Table 4.7 : Computed relative error estimations for Example 3 from some values of N.

Example 4.4.14. *We consider $[a, b] = [0, 1]$ and the following Volterra integro-differential problem of order 4*

$$\begin{cases} u^{iv}(t) + u(t) - \int_0^t u(s)ds = -\frac{t^5}{5} + t^4 + 24, \quad 0 < t < 1 \\ u(0) = u'(0) = 0, \quad u(1) = -1, \ u'(1) = 4. \end{cases}$$

The exact solution is

$$u(t) = t^4.$$

Table 4.8 shows the relative error estimations for distinct values of N.

N	E_1	E_2
20	2.4411×10^{-1}	1.4699×10^{-1}
40	7.3201×10^{-2}	4.6247×10^{-2}
80	1.9593×10^{-2}	1.3083×10^{-2}
160	5.0002×10^{-3}	3.6938×10^{-3}
320	1.1289×10^{-3}	9.8196×10^{-4}
640	3.1596×10^{-4}	2.3896×10^{-4}

Table 4.8 : Computed relative error estimations for Example 4 from some values of N.

Chapter 5

Generalized Wendland RBFs for bivariate functions

5.1 Introduction

Frequently, positive kernels reproducing Hilbert spaces of continuous functions appear in some applications and they are presented as radial basis functions

$$\Psi(x, y) = \psi(\langle x - y \rangle_n), \quad \forall\, x, y \in \mathbb{R}^n,$$

where $\langle \cdot \rangle_n$ denotes the Euclidean norm in $\mathbb{R}^n$, and $\psi : [0, +\infty) \to \mathbb{R}$ is a given smooth univariate function.

The Wendland functions [114] yield compactly supported and differentiable functions in $\mathbb{R}^n$ that reproduce kernels of Hilbert spaces isomorphic to the Sobolev space $H^{n/2+k+1/2}(\mathbb{R}^n)$. Thus, when the dimension n is even, the order of this Sobolev space is not integer.

Robert Shaback [100] extend the classical Wendland functions to the missing Wendland functions that reproduce kernels of Hilbert spaces isomorphic to the Sobolev spaces of integer order in even dimensions. Moreover, they have compact support.

To better understand the objective of this work, we believe that we should cite a brief history of the theory of the approximation problem using the variational spline functions. The theory of the approach using the variational splines has been introduced by Attéia [8] based on the D^m-splines functions, after Duchon [38] developed the idea using the technique of the minimization

of quadratic functionals. We have enriched this generic idea by minimizing various types of quadratic functionals, first in Hilbert spaces and secondly in a finite element space, such as in [71]. We have studied some interpolation and smoothing methods for constructing free-form curves and surfaces from a given Lagrangian and/or Hermite data set. The methods consist in the minimization of a certain quadratic functional in a Sobolev space.

In recent years, some authors related with this thesis have started some works of approximation using the Wendland radial basic functions.In [72] we have presented an approximation method from a given scattered data set, by minimizing a quadratic functional in a parametric finite element space. In [73] we consider the same problem from a given noisy data set; meanwhile, in [74] we study these problems in a bicubic spline functional space and the optimal solution is obtained by a suitable optimization of some parameters that appear in the minimization functional. The recent publications were the result of them, see for example [49], where the authors proposed an approximation method for solving second kind Volterra integral equation systems by radial basis functions.

Specially, in this chapter we deal with the smoothing problem in a finite-dimensional Generalized Wendland functions space; formulating the problem of smoothing variational splines by Generalized Wendland functions, we show how to compute in practice the solution of such problem and the method is justified by proving the corresponding convergence result. In order to illustrate the method, some graphical and numerical examples are presented in $\mathbb{R}^2$ and also comparison with other works are analyzed.

The remainder of this chapter is organized as follows. In section 2 we present some notations and preliminaries that are necessary to formulate the problem. Section 3 is devoted to study the Generalized Wendland compactly supported radial basis functions while section 4 is dedicated to show the problem of the smoothing variational splines by Generalized Wendland functions. In the last section, we finish this work by illustrating some numerical and graphical examples and a study of comparisons with another work.

5.2 Generalized Wendland CSRBFs

Definition 5.2.1. *Let be* $\psi : [0, +\infty) \to \mathbb{R}$ *a continuous function, a set* $\Omega \subset \mathbb{R}^2$*, and a finite set* $T_N = \{\boldsymbol{\xi}_1, \ldots, \boldsymbol{\xi}_N\}$ *of points of* Ω*, the linear space*

generated by the functions set

$$S_N = \{\psi(\langle \cdot - \boldsymbol{\xi}_1 \rangle_2), \ldots, \psi(\langle \cdot - \boldsymbol{\xi}_N \rangle_2)\} \tag{5.1}$$

is called the radial basis functions space relative to the function ψ and the centers set T_N, bein $< \cdot, \cdot >_2$ the Euclidean inner-product in $\mathbb{R}^2$.

Definition 5.2.2. *Consider a function $u \in C(\Omega)$ and the radial basis function $s_{u,T_N} \in S_N$ given by*

$$s_{u,T_N}(\boldsymbol{x}) = \sum_{i=1}^{N} c_i \psi(\langle \boldsymbol{x} - \boldsymbol{\xi}_i \rangle_2), \quad \boldsymbol{x} \in \Omega, \tag{5.2}$$

where $c_1, \ldots, c_N \in \mathbb{R}$ are determined by the interpolating conditions

$$s_{u,T_N}(\boldsymbol{\xi}_i) = u(\boldsymbol{\xi}_i), \quad 1 \leq i \leq N. \tag{5.3}$$

Then s_{u,T_N}, if it exists, is called the interpolation radial basis function (RBF) of u in S_N (relative to ψ and T_N).

Remark 5.2.3. *The interpolation RBF s_{u,T_N} exists and it is unique if and only if*

$$\det((\psi(\langle \boldsymbol{\xi}_i - \boldsymbol{\xi}_j \rangle_2))_{1 \leq i,j \leq N}) \neq 0.$$

Robert Shaback in [100] consider the integral operator

$$I_\alpha(f)(t) = \int_t^\infty f(s) \frac{(s-t)^{\alpha-1}}{\Gamma(\alpha)} ds$$

for all $\alpha > 0$, $t \geq 0$.
Consider the truncated power functions for all $\mu > 0$.

$$a_\mu(s) = (1 - \sqrt{2s})_+^\mu.$$

Since the I_α operators preserve compact supports and are applicable to a_μ for all $\alpha, \mu > 0$, we can define $a_{\mu,\alpha} = I_\alpha(a_\mu)$.

Definition 5.2.4. *We call Generalized Wendland functions The functions* $\Psi_{\mu,\alpha}$ *given by*

$$\Psi_{\mu,\alpha}(r) = a_{\mu,\alpha}(\frac{r^2}{2}), \quad \forall\, \alpha, \mu > 0,$$

which are well defined and supported in $[0,1]$

Remark 5.2.5. *Taking into account the above definition, we have that*

$$\Psi_{\mu,\alpha}(t) = \int_t^1 s(1-s)^\mu \frac{(s^2-t^2)_+^{\alpha-1}}{\Gamma(\alpha)2^{\alpha-1}} ds, \quad \forall t \in [0,1].$$

In [100] it deduces an algorithm for constructing the Generalized Wendland functions for even dimensions $2m$ in the following way

$$\Psi_{2m,(2\ell-1)/2}(r) = r^{2\ell} p_{m,\ell}(r^2) L(r) + q_{m,\ell}(r^2) S(r), \quad r \in [0,1],$$

for any integers $m, \ell \geq 0$, being

$$L(r) = \log\left(\frac{r}{1+\sqrt{1-r^2}}\right), \quad S(r) = \sqrt{1-r^2},$$

and $p_{m,\ell}, q_{m,\ell}$ two associated polynomials of degree $m-1$ and $m-1+\ell$, respectively.

$$\begin{aligned}
\Psi_{2,1/2}(r) &= \frac{\sqrt{2}}{3\sqrt{\pi}}(3r^2 L(r) + (2r^2+1)S(r)),\\
\Psi_{2,3/2}(r) &= -\frac{\sqrt{2}}{60\sqrt{\pi}}(15r^4 L(r) + (8r^4+9r^2-2)S(r)),\\
\Psi_{2,5/2}(r) &= \frac{\sqrt{2}}{2520\sqrt{\pi}}(105r^6 L(r) + (48r^6+87r^4-38r^2+8)S(r)),\\
\Psi_{4,1/2}(r) &= \frac{\sqrt{2}}{30\sqrt{\pi}}((45r^4+60r^2)L(r) + (16r^4+83r^2+6)S(r)),\\
\Psi_{4,3/2}(r) &= -\frac{\sqrt{2}}{420\sqrt{\pi}}((105r^6+210r^4)L(r) + (32r^6+247r^4+40r^2-4)S(r)),
\end{aligned}$$

Table 5.1 : Some Generalized Wendland functions in even dimensions.

Theorem 5.2.6. *Let be* $\Omega \subset \mathbb{R}^2$, $T_N = \{\boldsymbol{\xi}_1, \ldots, \boldsymbol{\xi}_N\} \subset \Omega$ *a centers set and* $n, k \in \mathbb{N}$ *with* $k \geq 0$. *Let be* s_{f,T_N} *the interpolation RBF of* $f \in H^{k+2}(\Omega)$ *relative to* T_N *from* $\Psi_{k+2,k+1/2} = \Psi_{\alpha+3/2,\alpha}$ *with* $\alpha = k+1/2$.

Let

$$h = \sup_{\boldsymbol{x}\in\Omega} \min_{1\leq i\leq N} \langle \boldsymbol{x} - \boldsymbol{\xi}_i \rangle_2$$

be the fill-distance of T_N *in* Ω*, where* $< \cdot >_2$ *denote the Euclidean norm in* $\mathbb{R}^2$*.*

Then

$$|f - s_{f,T_N}|_j \leq Ch^{k+2-j}\|f\|_{k+2}, \quad \forall\, j = 0, \ldots, k+2, \tag{5.4}$$

where C *is independent of* f*.*

Proof. Applying [91, Proposition 3.2] for $\alpha = 0$, $s = 0$ and $\tau = k + 2$ it is verified that $k + 2 > \alpha + 1$ and thus there exists a real constant $C > 0$, independent of f, such that

$$\|f - s_{f,T_N}\|_0 \leq Ch^{k+2}\|f\|_{k+2} \tag{5.5}$$

From Madych-Nelson Theorem[59, Theorem 6] it is verified that

$$(\Psi_{k+2,k+1/2}(\langle \cdot - \boldsymbol{\xi}_j \rangle_2), s_{f,T_N}) = s_{f,T_N}(\boldsymbol{\xi}_j)$$

and

$$(\Psi_{k+2,k+1/2}(\langle \cdot - \boldsymbol{\xi}_j \rangle_2), f) = f(\boldsymbol{\xi}_j) = s_{f,T_N}(\boldsymbol{\xi}_j),$$

where $(\,\cdot\,,\,\cdot\,)$ denotes de inner product in the dual space of S_N. Then $(\Psi_{k+2,k+1/2}(\langle \cdot - \boldsymbol{\xi}_j \rangle_2), s_{f,T_N} - f) = 0$, for all $i = 1, \ldots, N$ and here we have that $s_{f,T_N} - f$ is orthogonal to S_N.

Thus, for any $s \in S_N$ it is verified $((s_{f,T_N} - s, s_{f,T_N} - f))_{k+2} = 0$ and we obtain that

$$\|s - f\|_{k+2}^2 = \|s - s_{f,T_N} + s_{f,T_N} - f\|_{k+2} = \|s - s_{f,T_N}\|_{k+2}^2 + \|s_{f,T_N} - f\|_{k+2}^2.$$

Hence we have

$$\|s_{f,T_N} - f\|_{k+2}^2 \leq \|s - f\|_{k+2}^2$$

and taking $s = 0$ we conclude that

$$\|s_{f,T_N} - f\|_{k+2} \leq \|f\|_{k+2}. \tag{5.6}$$

From (5.5)– (5.6) and [62, Lemma 3.3.3] we can affirm that there exists $C > 0$, independent of f, such that

$$\|f - s_{f,T_N}\|_j \leq Ch^{k+2-j}\|f\|_{k+2}, \quad \forall\, j = 0, \ldots, k+2.$$

Then, there exists $C > 0$, independent of f such that

$$|f - s_{f,T_N}|_j \leq Ch^{k+2-j}\|f\|_{k+2}, \quad \forall\, j = 0, \ldots, k+2$$

and (5.4) holds. □

5.3 Smoothing variational splines by Generalized Wendland functions

Given a function $f \in H^{k+2}(\Omega)$ with $k \geq 0$ and a finite set of points $A = \{\boldsymbol{a}_1, \ldots, \boldsymbol{a}_n\} \subset \Omega$, we consider the functional $\theta : H^{k+1}(\Omega) \to \mathbb{R}^n$ given by

$$\theta v = (v(\boldsymbol{a}_i))_{1 \leq i \leq n} \in \mathbb{R}^n$$

and let Γ be the functional defined on $H^{k+2}(\Omega)$ by

$$\Gamma(v) = \langle \theta v - \theta f \rangle_n^2 + \varepsilon |v|_{k+2}^2.$$

Remark 5.3.1. *The first term of* $\Gamma(v)$ *indicates how well* v *approaches* f *in a least discrete square sense. The second term represents a classical smoothness measure weighted by the parameter* ε*.*

Let S_N be the radial basis functions space relative to the function $\psi_{k+2,k+\frac{1}{2}}$ and the centers set T_N and consider the following minimization problem: Find $\sigma \in S_N$ such that

$$\forall\, v \in S_N, \quad \Gamma(\sigma) \leq \Gamma(v). \tag{5.7}$$

Suppose that A is a $\mathbb{P}_{k+1}$-unisolvent set, that is,

$$\ker\theta \cap \mathbb{P}_{k+1}(\Omega) = \{0\} \tag{5.8}$$

and suppose that

$$\sup_{\boldsymbol{x}\in\Omega}\min_{\boldsymbol{a}\in A}\langle \boldsymbol{x}-\boldsymbol{a}\rangle_2 = o(\frac{1}{n}), \quad n\to+\infty. \tag{5.9}$$

Theorem 5.3.2. *Problem (5.7) has a unique solution, called smoothing variational spline in S_N associated with A, θf and ε, which is the unique solution of the following variational problem: Find $\sigma_n \in S_N$ such that*

$$\forall\, v\in S_N, \quad \langle\theta\sigma_n,\theta v\rangle_n + \varepsilon(\sigma_n,v)_{k+2} = \langle\theta f,\theta v\rangle_n. \tag{5.10}$$

Proof. From (5.8) we have that the bilinear application $\eta : H^{k+2}(\Omega)\times H^{k+2}(\Omega)\to\mathbb{R}$ given by

$$\eta(u,v) = 2(\langle\theta u,\theta v\rangle_n + \varepsilon(u,v)_{k+2})$$

is continuous and $H^{k+2}(\Omega)$-elliptic. Applying Lax-Milgram Lemma [7, Theorem 3.8.2] for η and the continuous linear application $\ell : H^{k+2}(\Omega)\to\mathbb{R}$ given by $\ell(v) = 2\langle\theta f,\theta v\rangle_n$ there exists $\sigma_n\in S_N$ such that

$$\forall\, v\in S_N, \quad \eta(\sigma_n,v) = \ell(v)$$

and (5.10) holds. Moreover σ_n minimizes the functional $\varphi(v) = \frac{1}{2}a(\sigma_n,v) - \ell(v) = \Gamma(v) - \langle\theta f\rangle_n^2$ and thus σ_n is the solution of Problem (5.7). □

For computing the solution function σ_n, for $i=1,\dots,N$, let $w_i\in S_N$ be the function

$$w_i(\boldsymbol{\xi}) = \psi_{k+2,k+\frac{1}{2}}(\langle\boldsymbol{\xi}-\boldsymbol{\xi}_i\rangle_2), \quad \forall\,\boldsymbol{\xi}\in\Omega,$$

then $\sigma_n = \sum_{i=1}^{N}\alpha_i w_i$. Applying Theorem 5.3.2 we obtain that $\boldsymbol{c} = (c_1,\dots,c_N)^\top \in \mathbb{R}^N$ is the solution of the linear system

$$(\mathcal{A}\mathcal{A}^\top + \varepsilon\mathcal{R})\mathbf{c} = \mathcal{A}\theta\mathbf{f},$$

where its coefficients are given as follows

$$\mathcal{A} = (\theta w_i)_{1\leq i\leq N} \in \mathbb{R}^{N,n}$$

and

$$\mathcal{R} = ((w_i, w_j)_{k+2})_{1\leq i,j\leq N}.$$

Now, we are going to prove that the smoothing variational spline σ_n converges to the function f under suitable hypotheses.

Theorem 5.3.3. *Suppose hypotheses (5.8)–(5.9) hold and that*

$$\varepsilon = o(1), \quad n \to +\infty \tag{5.11}$$

and

$$\frac{n^2 h^{2k+4}}{\varepsilon} = o(1), \quad n \to +\infty. \tag{5.12}$$

Then

$$\lim_{n\to+\infty} \|\sigma_n - f\|_{k+2} = 0.$$

Proof. Let s_{f,T_N} be the interpolation RBF of f relative to T_N from $\psi_{k+2,k+1/2}$, then $\Gamma(\sigma_n) \leq \Gamma(s_{f,T_n})$ and one has

$$\langle \theta\sigma_n - \theta f\rangle_n^2 + \varepsilon|\sigma_n|_{k+2}^2 \leq \langle \theta s_{f,T_N} - \theta f\rangle_n^2 + \varepsilon|s_{f,T_N}|_{k+2}^2. \tag{5.13}$$

From(5.4) there exists $C > 0$ such that

$$|s_{f,T_N}|_{k+2}^2 \leq C\|f\|_{k+2}^2 \tag{5.14}$$

and

$$\langle \theta f - \theta s_{f,T_N}\rangle_n^2 \leq n^2 C h^{2k+4}\|f\|_{k+2}^2. \tag{5.15}$$

Thus, from (5.13)–(5.15) we have that

$$|\sigma_n|_{ks2}^2 \leq \frac{1}{\varepsilon}\langle \theta f - \theta s_{f,T_N}\rangle_n^2 + |s_{f,T_N}|_{k+2}^2 \leq (\frac{n^2 h^{2k+4}}{\varepsilon} + 1)C\|f\|_{k+2}^2$$

and, from (5.12) we conclude that there exists $C_1 > 0$ and $n_1 \in \mathbb{N}$ such that

$$|\sigma_n|_{k+2}^2 \leq C_1, \quad \forall\, n \geq n_1. \tag{5.16}$$

Moreover, from (5.13)–(5.15) we have that

$$\langle \theta\sigma_n - \theta f\rangle_n^2 \leq (n^2 h^{2k+4} + \varepsilon) C |f|_{k+2}^2$$

and, from (5.11)–(5.12) there exists $C_2 > 0$ and $n_2 \in \mathbb{N}$ such that

$$\langle \theta\sigma_n - \theta f\rangle_n \leq C_2, \quad \forall\, n \geq n_2. \tag{5.17}$$

From (5.16)–(5.17) we can deduce that there exists a real constant $C > 0$ and $n_0 \in \mathbb{N}$ such that

$$\|\sigma_n\|_{k+2} \leq C, \quad n \geq n_0,$$

which means that the family $(\sigma_n)_{n\geq n_0}$ is bounded in S_N. It follows that there exists a subsequence $(\sigma_{n_l})_{l\in\mathbb{N}}$ with $\lim_{l\to+\infty} n_l = +\infty$ and an element $f^* \in H^{k+2}(\Omega)$ such that

$$\sigma_{n_l} \text{ converges weakly to } f^* \text{ in } H^{k+2}(\Omega).$$

Finally, reasoning as the points 3), 4) and 5) of the proof of [3, Theorem VI-3.2], we obtain the result. □

5.4 Numerical and graphical examples

To show the effectiveness of the method, we have computed two relative error estimations given by

$$E_i = \sqrt{\frac{\sum_{i=1}^{5000} (s_{f,T_N}(a_i) - f(a_i))^2}{\sum_{i=1}^{5000} f(a_i)^2}}, \quad E_s = \sqrt{\frac{\sum_{i=1}^{5000} (\sigma_n(a_i) - f(a_i))^2}{\sum_{i=1}^{5000} f(a_i)^2}},$$

being $\{a_1, \ldots, a_{5000}\} \subset I$ five thousands distinct random points, which are some approximations of the relative error of s_{f,T_N} and σ_n respectively, with respect to f in $L^2(I)$.

From Theorem 5.3.3, these relative error estimations E_i and E_s tends to 0 as n tends to $+\infty$, under adequate conditions.

Consider the Franke function given by

$$\begin{aligned} f(x,y) = \; & 0.75e^{-\frac{1}{10}(9x+1)^1-\frac{1}{49}(9y+1)^2} - 0.2e^{-\left((9x-7)^2+(9y-4)^2\right)}+ \\ & 0.5e^{-\frac{1}{4}\left((9x-3)^2+(9y-7)^2\right)} + 0.75e^{-\frac{1}{4}\left((9x-2)^2+(9y-2)^2\right)}, \end{aligned}$$

for any $(x,y) \in \Omega = (0,1) \times (0,1)$.

Moreover, the discrete space that we use to calculate the approximated solution σ_n is the RBFs space constructed from the Generalized Wendland function $\Psi_{2,1/2}$ and the centers set

$$T_N = \left\{ (\frac{i}{r-1}, \frac{j}{r-1}) \;\; i,j = 0,\ldots,r-1 \right\},$$

being $N = r^2$.

Table 5.2 shows the relative error estimation E_s from $r = 10$ ($N = \dim S_N = 100$) and $n = 1000$ for different values of ε. In this case $E_i = 5.8496 \times 10^{-3}$. We observe that there exists an optimum value of ε that could be estimated minimizing E_s.

ε	E_s
10^{-3}	6.1827×10^{-3}
10^{-6}	3.1421×10^{-3}
10^{-9}	2.9671×10^{-3}
10^{-12}	3.0629×10^{-3}
10^{-15}	3.0927×10^{-3}

Table 5.2 : Computed relative error estimation E_s from $r = 10$ and $n = 1000$ for different values of ε. $E_i = 5.8496 \times 10^{-3}$.

Table 5.3 shows the relative error estimation E_s from $r = 10$ ($N = \dim S_N = 100$) and $\varepsilon = 10^{-9}$ for different values of n. In this case $E_i = 5.8496 \times 10^{-3}$. We observe that E_s decreases when n increases and it seems that it tends to stabilize.

n	E_s
100	5.7736×10^{-3}
500	3.5199×10^{-3}
1000	3.0276×10^{-3}
2500	2.9316×10^{-3}
5000	2.7236×10^{-3}

Table 5.3 : Computed relative error estimation E_s from $r = 10$ and $\varepsilon = 10^{-9}$ for different values of n. $E_i = 5.8496 \times 10^{-3}$.

Table 5.4 shows the relative error estimations E_i and E_s from $n = 1000$ and $\varepsilon = 10^{-9}$ for different values of r. We observe that E_i and E_s decrease when r increases.

r	E_i	E_s
5	5.9404×10^{-2}	4.4007×10^{-2}
7	3.1667×10^{-2}	2.5946×10^{-2}
10	5.8496×10^{-3}	3.0276×10^{-3}
12	3.9227×10^{-3}	1.8972×10^{-3}

Table 5.4 : Computed relative error estimation E_s from $n = 1000$ and $\varepsilon = 10^{-9}$ for different values of r.

Figure 5.4.1 shows the graphs of the function f and Figure 5.4.2 shows the interpolation RBF s_{f,T_N} and the smoothing variational spline σ_n for $r = 10$, $n = 1000$ and $\varepsilon = 10^{-9}$, from left to right. We have obtained that $E_i = 5.8496 \times 10^{-3}$ and $E_s = 3.0276 \times 10^{-3}$.

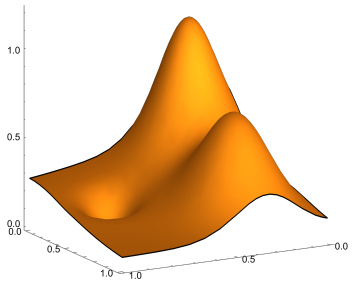

Figure 5.4.1: Graph of the function f.

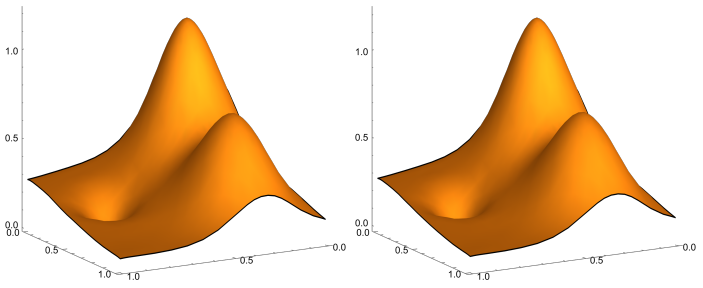

Figure 5.4.2: Graphs of the interpolation RBF s_{f,T_N} and the smoothing variational spline σ_n for $r = 10$, $n = 1000$ and $\varepsilon = 10^{-9}$, from left to right.

Chapter 6

Non-parametric Density Estimation

6.1 Introduction

The foundational statistical method of density estimation, as articulated by Silverman [106], boasts a multitude of applications spanning diverse fields. In the intricate landscape of finance, density estimation serves as a key element for risk assessment and asset pricing. It unveils market volatility, offering valuable insights that guide investment choices, as highlighted by Johannes [65]. Transitioning to healthcare, experts leverage density estimation for in-depth illness analysis and medical imaging. This strategic application facilitates the identification of irregularities, fostering a comprehensive understanding of how diseases propagate within populations [93].

Moreover, density estimation plays a pivotal role in environmental science, where it functions as a predictive tool for pollution levels [30]. Its contribution to supporting the formulation of effective environmental laws cannot be overstated [76]. Beyond these applications, density estimation emerges as an indispensable tool for anomaly detection and generative modeling within the realms of machine learning and artificial intelligence. Its impact resonates in applications such as fraud detection and data synthesis, underscoring its relevance in cutting-edge technological domains [50].

The utility of density estimation extends into the social sciences and urban planning, as noted by McArthur [84]. Criminologists employ its analytical power to dissect crime trends and craft preventive strategies [63].

Similarly, sociologists use it for meticulous population research and resource allocation. Urban planners, grappling with the complexities of modern cities, heavily rely on density estimation. It aids in examining complex issues like traffic congestion, land use, and the strategic direction of infrastructure development. The pervasive influence of density estimation is further exemplified in its role in refining chat-bots and recommendation engines. By enhancing language modeling, sentiment analysis, and recommendation systems in natural language processing, density estimation significantly contributes to the effective functioning of these technological applications [80]. These real-world use cases collectively emphasize the overarching importance of density estimation across a spectrum of academic disciplines and practical domains.

Nonparametric density estimation avoids the parametric assumptions in probabilistic modeling and reasoning, which achieves flexibility in data modeling while reducing the risk of model misspecification [105],[47]. Hence, nonparametric density estimation is an important research area in statistics. In this chapter, we focus on the estimation of univariate density functions, which is a classic problem in nonparametric statistics.

There are four main techniques for nonparametric estimation, i.e., histograms, orthogonal series, kernels, and splines. Histograms transform the continuous data into discrete data, while important information may be lost during the discretization process [45]. Kernel density estimation is one of the most famous methods for density estimation, which still remains an active research area (see [15] and references therein).

Asymmetric kernel estimators have been suggested as a solution to the well-known problem of boundary bias. This problem arises from using symmetric kernels, which assign weights outside the density support near zero. The statistical literature has introduced several kernels with asymmetric densities, including the gamma and modified gamma kernels [28], inverse and reciprocal inverse Gaussian kernels [20], lognormal and Birnbaum-Saunders (BS) kernels [64], and more recently, the generalized Birnbaum-Saunders (GBS) [88] and skewed GBS kernels [98]. It's important to note that the GBS kernels include special cases like the BS-power-exponential (BS-PE) and the BS-Student-t (BS-t) kernels. These kernels, such as lognormal, BS, GBS, and skewed GBS, are primarily designed for analyzing the densities of nonnegative heavy-tailed HT data, which are considered irregular data and are encountered in various fields like finance, actuarial science, web traffic, environmental science, and more. Research [88] has shown that the BS-PE kernel estimator for an unknown probability density function of nonnegative HT data can outperform other estimators, such as those using lognormal, BS, and BS-t kernels, in terms of integrated squared error (ISE).

The important part of any estimation procedure is the bandwidth selec-

tion method. The existing literature on bandwidth is quite rich (see [70],[79] and references therein). It should be noted that the least squares cross-validation (LSCV) formula in closed form was proposed in [70], which can be used to determine the bandwidth efficiently. In this paper, we use nonuniform kernel density estimators. By introducing the local error indicator attached to the class of data points, we design an adaptive refinement strategy, which increases the approximation capability of the local density estimator. The numerical experiments show that our adaptive local density estimation produces a smaller approximation errors. The adaptive approach we used yielded reasonable results, which are shown in graphs at the end of this work.

The remainder of the chapter is organized as follows. In the next section we give the basic notions of non-parametric density estimation. In Section 3, we detail the proposed methodology for density estimation with the adaptive bandwidth refinement strategy. Numerical experiments are provided in Section 4. Finally, conclusions will be included in Chapter 7.

6.2 Density estimation

In practice, the probability density function (PDF) of some observable random variable X is in general unknown. All we have are n observations $X_1, ..., X_n$ of X and our task is to use these n values to estimate $f(x)$. We shall assume that the n observations are independent and that they all indeed come from the same distribution, namely $f(x)$. That is, we will be concerned with estimating $f(x)$ at a certain value x from *i.i.d.* data (independent and identically distributed).

A density estimate is created by extrapolating the density function from the observed data. Basically, we are interested in finding an unknown function $f(x)$ given only random samples or observations spread over this function. More formally, the goal of density estimation is to infer the probability density function, or pdf, from observations of a random variable.

The distribution from which the data set is produced is a crucial question when a dataset is accessible. In parametric estimation, a distribution is hypothesized before the parameters are estimated; nevertheless, the validity of the analysis is called into doubt if the assumed distribution is incorrect. However, no distributional presumptions are assumed while doing nonparametric density estimation. As a result, it became a widely used technique for estimating density. In this research, we use kernel density estimation which is one of the most effective methods for nonparametric density estimation.

6.2.1 Kernel density estimation

Kernel Density Estimation (KDE) stands as an effective non-parametric statistical technique employed to estimate the probability density function of continuous random variables. Its versatility lies in its ability to capture the inherent distributions of data without imposing restrictive assumptions on their forms. This adaptability has led to KDE's widespread adoption across diverse fields, ranging from environmental research to the complexities of finance. The foundations of KDE were laid by Rosenblatt (1956) [96] and Parzen (1962) [92], whose pioneering work laid the theoretical groundwork for this powerful method. Over the years, KDE has undergone significant evolution, emerging as an indispensable tool for contemporary statistical analysis and data visualization.

The applicability of KDE extends across various scientific domains owing to its adaptability and wide-ranging utility. Silverman (1986) [106] played a pivotal role in advancing adaptive KDE in the realm of ecology, enhancing its ability to adjust to dynamic spatial structures and evolving data patterns. Scott (1992) [102] further broadened the scope of KDE by introducing methods to handle spatial data within spatial statistics. This extension opened avenues for KDE's application in Geographic Information Systems (GIS) and spatial modeling, making it a valuable tool for researchers dealing with geographical data.

Beyond its contributions to ecology and spatial statistics, KDE has found practical applications in the financial sector. Fan (1996) [42] notes its significance in offering insights into asset return distributions, thereby aiding in risk assessment and portfolio optimization. These references underscore the pivotal role of KDE in modern statistical practices and its expansive use in domains requiring precise estimates of data densities. However, it is essential to recognize that these references represent only a fraction of the extensive literature on KDE, emphasizing its enduring impact and continuous relevance in advancing statistical methodologies. The versatility of KDE, coupled with its continuous refinement, positions it as a cornerstone in contemporary statistical analysis, offering a robust and flexible approach to estimate probability density functions across a multitude of scientific and applied disciplines.

It is easy to generalize the naive estimator to overcome some of its difficulties. Replace the weight function w by a kernel function K which satisfies the condition

$$\int_{-\infty}^{\infty} K(x)dx = 1.$$

Usually, but not always, K will be a symmetric probability density function,

the normal density, for instance, or the weight function w used in the definition of the naive estimator. By analogy with the definition of the naive estimator, the kernel estimator with kernel K is defined by

$$\widehat{f}_n(x) = \frac{1}{nh} \sum_{i=1}^{n} K\left(\frac{x_i - x}{h}\right), \tag{6.1}$$

where h is the window width, also called the smoothing parameter or bandwidth by some authors. We shall consider some mathematical properties of the kernel estimator later, but first of all an intuitive discussion with some examples may be helpful.

Just as the naive estimator can be considered as a sum of 'boxes' centred at the observations, the kernel estimator is a sum of 'bumps' placed at the observations. The kernel function K determines the shape of the bumps while the window width h determines their width where the individual bumps $n^{-1}h^{-1}K\left\{\left(x - X_{\mathrm{i}}\right)/h\right\}$ are shown as well as the estimate $\hat{f}$ constructed by adding them up.

According to Hart (1997)[53], a kernel function that satisfies the following equations would allow for the minimization of the mean integrated squared error.

(i) $\int K(u)du = 1$

(ii) $\int uK(u)du = 0$

(iii) $\int u^2K(u)du = k_2 \neq 0 < \infty$

(iv) $\int K^2(u)du = I_2 < \infty$

The kernel must be a probability density function with a mean of zero according to the first two equations. These two requirements enable the function to be symmetric and have a maximum near zero, which are great characteristics for estimating data with an unknown distribution. To enable the computation of the AMISE, the other two equations must be finite. According to B.W. Silverman (1986) [106], the kernel functions must also be continuous and differentiable in order for $f(x)$ to inherit these characteristics. As we mentioned before, some kernels don't satisfy some of these conditions. Nevertheless, they can still be used. However, many density functions can satisfy these requirements, hence a list of some of the most popular choices as stated in Silverman (1986)[106] is provided. As examples, Gaussian, Epanechnikov and Quartic kernels could be considered.

6.2.2 Approximated mean integrated squared error

Mean integrated squared error (MISE) is the most popular used measure of accuracy of $\widehat{f}(x)$ according to Silverman (1986)[106]. It can be expressed as following:

$$MISE\left(\widehat{f}(x)\right) = \int E\left\{\widehat{f}(x) - f(x)\right\}^2 dx.$$

As stated in Parzen(1962)[92], the the minimization of the approximated mean integrated squared error AMISE will be given by:

$$AMISE\left(\widehat{f}(x)\right) = \frac{1}{4}h^4 k_2^2 \int \left(f^{(2)}(x)\right)^2 dx + \frac{1}{nh}\int K^2(u)du.$$

It is also shown in Parzen(1962)[92] that the optimal value of h can be given by:

$$h_a = k_2^{-\frac{2}{5}} \left(\int K^2(u)du\right)^{\frac{1}{5}} \left(\int \left(f^{(2)}(x)\right)^2 dx\right)^{-\frac{1}{5}} n^{-\frac{1}{5}}. \tag{6.2}$$

These approximation equations may be solved by substitution if the density function $f(x)$ of our observed data is known. With the exception of $\int \left(f^{(2)}(x)\right)^2 dx$, this equation's components have all been solved for. The observed data's density function will usually be unknown. $f^{(2)}(x)$ will likewise be unknown as a result. As stated by Rahman et al. (1996)[94], an estimate of $f^{(2)}(x)$ is required in this situation and will be defined as follows:

$$\widehat{f}^{(2)}(x) = \frac{1}{nh}\sum_{i=1}^{n} K^{(2)}\left(\frac{x - X_i}{h}\right).$$

Using a standard family of distributions to give the term $\int \left(f^{(2)}(x)\right)^2 dx$ in the formula (6.2) a value is a fairly simple and straightforward method (see Silverman (1986)[106]).

$$\int \left(f^{(2)}(x)\right)^2 dx = \frac{3}{8\sigma^5\sqrt{\pi}}.$$

Hence, for the Gaussian kernel, we can conclude that

$$AMISE = \frac{3h_a^4}{32\sigma^5\sqrt{\pi}} + \frac{1}{2nh_a\sqrt{\pi}}$$

And, in this case, an optimal value of the smoothing parameter h will be

$$h_a = \left(\frac{4}{3n}\right)^{\frac{1}{5}} \sigma \simeq 1.06\sigma n^{-\frac{1}{5}}.$$

This last result was concluded by Silverman (1986)[106] and what is now called the normal distribution approximation, Gaussian approximation, or Silverman's *rule of thumb*.

When an h value enhances the fit for long-tailed, skewed, or bimodal mixed distributions, it is seen as more robust. Empirically, this is frequently accomplished by substituting the following parameter A for the standard deviation σ:

$$A = \min\left(\sigma, \frac{IQR}{1.34}\right)$$

where IQR is the interquartile range.

Another modification was suggested by Silverman (1986)[106], that will improve the model, is to reduce the factor from 1.06 to 0.9. The final formula would therefore be:

$$h = 0.9 \min\left(\sigma, \frac{IQR}{1.34}\right) n^{-\frac{1}{5}} \tag{6.3}$$

where n is the sample size.

6.2.3 BS-PE kernel estimator

Given the observations $x_1, \ldots, x_n$ from a random sample $X_1, \ldots, X_n$, the classical kernel estimator of the unknown true density f is given in (6.1) where K is a function called kernel that satisfies $\int K(x)dx = 1$ and h a smoothing parameter known as bandwidth. Generally, K corresponds to a symmetric density, as in the case of the Gaussian kernel. As aforementioned, expression given in (6.1) is classically used for estimating nonparametrically a density with support in $\mathbb{R}$. However, when nonnegative data are modeled, (6.1) leads to the boundary bias problem, because it assigns weight outside the density support near $x = 0$. Consider the Birnbaum-Saunders power-exponential (BS-PE) kernel estimator of unknown asymmetric densities with nonnegative support, which is is given by [88]

$$\widehat{f}(x) = \frac{1}{n}\sum_{i=1}^{n} K_{h,x}\left(x_i\right), \tag{6.4}$$

where $K_{h,x}$ is a kernel corresponding to an asymmetric density with nonnegative support of parameters h (bandwidth) and x (point where the density is estimated) and

$$K_{h,x}(x_i) = \frac{a}{2^{\frac{1}{2a}}\Gamma(\frac{1}{2a})\sqrt{4h}} \left(\frac{1}{\sqrt{xx_i}} + \sqrt{\frac{x}{x_i^3}} \right) exp\left(\frac{-1}{2h^a} \left(\frac{x_i}{x} + \frac{x}{x_i} - 2 \right)^a \right) (6.5)$$

where $x > 0$ is the point where the density is estimated, $h > 0$ is a smoothing parameter and $a > 0$ is a fixed parameter.

6.3 Methodology

The primary phases of our approach to creating a probability density function for n-independent, identically distributed (iid) continuous random variables are covered in this section. The next subsections provide a detailed explanation of our methodology using algorithms.

6.3.1 Grouping procedures

Let $X_1, \ldots, X_n$ be independent and identically distributed (iid) continuous random variables with an unknown probability density function (pdf) f.

In the following, we present examples generated according to the normal and exponential densities for different sample size $n = 100, 50$.

From Graphics 1 and 2 in Figure 6.3.1, it is easy to observe the benefit of decomposition of the sample into different regions with respect to its densities. We note that the decomposition delimits in a rather efficient way the two or more regions of the densities. This will be efficiently performed through the coming algorithm.

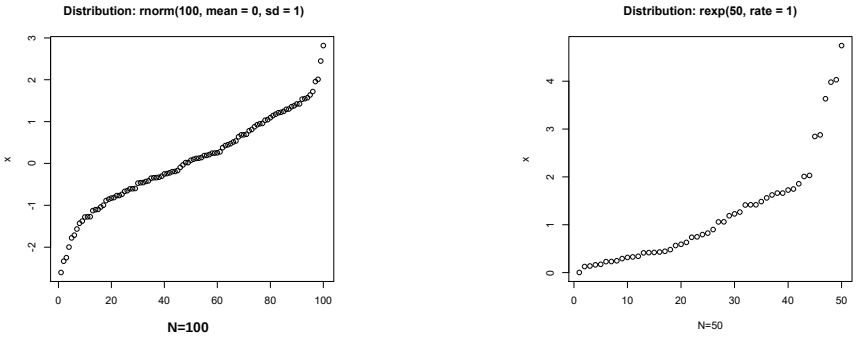

Figure 6.3.1: Examples of datasets of normal and exponential distributions.

We propose an algorithm for grouping data. It is based on the notion of distance between observations [124].
Let $Y_1, \ldots, Y_k$, with $k \leq n$, be a subset of $X_1, \ldots, X_n$.

Algorithm 1

1. We start with the data $y_1, \ldots, y_k$ placed in order, i.e., $y_{(1)} \leq y_{(2)} \leq \ldots \leq y_{(k)}$.

2. Compute the distance d_i for each pair of observations (y_i, y_{i+1}), where $d_i(y_i, y_{i+1}) = |y_i - y_{i+1}|$.

3. We define the constant ε which displays the dispersion distances already calculated as $\varepsilon = \sqrt{Var(d_i)}$.

4. Grouping procedure:

   (i) $S_1^k = \{y_i; d_i \leq \varepsilon\}$;

   (ii) Once $d_i > \varepsilon$, we stop the test, and we consider the rest of observations as being the set low-density region S_2^k.

Suppose that the algorithm decomposes the sample with respect to its density into k regions $S_1, S_2, \ldots, S_k$. Let h_j, $j = 1, \ldots, k$, denote the band-

width assigned to the observations of S_j, respectively. Then

$$\widehat{f}(x) = \sum_{j=1}^{k} \sum_{i=1}^{N_j} \frac{1}{nh_j} K\left(\frac{x - x_{(j)}^i}{h_j}\right) \chi_{x_{(j)}^i \in S_{(j)}}.$$

6.3.2 A residual-based posteriori error estimator

Since the true density function f is unknown, we define, as suggested in [125], a local error indicator attached with the class S_i as follows:

$$\tau_i = -\sum_{j=1}^{N_i} \frac{1}{N_i} \log\left(\widehat{f}(x_i^j)\right), \tag{6.6}$$

where $x_i^1, \ldots, x_i^{N_i}$ be all the sampling points in $\{x_j, j \in \{1, \ldots, N\}\}$ located in the class S_i. Note that τ_i is an estimate of information entropy restricted on the class S_i;

$$H(f, \widehat{f}) \mid_{S_i} = -\int_{I_i} f(x) \log(\widehat{f}(x)) dx,$$

and $I_i = [\min(S_i), \max(S_i)]$.

6.3.3 Adaptive refinement strategy

Compute bandwidth $\longrightarrow$ Error Estimate for each bandwidth $\longrightarrow$ Mark and Refine.

Inspired by the adaptive refinement strategy [89], in the numerical analysis, we introduced the adaptive refinement strategy to compute a sequence of estimates that converged to the true probability density function. As the error indicator for each interval was available, we marked each class S_i to be refined that had a large error. In order to find the intervals with a large error efficiently, we adopted the refinement strategy given in Algorithm 2.

Algorithm 2:

Input: $X_1, \ldots, X_n$; d_i; $\varepsilon = \sqrt{Var(d_i)}$, S_1, S_2, errors indicators τ_i, $i = 1, 2$, parameters $0 < \theta$ and $\nu < 1$, $S := [S_1, S_2]$.

Output: A new classification S'.

Calculate $\tau_{max} = \max(\tau_i)$ and $\tau := \sum \tau_i$,

$Sum := 0, \mu = 1;$
while $sum < \theta\tau$
$\mu = \mu - \nu$
for all S_i
if S_i is not marked
if $\tau_i > \mu\tau_{max}$ then mark the interval S_i, refine S_i, by a new class.

$sum := sum + \tau_i$

Morin et al. [89] employed **Algorithm 2**, specifically referred to as Algorithm 5.1 (Marking algorithm), drawing on Dörfler's foundational work [36]. The convergence proof, expounded in those references, establishes the algorithm's reliability in practical applications. This integration of insights ensures **Algorithm 2** not only addresses computational challenges effectively but also boasts a robust theoretical underpinning, as outlined in the cited works.

We have already covered the grouping procedure in **Algorithm 1** and then constructed a new classification utilizing the adaptive refinement strategy in **Algorithm 2.** It is now time to demonstrate **Algorithm 3**, which completes the task and yields the final density estimation $\widehat{f}(x)$.

Algorithm 3:

Input: $X_1, \ldots, X_n$;

Output: $\widehat{f}(x) = \sum_{j=1}^{k} \sum_{i=1}^{N_j} \frac{1}{nh_{(j)}} K\left(\frac{x - x^i_{(j)}}{h_{(j)}}\right) \chi_{x^i_{(j)} \in S_{(j)}}$.

Step 1 Grouping

Step 2 Initialize $S = [S_1, S_2, \ldots]$

Step 3 Compute h_i, $1 \leq i \leq card(S)$

Step 4 Evaluate the error τ_i

Step 5 Apply **Algorithm 2** to get a refined S'

Step 6 If $S' \neq S$, update $S = S'$ and go to Step 3

Step 7 $\widehat{f}(x)$.

6.4 Numerical experiments

In this section, we shall operationalize our methodology. Specifically, we will conduct estimations for two probability density functions, one characterized by symmetry, and the other displaying asymmetry. These estimations will be documented in the ensuing table, incorporating the respective kernel functions employed. Subsequently, we will present a thorough exposition of the results, complemented by accompanying graphical representations.

Table 1. Distributions in our experiments.

	Distribution	Density	Parameters
D1	Normal	$\frac{1}{\sigma\sqrt{2\pi}} \exp\left(-\frac{1}{2}\left(\frac{x-\mu}{\sigma}\right)^2\right)$	$(\mu, \sigma) = (0, 1)$
D2	lognormal	$\frac{1}{x\sigma\sqrt{2\pi}} \exp\left(\frac{-1}{2\sigma^2}(\ln(x) - \mu)^2\right), x > 0$	$(\mu, \sigma) = (1, 1)$

6.4.1 Density estimation for rnorm distribution

In this subsection, we implement our strategy to investigate the probability density function of a normal distribution, utilizing the Gaussian function as our kernel density estimator. Our initial dataset is visualized in Figure 6.4.2, comprising 200 randomly sampled points from a normal distribution, denoted as D1 with parameters $(\mu, \sigma) = (0, 1)$.

Firstly, to decompose the dataset, we apply **Algorithm 2** resulting in the dataset's division into three distinct classes, as illustrated in Figure 6.4.2.

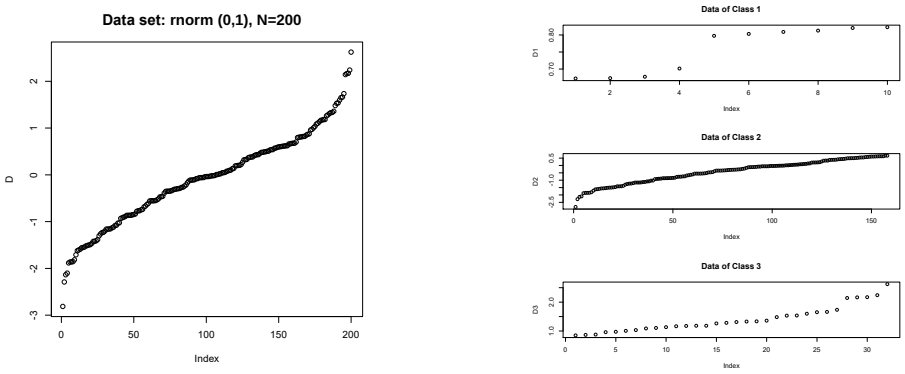

Figure 6.4.2: Normal distribution dataset (left), and its decomposition (right).

Secondly, it is necessary to construct the density estimations for all classes. This is in order to obtain the local error τ_i which is defined above in formula (6.6) and the associated bandwidth at each class. In this step, we use the

Gaussian function as a kernel estimator and Silverman's *rule of thumb* for bandwidth selection. Figure 6.4.3 shows the density estimation for each class.

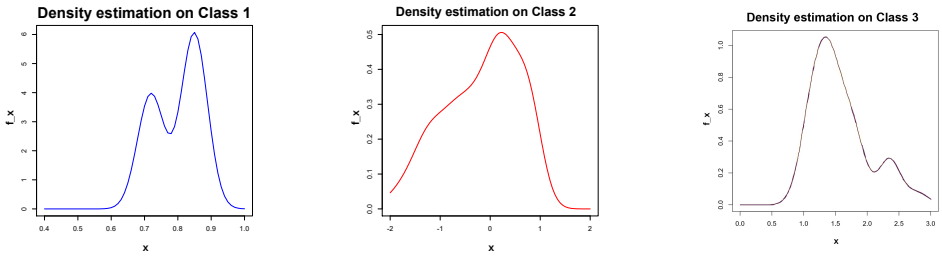

Figure 6.4.3: Density estimation for each class.

Finally, we are in a position to apply **Algorithm 3** to obtain an estimation for our probability density function. In this case the final estimation will be defined as follows

$$\widehat{f}(x) = \sum_{j=1}^{3} \sum_{x_{(j)}^i \in S_{(j)}} \frac{1}{nh_j} K\left(\frac{x - x_{(j)}^i}{h_j}\right) .$$

The final density estimation, displayed alongside the original probability density function, is visualized in Figure 6.4.4.

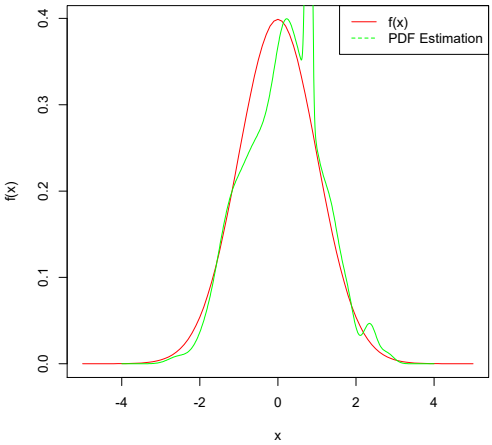

Figure 6.4.4: True pdf and final kernel estimator for D1(rnorm) with $n = 200$.

6.4.2 Density estimation for Log-normal distribution

In this section, we apply our approach to estimate the probability density function of an asymmetric distribution which is Log-normal distribution. We employ the (BS-PE) function, mentioned above in Equation (6.5) with $a = 2$, as our kernel density estimator. The initial dataset is depicted in Figure 6.4.5, consisting of 800 randomly sampled points from a Log-normal distribution, which was denoted in the table above as **D2** with parameters $(\mu, \sigma) = (0, 1)$.

Firstly, to regroup the dataset, we implement **Algorithm 2**, resulting in the dataset's division into four distinct classes, as depicted in Figure 6.4.5.

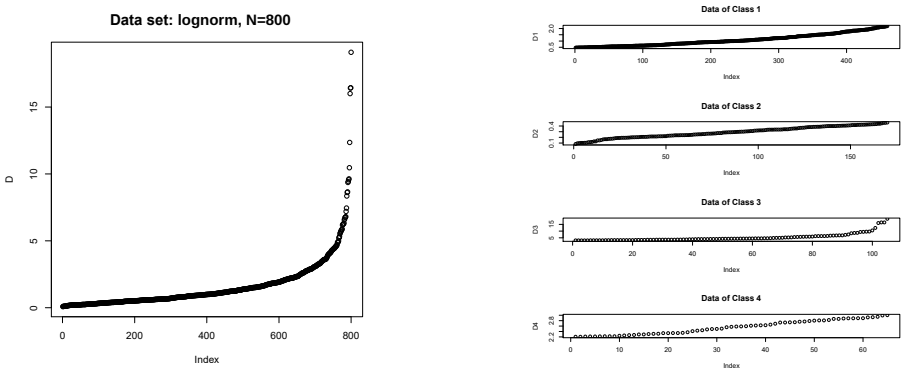

Figure 6.4.5: Log-normal distribution dataset (left), and its decomposition (right).

Secondly, it is necessary to construct the density estimations for all classes. This is in order to obtain the local error τ_i which is defined above in formula (6.6) and the associated bandwidth at each class. In this step, we use the (BS-PE) function as a kernel estimator. Figure 6.4.6 shows the density estimation for each class.

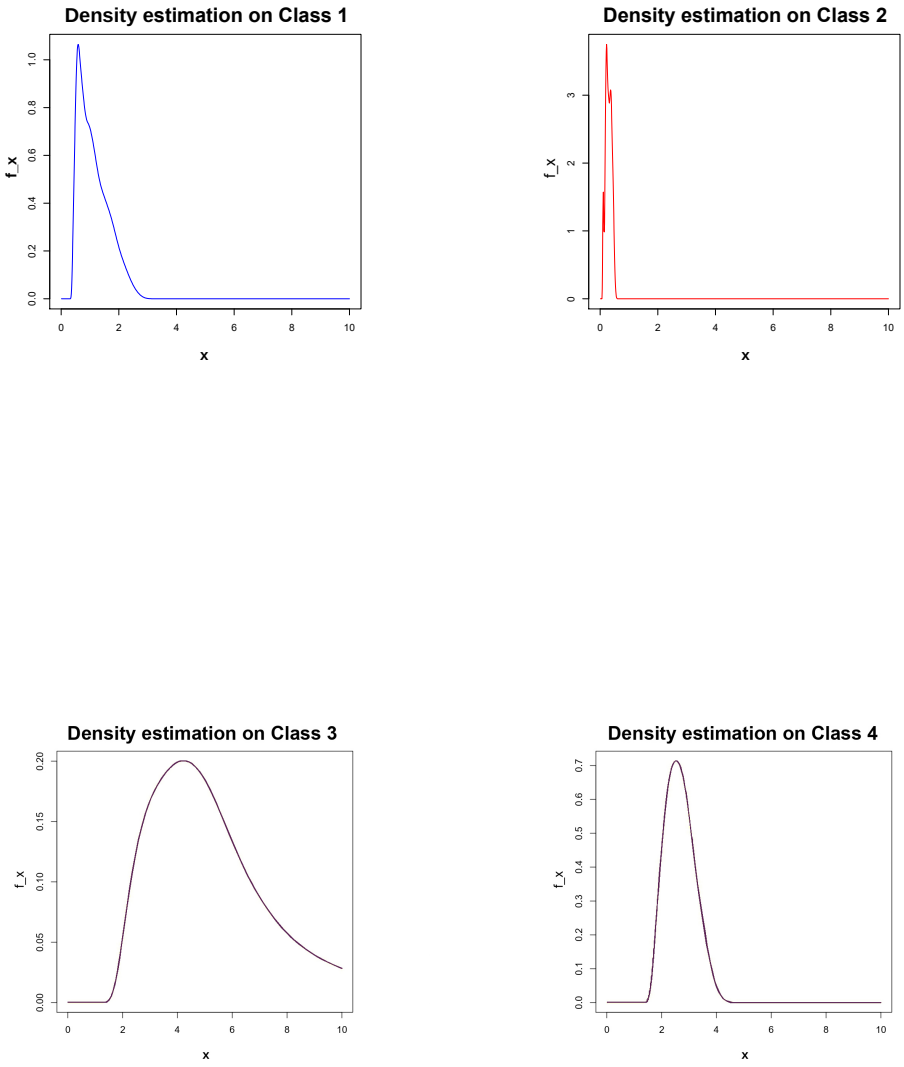

Figure 6.4.6: Density estimation for each class.

Finally, we are in a position to apply **Algorithm 3** to obtain an estimation for our probability density function. In this case the final estimation

will be defined as follows

$$\widehat{f}(x) = \sum_{j=1}^{4} \sum_{x_{(j)}^i \in S_{(j)}} \frac{1}{n} K_{h_j,x}\left(x_{(j)}^i\right),$$

where $K_{h_j,x}$ is the (BS-PE) function, mentioned above in Equation (6.5) with $a = 2$, as our kernel density estimator.

The final density estimation, displayed alongside the original probability density function, is visualized in Figure 6.4.7.

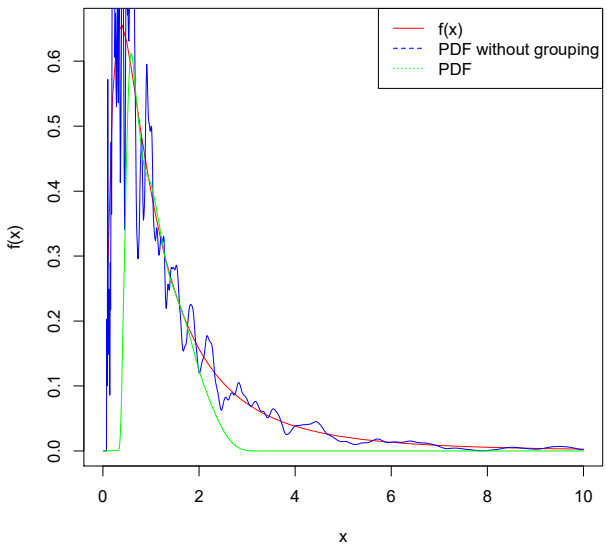

Figure 6.4.7: True pdf and final density estimator for D2(lognorm) with $n = 800$.

Chapter 7

Conclusions and future work

7.1 Conclusions

In this concluding chapter, we synthesize the novel insights gleaned from our exploration into the applications of Radial Basis Functions (RBFs) in diverse mathematical domains. Through our four key applications addressing Second Kind Volterra Integral Equation Systems, Numerical Solutions of Linear Volterra Integro-Differential Problems, Approximation of bivariate functions by Generalized Wendland RBFs and Nonparametric Density Estimation, our conclusions illuminate the collective impact on interpolation, approximation, and data science. As we disclose the significance of these new developments, this chapter serves as the culmination of our research journey, offering insights, reflections, and paving the way for future investigations in the dynamic field of RBF applications. We have also prepared some articles with the content of some of the chapters:

- The content of our first article titled "Numerical Solution of Linear Volterra Integral Equation Systems of Second Kind by RBFs" was shown in Section 4.3. We conclude that the above presented experiments (see Tables 4.2 – 4.4) confirm the validity of the method and justify the convergence results given in Theorem 4.3.3 and Corollary 4.3.7. In fact, in all our experiments (see the Examples 4.3.8–4.3.10), by using small values of N, we obtain a significant good order of approximation using the relative errors E_1 and E_2 considered. So, our original goal to devise an appropriate variational procedure that is capable of solving this type of problems in a precise and efficient way has been completely

accomplished.

As compared with the other recently published works, for example [60, 57, 69, 90, 68], they do not study convergence results. Likewise, our technique gives an acceptable accuracy with a small use of data, resulting also a low computational cost.

In ([57], Tables 1 and 2) the mean of the error is of the order 10^{-5}. We have obtained the same order of error with only 50 points.

In [90] the authors use Bernstein polynomials and the degree of its approximation is of order 10^{-4} in most of the tables. The same happens in ([68], Table 4), it uses the simple block-by-block method and its degree of approximation is about 10^{-3}.

- In section 4.4, the contents of our second article under the title "Numerical solution of a linear Volterra integro-differential equations" were presented. In this study, we proposed and developed an approximation method for solving numerically a linear Volterra integro-differential problem. This numerical method is based on the associated variational formulation of this type of problems, in the appropriate finite-dimensional space generated by a finite set of Wendland RBFs. Apart from proving the existence and uniqueness of the corresponding solution of the discrete problem, we have also given two convergence theoretical results which have also been finally endorsed by the numerical experiments (see examples 4.4.11 – 4.4.14) carried out in the corresponding subsection 4.4.5. There, the tables (4.5 – 4.8) of the computed relative errors associated to the four chosen significant examples ratify both the convergence theoretical ratio, as well as the good approach of the numerical procedure.

- We included the content of our third article titled "Approximation of bivariate functions using Generalized Wendland RBFs" in Chapter 5. Apparently the method to develop this work is known, but in reality the use of the Generalized Wendland compactly supported RBFs is totally new. In fact, the question that one can be asked is why use these functions?. The answer totally convincing is that the time cost when programming these functions is quite reduced, if we compare it, for example, with the variational splines mentioned in the references. Moreover, the order of the degree of approximation, represented with the calculation of the estimate of the interpolation error E_i and smoothing error E_s, with 500-1000 approximation points are of order between 1.8972×10^{-3} and 3.0276×10^{-3} in most cases in tables 5.2 –5.4 while

in Table 2 subsection 5.2.2 of [71] the degree of approximation with 900 points of approximation are $8.8... \times 10^{-3}$. All this shows the improvement and the effectiveness of the approximation method studied in this article.

- In Chapter 6, we discussed adaptive nonparametric estimation of bandwidth using mixtures of kernel estimators for symmetric and length-biased data. Addressing the challenges of density estimation in the era of Big Data, our research highlights the significance of efficient tools for estimating probability distributions from extensive datasets. The incorporation of local adaptation techniques and genetic algorithms proves crucial, emphasizing the need to identify optimal combinations for real-world applications. Experimental results validate the effectiveness of our refinement procedures and algorithms, demonstrating satisfactory outcomes for both symmetric (See Figures 6.4.2 to 6.4.4) and asymmetric distributions (See Figures 6.4.5 to 6.4.7).

These conclusions collectively mark significant strides in the understanding and application of Radial Basis Functions, offering valuable insights into their performance across diverse problem domains.

7.2 Future work

In order to do more research on these topics in the future, among some of the open problems that we consider are:

- Regarding the methods we used to solve Volterra integral and integro-differential equations in Chapter 4 and the approximation method we used in Chapter 5:
  - Numerical comparisons between our methods and many others in the literature.
  - The theoretical study of the order of convergence of the presented methods.
  - The adaptation of our first procedure (in Section 4.3) to find a numerical solution of the linear systems of 2D Volterra integral equations of second kind by means of appropriate radial basis functions.
  - The adaptation of our second procedure (in Section 4.4) to find a numerical solution of a linear system of Volterra integro-differential equations.

– The application of Generalized Wendland RBFs in solving integral or/and differential equations.

- Regarding the procedures we used for nonparametric density estimation:

– Future work will focus on further testing with real data samples and exploration of additional kernels and bandwidth selection methods to enhance the versatility and applicability of our proposed strategies.

– The theoretical study of the order of convergence of the presented methodology shown in Section 6.3.

Bibliography

[1] Aggarwal, S.; Gupta, A.R. Solution of Linear Volterra Integro-Differential Equations of Second Kind Using Kamal Transform. *J. Emerg. Technol. Innov. Res.* **2019**, *6*, 741–747. 37

[2] Aggarwal, S.; Sharma, N.; Chauhan, R. Solution of Linear Volterra Integral Equations of Second Kind Using Mohand Transform. *IJRAT* **2018**, *6(11)*, 3098–3102. 37

[3] Arcangéli, R.; López de Silanes, M. C.; Torrens, J. J. *Multidimensional Minimizing Splines, Theory and Applications*. Kluber Academic Publisher, Boston, 2004. 75

[4] Assari, P.; Dehghan, M. A meshless local Galerkin method for solving Volterra integral equations deduced from nonlinear fractional differential equations using the moving least squares technique. *Appl. Numer. Math.* **2019**, *143*, 276–299. 41

[5] Atkinson, K. E. A survey of numerical methods for Fredholm integral equations of the second kind. *IAM, Philadelphia,* 1976.

[6] Atkinson, K. *The Numerical Solution of Integral Equations of the Second Kind*. Cambridge University Press, 1997. 39, 40

[7] Atkinson, K.; Weiman, H. *Theoretical Numerical Analysis. A Functional Analysis Framework*, 2nd ed.; Springer: New York, NY, USA, 2005. 9, 10, 41, 44, 45, 49, 73

[8] Attéia, M. Fonctions splines définies sur un ensemble convexe. *Numer. Math.* **1968**, *12*, 192–210. 67

[9] Aziz, I.; Siraj-ul-Islam. New algorithms for the numerical solution of nonlinear Fredholm and Volterra integral equations using Haar wavelets. *J. Comput. Appl. Math.* **2013**, *239*, 333–345. 36

[10] Babolian, E.; Shahsavaran, A. Numerical solution of nonlinear Fredholm integral equations of the second kind using Haar wavelets. *J. Comput. Appl. Math.* **2009**, *225*, 87–95. 36

[11] Baker, C.T.H. Numerical Analysis of Volterra Functional and Integral Equations. In *The State of the Art in Numerical Analysis*; Duff, I.S., Watson, G.A., Eds.; Oxford University Press, New York, NY, USA, 1997; pp. 193–222. 35, 36

[12] Balakumar, V.; Murugesan, K. Numerical solution of Volterra integral-algebraic equations using block pulse functions. *Appl. Math. Comput.* **2015**, *263*, 165–170. 37

[13] Berenguer, M.I.; Gámez, D. ; Garralda-Guillém, A.I. ; Ruiz Galán, M. ; Serrano Pérez, M.C. Analytical Techniques for a Numerical Solution of the Linear Volterra Integral Equation of the Second Kind. *Abstr. Appl. Anal.* **2009**, 149367. doi.org/10.1155/2009/149367. 37

[14] Berenguer, M.I.; Gámez, D. ; Garralda-Guillém, A.I. ; Serrano Pérez, M.C. Nonlinear Volterra Integral Equation of the Second Kind and Biorthogonal Systems. *Abstr. Appl. Anal.* **2010**, 135216. doi:10.1155/2010/135216. 37

[15] Bhattacharya, A.; Dunson, D.B. Nonparametric Bayesian density estimation on manifolds with applications to planar shapes. *Biometrika* **2010**, *97*, 851–865. https://doi.org/10.1093/biomet/asq044. 80

[16] Bjornsson, H.; Hafstein, S. Advanced algorithm for interpolation with Wendland functions. In *Informatics in Control, Automation and Robotics (ICINCO 2019)*; Lecture Notes in Electrical Engineering; Gusikhin O., Madani K., Zaytoon J., Eds.; Springer: New York, NY, USA, 2019; pp. 99–117. 41

[17] Bochner, S. Monotone funktionen, stieltjessche integrale and harmonische analyse, *Math. Ann.* Vol 108, pp. 378–410, 1933. 25, 30

[18] Brézis, H. *Analyse fonctionnelle. Théorie et applications.* Collection of Applied Mathematics for the Master's Degree. Masson, Paris, 1983. ISBN: 2-225-77198-7. 5, 6, 7, 8, 9

[19] Brézis, H. *Functional Analysis, Sobolev Spaces and Partial Differential Equations*, Springer, New York, 2011. 3, 5, 57

[20] Brunner, H. 1896–1996: One hundred years of Volterra integral equations of the first kind. *Appl. Numer. Math.* **1997**, *24*, 83–93. 36

[21] Brunner, H.; Pedas, A.; Vainikko, G. The piecewise polynomial collocation method for nonlinear weakly singular Volterra equations. *Math. Comp.* **1999**, *68*, 1079–1095. 36

[22] Buhmann, M. D. Radial functions on compact support, *Proc. Edin. Math. Soc. II.* Vol. 41 , pp. 33–46, 1998. 33

[23] Buhmann, M. D. *Radial Basis Functions: Theory and Implementations.* Cambridge University Press, 2003. 26

[24] Buhmann, M. D. ;Michelli, C.A. Multivariate interpolation in odd-dimensional Euclidean spaces using multiquadrics, *Const. Approx.* Vol. 6 (12) , pp. 21–34, 1990. 23

[25] Buhmann, M. D.; Michelli, C.A. Multiquadric interpolation improved, *Computers Math. Applic.* Vol. 24 (12) , pp. 21–26, 1992. 23

[26] Cahlon, B. Numerical solution of nonlinear Volterra integral equations. *J. Comput. Appl. Math.* **1981**, *7*, 121–128. 35

[27] Chauhan, R.; Aggarwal, S. Laplace Transform for Convolution Type Linear Volterra Integral Equation of Second Kind. *J. Adv. Res. Appl. Math. Stat.* **2019**, *4*, 1–7. 37

[28] Chen, S.X. Probability Density Function Estimation Using Gamma Kernels. *Ann. Instit. Statist. Math.* **2000**, *52*, 471–480. `https://doi.org/10.1023/A:1004165218295`. 80

[29] Chui, C.K.; Stoeckler, J.; Ward, J. D. Analytic wavelets generated by radial functions, *Adv. Comput. Math.* Vol. 5 , pp. 95–123, 1996. 23

[30] Comess, S.; Chang, H.H.; Warren, J.L. A Bayesian framework for incorporating exposure uncertainty into health analyses with application to air pollution and stillbirth. *Biostatistics* **2024**, *25*, 20–39. `https://doi.org/10.1093/biostatistics/kxac034`. 79

[31] Corduneanu, C.; Sandberg, I.W. *Volterra Equations and Applications.* Gordon and Breach, Amsterdam, The Netherlands, 2000. 35

[32] Şahn, N.; Yüzbaşi, Ş.; Glsu, M. A collocation approach for solving systems of linear Volterra integral equations with variable coefficients. *Comput. Math. Appl.* **2011**, *62*, 755–769. 37

[33] Daubechies I. *Ten Lectures on Wavelets*; CBMS-NSF Regional Conference Series in Applied Mathematics; SIAM: Philadelphia, PA, USA, 1992. 36

[34] Deb, A.; Sarkar, G.; Sengupta, A. *Triangular Orthogonal Functions for the Analysis of Continuous Time Systems*; Elsevier: New Delhi, India, 2007. 36

[35] Delves, L.M.; Mohamed, J.L. *Computational Methods for Integral Equations*; Cambridge University Press: New York, USA, 1985. 37

[36] Dörfler, W. A convergent adaptive algorithm for Poisson's equation. *SIAM J. Numer. Anal.*, **1996**, *33*, 1106–1124. 89

[37] Draidi, W.; Qatanani, N. Numerical Schemes for solving Volterra integral equations with Carleman kernel. *Int. J. Appl. Math.* **2005**, *31*, 647–669. 37

[38] Duchon, J. Interpolation des fonctions de deux variables suivant le principe de la flexion des plaques minces. *RAIRO* **1976**, *10*(12), 5–12. 67

[39] El-Borai, M.; Abdou, M.A.; Badr, A.A.; Basseem, M. Chebyshev Polynomials and Fredholm-Volterra integral equation. *Int. J. of Appl. Math. Mech.* **2008**, *4*, 78–92. 37

[40] Elnagar, G.N.; Kazemi, M. Chebyshev spectral solution of nonlinear Volterra-Hammerstein integral equations. *J. Comput. Appl. Math.* **1996**, *76*, 147–158. 36

[41] Epperson, J. F. On the Runge Example, *The American Mathematical Monthly* **1987**, *94(4)*, 329–341. `https://doi.org/10.2307/2323093`. 16

[42] Fan, J.; Gijbels, I. *Local Polynomial Modelling and Its Applications*, Chapman and Hall: London, UK, 1996. 82

[43] Farshadmoghadam, F.; Azodi, H.D. ; Yaghouti, M.R. An improved radial basis functions method for the high-order Volterra-Fredholm integro-differential equations. *Math. Sci.* **2021,** 1–14. https://doi.org/10.1007/s40096-021-00432-2 41

[44] Fasshauer, G. E. *Meshfree Approximation Methods with Matlab* World Scientific Publishing, Interdisciplinary Mathematical Sciences Vol. 6, 520 pages, 2007. 17, 18, 20, 24, 25, 26, 30

[45] García, S.; Luengo, J.; Sáez, J. A.; López, V.; Herrera F. A Survey of Discretization Techniques: Taxonomy and Empirical Analysis in Supervised Learning. *IEEE Trans. Knowl. Data Eng.* **2013**, vol. 25 *4*, 734–750. doi:10.1109/TKDE.2012.35 80

[46] Ghasemi, M.; Tavassoli Kajani, M.; Babolian, E. Numerical Solutions of the Nonlinear Volterra-Fredholm Integral Equations by Using Homotopy Perturbation Method. *Appl. Math. Comput.* **2007**, *188*, 446–449. 37

[47] Gibbons, J.D.; Chakraborti, S. *Nonparametric Statistical Inference*, CRC Press: Boca Raton, FL, USA, 2014. 80

[48] Clough, R. The finite element method in plane stress analysis. In *Proceedings 2nd ASCE conference on Electronic Computation*, Pittsburgh, PA, 1960.

[49] González-Rodelas, P.; Pasadas, M.; Kouibia, A.; Mustafa, B. Numerical Solution of Linear Volterra Integral Equation Systems of Second Kind by Radial Basis Functions. *Mathematics* **2022**, *10*, 223. https://doi.org/10.3390/math10020223 57, 61, 68

[50] Guo, M.; Liu, H.; Li, Y.; Li, W.; Gao, F.; Qin, S.; Wen, Q. Quantum algorithms for anomaly detection using amplitude estimation. *Physica A: Statistical Mechanics and its Applications* **2022**, *604*, 127936. https://doi.org/10.1016/j.physa.2022.127936. 79

[51] Hardy, R. L. Multiquadric equations of topography and other irregular surfaces, *J. Geophys. Res.* **1971**, Vol. 76 (8), pp. 1905–1915. 22, 23

[52] Hardy, R. L. Theory and applications of the multiquadric-biharmonic method: 20 years of discovery 1968-1988, *Computers Math. Applic.* **1990**, Vol. 19 (8/9), pp. 163–208. 21, 23

[53] Hart, J. D. *Nonparametric Smoothing and Lack-of-fit Tests*, Springer-Verlag: New York, USA, 1997. 83

[54] Hon, Y. C. An efficient numerical scheme for Burgers' equation, *Appl. Math. Comput.* Vol. 95 , pp. 37–50, 1998. 23

[55] Hon, Y.C.; Wong,A.S.M.; Li, T.S.; Chung, S.L.; Kansa, E.J. Multizone decomposition for simulation of time-dependent problems using the multiquadric scheme, *Computers and Mathematics with Applications,* V. 37, Issue 8, 1999, pp. 23-43, ISSN 0898-1221, https://doi.org/10.1016/S0898-1221(99)00098-X. 29

[56] Hon, Y.C.; Wong, S.M.; Golberg, M.A. Compactly supported radial basis functions for shallow water equations, *Applied Mathematics and Computation,* V. 127, Issue 1, 2002, pp. 79–101, ISSN 0096-3003, https://doi.org/10.1016/S0096-3003(01)00006-6. 29

[57] Hong, Z.; Fang, X.; Yan, Z., Hao, H. On Solving a System of Volterra Integral Equations with Relaxed Monte Carlo Method. *J. Appl. Math. Phys.* **2016**, *4*, 1315–1320. 37, 96

[58] Ikebe, Y. New fixed point theorems for countably condensing maps with an application to functional integral inclusions. *SIAM Rev.* **1972**, 14, 465–491.

[59] Iske, A. Scattered data approximation by positive definite kernel functions. *Rend. Sem. Mat. Univ. Politec. Torino* **2011**, *69*(3), 217–246. 71

[60] Islam, M.S.; Islam, M.S.; Bangalee, M.Z.I.; Khan, A.K.; Halder, A. Approximate Solution of Systems of Volterra Integral Equations of Second Kind by Adomian Decomposition Method. Dhaka. *Univ. J. Sci.* **2015** *63*, 15–18. 37, 96

[61] Issa, A.; Qatanani, N.; Daraghmeh, A. Approximation Techniques for Solving Linear Systems of Volterra Integro-Differential Equations. *J. Appl. Math.* **2020**, 2360487. https://doi.org/10.1155/2020/2360487. 37

[62] Jiayin, L. Quantifying uncertainty for an elliptic inverse problem with finite data. Thesis, Texas A&M University, 2015. 72

[63] Jiang, C.; Liu, L.; Qin, X.; Zhou, S.; Liu, K. Discovering Spatial-Temporal Indication of Crime Association (STICA). *ISPRS Int. J. Geo-Inf.* **2021**, *10*, 67. https://doi.org/10.3390/ijgi10020067. 79

[64] Jin, X.; Kawczak, J. Birnbaumí-Saunders and lognormal kernel estimators for modelling durations in high frequency financial data. *Ann. Econ. Fin.* **2003**, *4*, 103–124. 80

[65] Johannes, M. ; Polson, N. *MCMC Methods for Continuous-Time Financial Econometrics*, Handbook of Financial Econometrics: Applications, Vol. 2; Elsevier, 2010; pp. 1–72. https://doi.org/10.1016/B978-0-444-53548-1.50003-9. 79

[66] Kansa, E. J. Multiquadrics - a scattered data approximation scheme with applications to computational fluid-dynamics- surface approximations and partial derivative estimates *I. Comput. Math. Applic.* Vol. 19, No. 8, pp, 127–145, 1990. 23

[67] Kansa, E. J. Multiquadrics -a scattered data approximation scheme with applications to computational fluid-dynamics-solutions to parabolic, hyperbolic and elliptic partial differential equations, *I. Comput. Math. Applic.* Vol. 19, No. 8, pp, 147–161, 1990. 23

[68] Kasumo, C. On the Approximate Solutions of Linear Volterra Integral Equations of the First Kind. *Appl. Math. Sci.* **2020**, *14*, 141–153. 38, 96

[69] Khan, F.; Omar, M.; Ullah, Z. Discretization method for the numerical solution of 2D Volterra integral equation based on two-dimensional Bernstein polynomials. *AIP Adv.* **2018**, *8*, 125209. 37, 96

[70] Kirkby, J.L.; Leitao, A.; Nguyen, D. Nonparametric density estimation and bandwidth selection with b-spline bases: A novel galerkin method. *Comput. Stat. Data Anal.* **2021**, *159,107202*, `https://doi.org/10.1016/j.csda.2021.107202`. 81

[71] Kouibia, A.; Pasadas, M. Smoothing variational spline. *Appl. Math. Lett.* **2000**, *13*, 71–75. 68, 97

[72] Kouibia, A.; Pasadas, M. Approximation by discrete variational splines. *J. Comput. Appl. Math.* **2000**, *116*, 145–156. 68

[73] Kouibia, A.; Pasadas, M. Approximation by smoothing variational vector splines for noisy data. *J. Comput. Appl. Math.* **2008**, *211*, 213–222. 68

[74] Kouibia, A.; Pasadas, M. Optimization of the parameters of surfaces by interpolating variational bicubic splines. *Mathematics and Computers in Simulation* **2014**, *102*, 76–89. 68

[75] Kouibia, A.; Pasadas, M.; Rodriguez, M.L. A variational method for solving Fredholm integral systems. *Appl. Numer. Math.* **2012**, *66*, 1041–1049. 41, 44

[76] Lei, L.; Zhang, L.; Han, Z.; Chen, Q.; Liao, P.; Wu, D.; Tai, J.; Xie, B.; Su, Y. Advancing chronic toxicity risk assessment in freshwater ecology by molecular characterization-based machine learning. *Environmental*

Pollution **2024**, *342*, 123093. https://doi.org/10.1016/j.envpol.2023.123093. 79

[77] Lepik, Ü. Solving integral and differential equations by the aid of non-uniform Haar wavelets. *Appl. Math. Comput.*, **2008** , *198 (1)*, 326–332. 36

[78] Linz, P. *Analytical and Numerical Methods for Volterra Equations*, SIAM, Philadelphia, PA, 1985. 40

[79] Loader, C. Bandwidth selection: Classical or plug-in?. *Ann. Stat.* **1999**, *27*, 415–438. https://doi.org/10.1214/aos/1018031201. 81

[80] Ma, M.; Gao, Q.; Xiao, Z.; et al. Analysis of public emotion on flood disasters in southern China in 2020 based on social media data. *Nat Hazards* **2023**, *118*, 1013–1033. https://doi.org/10.1007/s11069-023-06033-7. 80

[81] Maleknejad, K.; Kajani, M.T. Solving integro-differential equation by using Hybrid Legendre and block-pulse functions. *Int. J. Appl. Math.* **2002**, *11*, 67–76. 37

[82] Maleknejad, K.; Mirzaee, F. Using rationalized Haar wavelet for solving linear integral equations. *Appl. Math. Comput.* **2005**, *160*, 579–587. 36

[83] Maleknejad, K.; Mohammadikia, H.; Rashidinia, J. A numerical method for solving a system of Volterra–Fredholm integral equations of the second kind based on the meshless method. *Afrika Mat.* **2018**, *29*, 955–965. 41

[84] McArthur, A.; McGregor, A.; & Stewart, R. Credit Unions and Low-income Communities. *Urban Stud.* **1993**, *30(2)*, 399–416. https://doi.org/10.1080/00420989320080371. 79

[85] Mirzaae, F. Numerical computational solution of the linear Volterra integral equations systems via rationalized Haar functions. *J. King Saud Univ. Sci.* **2010**, *22*, 265–268. 36

[86] Mahgoub, M.M.A. The new integral transform: Sawi transform. *Adv. Theor. Appl. Math.* **2019**, *14*, 81–87. 37

[87] Maleknejad, K.; Almasieh, H.; Roodaki, M. Triangular functions (TF) method for the solution of nonlinear Volterra–Fredholm integral equations. *Comm. Nonlinear Sci. Numer. Simulat.* **2010**, *15*, 3293–3298. 36, 37

[88] Marchant, C.; Bertin, K.; Leiva, V.; Saulo, H. Generalized Birnbaum-Saunders kernel density estimators and an analysis of financial data. *Comput. Stat. Data Anal.* **2013**, *63*, 1–15. 80, 85

[89] Morin, P.; Nochetto, R.H.; Siebert, K.G. Data oscillation and convergence of adaptive FEM. *SIAM J. Numer. Anal.* **2000**, *38*, 466–488. https://doi.org/10.1137/S0036142999360044. 88, 89

[90] Muhammad, A.M.; Ayal, A.M. Numerical Solution of Linear Volterra Integral Equation with Delay using Bernstein Polynomial. *IEJME* **2019**, *14*, 735–740. 37, 96

[91] Narkawich, F. J.; Ward, J. D.; Wendland, H. Sobolev bounds on functions with scattered zeros, with applications to radial basis function surface fitting. *Mathematics of Computation* **2004**, *84*(250), 743–763. 71

[92] Parzen, E. On Estimation of a Probability Density Function and Mode. *Ann. Math. Statist.* **1962**, *33(3)*, 1065–1076. 82, 84

[93] Prastawa, M.; Gilmore, J. H.; Lin, W.; Gerig, G. Automatic segmentation of MR images of the developing newborn brain. *Med Image Anal.* **2005**,Vol. 9, Issue 5, 457–466. https://doi.org/10.1016/j.media.2005.05.007. 79

[94] Rahman, M.; Arnold, B. C.; Gokhale, D. V.; Ullah, A. Data-based selection of the smoothing parameter in kernel density estimation using exact and approximate MISE. Technical Report No. 229, *Depart. of Statistics, University of California Riverside* **1996**. 84

[95] Roodaki, M.; Almasieh, H. Delta basis functions and their applications to systems of integral equations. *Comput. Math. Appl.* **2012**, *63*, 100–109. 36

[96] Rosenblatt, M. Remarks on Some Nonparametric Estimates of a Density Function. *Ann. Math. Stat.* **1956**, *27(3)*, 832–837. 82

[97] Runge, C. *Über empirische Funktionen und die Interpolation zwischen àquidistanten Ordinaten* Z. Math. u. Physik 46, (1901), 224–243. 15, 16

[98] Saulo, H.; Leiva, V.; Ziegelmann, F.; Marchant, C. A nonparametric method for estimating asymmetric densities based on skewed Birnbaum-Saunders distributions applied to environmental data. *Stoch. Environ. Res. Risk* **2**013, *7*, 1479–1491. 80

[99] Sablonière, P. Univariate spline quasi-interpolants and applications to numerical analysis. *Rend. Sem. Mat. Univ. Pol. Torino* **2005**, *63*, 107–118. 51

[100] Schaback, R. The missing Wendland functions. *Adv. Comput. Math.* **2011**, *34*, 67–81. 67, 69, 70

[101] Schaback, R.; Wu, Z. Operators on radial functions, *J. Comput. Appl. Math.* Vol. 73, pp. 257–270, 1996. 31

[102] Scott, D.W. *Multivariate Density Estimation: Theory, Practice, and Visualization*, John Wiley & Sons Inc.: New York, USA, 1992. `http://dx.doi.org/10.1002/9780470316849`. 82

[103] Shampine, L.F. Solving Volterra integral equations with ODE codes. *IMA J. Numer. Anal.* **1988**, *8* , 37–41. 35

[104] Shaw, S., Whiteman, J.R. Applications and numerical analysis of partial differential Volterra equations: a brief survey. *Comput.Methods Appl. Mech. Eng.*, 150 (1997), pp. 397-409. 40

[105] Siegel, S. Nonparametric statistics. *Am. Stat.* **1957**, *11*, 13–19. 80

[106] Silverman, B. W. *Density estimation for statistics and data analysis*, Vol. 26; CRC press,: London, 1986. 79, 82, 83, 84, 85

[107] Singh, J.; Sandberg, I.W. *Integral equations and Calculus of variations.* Maharshi Dayanand University, ROHTAK, 2020. 38

[108] Sloan, I. H. A review of numerical methods for Fredholm equations of the second kind. In *The Application and Numerical Solution of Integral Equations.* Proc. Sem., Australian Nat. Univ., Canberra, Sijthoff and Noordhoff, Alphen aan den Rijn, 1978, 51-74.

[109] Van der Houwen, P.J.; Sommeijer, B.P. Euler-Chebyshev methods for integro-differential equations. *Appl. Numer. Math.* **1997**, *24*, 203–218. 37

[110] Volterra, V. *Leçons sur les équations intégrales et intégro-différentielles.* Gauthier-Villars, Paris, France, 1913. 35, 40, 41

[111] Uddin, M.; Ullah, N.; Ali-Shah, S.I. RBF Based Localized Method for Solving Nonlinear Partial Integro-Differential Equations. *Comput. Model. Eng. Sci.* **2020**, *123*, 957–972. 41

[112] Wazwaz, A.M. The combined Laplace transform–Adomian decomposition method for handling nonlinear Volterra integro–differential equations. *Appl. Math. Comput.* **2010**, *216*, 1304–1309. 37

[113] Wendland, W. L. On some mathematical aspects of boundary element methods for elliptic problems. In *The Mathematics of Finite Elements and Applications.* J. R. Whiteman, eds., Academic Press, London, 1985, 193-277.

[114] Wendland, H. Piecewise polynomial, positive definite and compactly supported radial functions of minimal degree. *Adv. Comput. Math.* **1995**, *4*, 389–396. 67

[115] Wendland, H. Error Estimates for Interpolation by Compactly Supported Radial Basis Functions of Minimal Degree. *J. Approx. Theory* **1998**, *93*, 258–272. 42, 43, 54

[116] Wendland, H. Meshless Garlekin Methods Using Radial Basis Functions. *Math. Comp.* **1999**, *228*, 1521–1531. 43, 55

[117] Wendland, H. *Scattered Data Approximation* Cambridge Monographs on Applied and Computational Mathematics, Cambridge University Press, Cambridge, 2005. 26, 27, 30, 31, 32

[118] Wu, Z. Compactly supported positive definite radial functions, *Adv. Comput. Math.* Vol. 4, pp, 283–292, (1995). 33

[119] Yang, L.-H.; Shen, J.-H.; Wang, Y. The reproducing kernel method for solving the system of the linear Volterra integral equations with variable coefficients. *J. Comput. Appl. Math.* **2012**, *236*, 2398–2405. 37

[120] Yousefi, S.; Razzaghi, M. Legendre wavelets method for the nonlinear Volterra–Fredholm integral equations. *Math. Comput. Simulat.* **2005**, *70*, 1–8. 37

[121] Youssri, Y.H.; Hafez, R. M. Chebyshev collocation treatment of Volterra–Fredholm integral equation with error analysis. *Arab. J. Math.* **2020**, *9* , 471–480. 37

[122] Zhang, H.; Chen, Y.; Nie, X. Solving the Linear Integral Equations Based on Radial Basis Function Interpolation. *J. Appl. Math.* **2014**, https://www.hindawi.com/journals/jam/2014/793582/ (accessed on 20 October 2021). 41

[123] Ziane, Y.; Zougab, N.; Adjabi, S. Adaptive Bayesian bandwidth selection in asymmetric kernel density estimation for nonnegative heavy-tailed data. *J. Appl. Stat.* **2015**, *42:8*, 1645–1658. https://doi.org/10.1080/02664763.2015.1004626.

[124] Ziane, Y.; Zougab, N.; Adjabi, S. Body tail adaptive kernel density estimation for nonnegative heavy-tailed data. *Monte Carlo Methods Appl.* **2021**, *1*, vol. 27, 57–69. https://doi.org/10.1515/mcma-2021-2082. 87

[125] Zhao, Y.; Zhang, M.; Ni, Q.; Wang, X. Adaptive Nonparametric Density Estimation with B-Spline Bases. *Mathematics* **2023**, *11*, 291. https://doi.org/10.3390/math11020291. 88